

The background of the cover is a vibrant yellow, filled with a complex, organic pattern of thin, dark yellow lines that resemble branches or veins. Interspersed among these lines are numerous small, solid yellow circles of varying sizes, creating a dense, textured effect that suggests a molecular or biological structure.

**CLINICAL PHARMACOLOGY
OF IMMUNO-MODULATORY
BIOTHERAPEUTICS**

INNOVATIONS
IN EARLY DRUG
DEVELOPMENT

MARLOUS R. DILLINGH



CLINICAL PHARMACOLOGY OF IMMUNO-MODULATORY BIOTHERAPEUTICS

INNOVATIONS IN EARLY DRUG DEVELOPMENT

PROMOTORES:
Prof. dr. J. Burggraaf
Prof. dr. A.F. Cohen

CO-PROMOTOR:
Dr. M. Moerland

LEDEN PROMOTIECOMMISSIE:
Prof. dr. H.J. Guchelaar
Prof. dr. R.E.M. Toes
Prof. dr. P.H. van der Graaf (Leiden Academic Centre for Drug Research, LACDR)
Dr. M. Wijsenbeek-Lourens (Erasmus Medical Center, Rotterdam)

ILLUSTRATIONS PAGE 13, 27, 98, 112
F.A. van Meurs

DESIGN
Caroline de Lint, Voorburg (caro@delint.nl)

ACKNOWLEDGEMENTS
The publication of this thesis was financially supported by the foundation
Centre for Human Drug Research (CHDR), Leiden, the Netherlands

CLINICAL PHARMACOLOGY OF IMMUNO-MODULATORY BIOTHERAPEUTICS

INNOVATIONS IN EARLY DRUG DEVELOPMENT

PROEFSCHRIFT
ter verkrijging van de graad van Doctor aan de Universiteit Leiden,
op gezag van Rector Magnificus prof.mr. C.J.J.M. Stolker,
volgens besluit van het College voor Promoties
te verdedigen op donderdag 9 november
klokke 15:00 uur

DOOR
Marlous R. Dillingh
Geboren te Dirksland in 1984

	CHAPTER 1
7	Introduction
	CHAPTER 2
15	Microdosing of a carbon-14 labelled protein in healthy volunteers accurately predicts its pharmacokinetics at therapeutic dosages
	CHAPTER 3
39	Recombinant human serum amyloid P in healthy volunteers and patients with pulmonary fibrosis
	CHAPTER 4
51	Recombinant human pentraxin-2 therapy in patients with idiopathic pulmonary fibrosis: safety, pharmacokinetics and exploratory efficacy
	CHAPTER 5
69	Characterization of inflammation and immune cell modulation induced by low-dose LPS administration to healthy volunteers
	CHAPTER 6
87	Clinical evaluation of Humira® biosimilar ONS-3010 in healthy volunteers: focus on pharmacokinetics and pharmacodynamics
	CHAPTER 7
105	Summary and discussion
	CHAPTER 8
115	Summary in Dutch
	APPENDICES
123	Curriculum Vitae
125	List of publications
126	Author affiliations
127	List of abbreviations



CHAPTER 1

Introduction

The development of new investigational medical products is complex and entails a comprehensive assessment of the value of the new compound. It takes on average 12 years before a new drug eventually becomes available for patients of the target population. After the new compound is considered to be safe for administration to humans based on preclinical data, the clinical development is traditionally divided into four phases, each with limited pertaining objectives:

- **PHASE I** – A new drug is administered to a small group of healthy volunteers or patients for the first time to assess safety, tolerability and pharmacokinetics.
- **PHASE II** – The drug is administered to (a larger group of) patients to further evaluate safety and assess the pharmacodynamic properties.
- **PHASE III** – The drug is administered to a large group of patients to confirm safety and efficacy.
- **PHASE IV** – After marketing authorization of the drug has been granted, data is gathered on the efficacy in larger patient populations and side effects associated with long-term use.

Although this classification has some merits, it also implicitly suggests that the drug development process is a linear process with well-demarcated phases, which have little overlap and most importantly, pays little attention to the pharmacodynamic effects of the new compound in the early phases of development. This approach appears to be particularly suitable for the development of drugs of which the pharmacology and clinical endpoints are well-known, the inter-individual variability is limited and hence a relatively high level of certainty to reach the market. However, since drugs that are currently being developed are more complex by targeting complicated, rather unexplored biological mechanism and do have a more uncertain future, novel approaches seem to be more suited.

Question-based drug development is a different, non-linear approach to clinical drug development. The major difference and also advantage compared to the more traditional, linear approach as described above, is the ability to resolve existing uncertainties already in early stages of development, by the definition of five research questions comprising five areas of interest: population, site, pharmacology, clinical (intended and adverse) and therapeutic window (Figure 1) (1, 2).

- **QUESTION 1** – Does the biologically active compound/active metabolites get to the site of action?
- **QUESTION 2** – Does the compound cause its intended pharmacological/functional effect(s)?

- **QUESTION 3** – Does the compound have beneficial effects on the disease or its pathophysiology?
- **QUESTION 4** – What is the therapeutic window of the new drug?
- **QUESTION 5** – How do the sources of variability in drug response in the target population affect the development of the product?

An increasing number of biotherapeutics such as recombinant proteins and monoclonal antibodies are developed for therapeutic and diagnostic purposes. The development of these compounds is particularly challenging since the immunogenicity of biotherapeutics is often intrinsically incompatible with preclinical animal models (3-5). In addition, a significant number of immunomodulatory biotherapeutics do not complete the process of drug development successfully, mainly due to a lack of efficacy when administered to patients (6-9). The identification of biomarkers and the use of *in vivo* or *ex vivo* challenge models in early clinical (pharmacology) studies play an important role in question-based drug development and may result in increased success rates for compounds of this class in the future or earlier abandonment of the development of a drug, with both outcomes equally important. This is exactly the reason why the Centre for Human Drug Research invested in the development of challenge models over the years. By the use of these challenge models we have been able to mimic specific diseases/conditions or to induce a specific pathway of interest. A few selected examples are: a tetrahydrocannabinol (THC) challenge model (10), a 5-hydroxytryptophan (5HTP) challenge model (11), a scopolamine challenge model (12) and a glucagon challenge model (13). In order to improve the process of drug development it is crucial to ask the right questions the right moment in time. Together with the performance of concurrent engineering this approach would result in a better data integration in the (early) stages of the development process.

This thesis describes the early clinical development of three immunomodulatory biotherapeutics, human recombinant placental alkaline phosphatase (hRESCAP), recombinant human pentraxin-2 (PRM-151) and an adalimumab biosimilar (ONS-3010).

Alkaline phosphatase (ALP) is an endogenous anti-inflammatory protein that is suggested to neutralize potentially harmful substrates in the human body. A bovine homologue of ALP has previously been investigated for treatment of acute ischemia-mediated and hypoxia-mediated inflammatory responses during invasive surgery and sepsis in humans (14, 15). However, because of its short plasma residence time, bovine ALP is not compatible with chronic disease management.

The development of a human recombinant ALP with the required pharmacokinetic properties might improve the treatment of an array of chronic inflammatory diseases.

Chapter 2 describes the first study in which the pharmacokinetics of human recombinant placental alkaline phosphatase (hRESCAP) was evaluated in human subjects, using microdosing combined with ultrasensitive accelerator mass spectrometry, as a first step in the drug development process. Microdosing is a relatively new approach and theoretically offers the advantage to obtain pharmacokinetic data with high statistical power, prior to the performance of a formal phase I study, in a small group of volunteers and after limited preclinical safety testing. In addition to the assessment of the pharmacokinetics of a single micro-dose of carbon-14 labelled (^{14}C)-hRESCAP, this study was performed to assess the applicability of microdosing as a technique to predict the pharmacokinetics of biotherapeutics in human subjects at therapeutic doses (question 1) without investigation of the intended pharmacological/functional effect(s).

PRM-151 is a recombinant human pentraxin-2 (PTX-2; also known as serum amyloid P, SAP), a protein that controls the differentiation of circulating monocytes into fibrocytes (16-18) and pro-fibrotic (M2) macrophages (19). PRM-151 is under development for the treatment of pulmonary fibrosis which is a chronic, progressive, irreversible and lethal disease.

The performance of extensive dose-finding studies is undesirable and sometimes even impossible in a vulnerable patient population like pulmonary fibrosis patients. The identification of selective, early phase (*and* non-invasive) biomarkers is highly important to be able to measure a potential pharmacologic effect. However, healthy volunteers don't show any inflammatory symptoms and are therefore no suitable study population to search for these biomarkers for this particular immunomodulatory biotherapeutic compound.

The single ascending dose study in healthy volunteers and a small number of patients with pulmonary fibrosis described in chapter 3 was designed to search for the target therapeutic dose resulting in the desired circulating SAP concentration (based on pre-clinical animal studies an approximate 2-fold increase in the normal circulating SAP concentration would be needed to achieve anti-fibrotic activity; dose-finding), for an initial comparison between the pharmacokinetic SAP profile in healthy volunteers and (idiopathic) pulmonary fibrosis patients and the identification of potential biomarkers in the patient population (questions 1 and 2).

In our search for these selective, early phase biomarkers, this study was also designed to investigate the pharmacological effect ('proof of concept') of PRM-151

treatment on the proportion of fibrocytes using a fluorescence activated cell sorter (FACS) analysis performed in a small cohort of (idiopathic) pulmonary fibrosis patients (question 2). Even though the patient number was small, these results suggested that circulating fibrocytes might be a biomarker for PRM-151 in patients with (idiopathic) pulmonary fibrosis studies. In a multiple dose follow-up study the therapeutic and beneficial effects of PRM-151 were investigated in more detail, in a larger number of idiopathic pulmonary fibrosis patients (chapter 4, question 3). The value of the biomarker identified in the preceding single dose study was also explored in this larger patient population in addition to the investigation of high-resolution computed tomography (HRCT) as a potential functional and relevant biomarker using a quantitative imaging modality (question 2).

As mentioned earlier, an LPS *in vivo/ex vivo* whole blood challenge model might be useful to evaluate the pharmacological effects of some classes of immunomodulatory compounds.

More specifically, an *in vivo/ex vivo* lipopolysaccharide (LPS) challenge is a human model of systemic inflammation which can be applied in clinical pharmacology studies to assess the effects of specific interventions (medicinal or non-medicinal) on the inflammatory response in non-diseased populations. It has proven to be specifically applicable for immunomodulatory biotherapeutics, to explore the molecular mechanisms and physiological significance of the systemic inflammatory response encountered in acute as well as chronic inflammatory conditions, in a controlled and standardized experimental setting.

In chapter 5, we explored the feasibility of a low-dose *in vivo* LPS challenge as a methodological tool for future clinical studies exploring pharmacological (or nutritional) immune-modulating effects (question 2). The reason for this research was to overcome the drawback of *in vivo* challenges that employ relatively high doses of LPS, making it impossible to be repeated frequently over time, because the challenge is burdensome for the volunteer and/or has potential sustained effects and/or is technically challenging or not even feasible. Therefore, cell-based (*in vitro/ex vivo*) challenge models have been developed to assess drug effects outside the human body, on primary human cells. The study results are presented in chapter 5 and answer the question if *in vivo* LPS administration in combination with repeated *ex vivo* LPS whole blood challenges can be valuably applied in future clinical pharmacology studies (question 2).

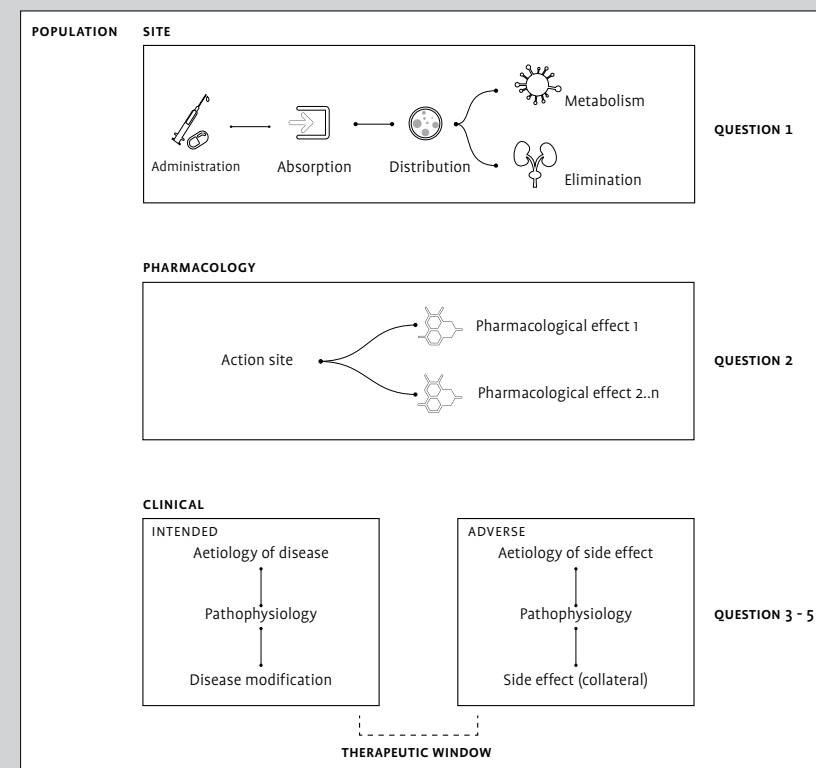
The development of products that are designed as a biosimilar of the original licensed product has gained interest over the last years because of expiring patents of originator's biotherapeutic products like adalimumab (Humira®).

Per US Food and Drug Administration (FDA) and European Medicines Agency (EMA) guidelines, demonstration of biosimilarity between test and reference biotherapeutics comprises quality characteristics, pharmacokinetic properties, biological activity, safety and efficacy (20-24). Assessing biological activity (e.g. pharmacodynamic effects) is commonly done only in advanced phases of clinical development bears the risk of late discovery of non-biosimilarity. Hence, de-risking the development of a compound using measures to demonstrate pharmacodynamic similarity as well can be of great value.

The study described in chapter 6 was performed to demonstrate pharmacokinetic biosimilarity between ONS-3010, developed as a biosimilar of adalimumab, and two reference products (Humira® EU and US) in healthy volunteers (question 1) and is an example of a clinical trial with an implemented *ex vivo* LPS/aluminium whole blood challenge. The reason to study the application of *ex vivo* LPS/aluminium whole blood challenges in this trial was not only to early assess the intended pharmacodynamic activity of ONS-3010 in comparison with the two reference products in healthy volunteers, but also to explore if mechanistic insight into the secondary effects of TNF- α blockade could be obtained (question 2).

In conclusion, the clinical pharmacology trials described in this thesis cover different aspects of question-based drug development, congruous in obtaining as much and as detailed product information as possible in the earliest stages of development to estimate the potential value of a new biotherapeutic compound.

FIGURE 1 Areas of interest of question-based drug development. *Population, site, pharmacology, clinical and therapeutic window, source A.F. Cohen 2010 (1).*



Microdosing of a carbon-14 labelled protein in healthy volunteers accurately predicts its pharmacokinetics at therapeutic dosages

Clinical Pharmacology and Therapeutics, 2015 Aug, 98(2):196-204

M.H.L. Vlaming, E. van Duijn, M.R. Dillingh, R. Brands, A.D. Windhorst, N.H. Hendrikse, S. Bosgra, J. Burggraaf, M.C. de Koning, A. Fidder, J.A.J. Mocking, H. Sandman, R.A.F. de Ligt, B.O. Fabriek, W.J. Pasman, W. Seinen, T. Alves, M. Carrondo, C. Peixoto, P.A.M. Peeters, W.H.J. Vaes

REFERENCE LIST

- Cohen AF. Developing drug prototypes: pharmacology replaces safety and tolerability? *Nat Rev Drug Discov.* 2010;9(11):856-65.
- de Visser SJ. A question based approach to drug development: Leiden University, The Netherlands; 2003.
- Brinks V, Jiskoot W, Schellekens H. Immunogenicity of therapeutic proteins: the use of animal models. *Pharm Res.* 2011;28(10):2379-85.
- Brinks V, Weinbuch D, Baker M, Dean Y, Stas P, Kostense S, et al. Preclinical models used for immunogenicity prediction of therapeutic proteins. *Pharm Res.* 2013;30(7):1719-28.
- Bugelski PJ, Treacy G. Predictive power of preclinical studies in animals for the immunogenicity of recombinant therapeutic proteins in humans. *Curr Opin Mol Ther.* 2004;6(1):10-6.
- Arrowsmith J. Trial watch: Phase II failures: 2008-2010. *Nat Rev Drug Discov.* 2011;10(5):328-9.
- Arrowsmith J. Trial watch: phase III and submission failures: 2007-2010. *Nat Rev Drug Discov.* 2011;10(2):87.
- Denayer T, Stöhr T, van Roy M. Animal models in translational medicine: Validation and prediction. *New Horizons in Translational Medicine* 2014.
- Hay M, Thomas DW, Craighead JL, Economides C, Rosenthal J. Clinical development success rates for investigational drugs. *Nat Biotechnol.* 2014;32(1):40-51.
- Strougo A, Zuurman L, Roy C, Pinquier JL, van Gerven JM, Cohen AF, et al. Modelling of the concentration-effect relationship of THC on central nervous system parameters and heart rate -- insight into its mechanisms of action and a tool for clinical research and development of cannabinoids. *J Psychopharmacol.* 2008;22(7):717-26.
- Jacobs GE, Kamerling IM, de Kam ML, Derijk RH, van Pelt J, Zitman FG, et al. Enhanced tolerability of the 5-hydroxytryptophane challenge test combined with granisetron. *J Psychopharmacol.* 2010;24(1):65-72.
- Liem-Moolenaar M, de Boer P, Timmers M, Schoemaker RC, van Hasselt JG, Schmidt S, et al. Pharmacokinetic-pharmacodynamic relationships of central nervous system effects of scopolamine in healthy subjects. *Br J Clin Pharmacol.* 2011;71(6):886-98.
- van Dongen MG, Geerts BF, Bhanot S, Morgan ES, de Kam ML, Moerland M, et al. Characterization of a standardized glucagon challenge test as a pharmacodynamic tool in pharmacological research. *Horm Metab Res.* 2014;46(4):269-73.
- Kats S, Brands R, Seinen W, de Jager W, Bekker MW, Hamad MA, et al. Anti-inflammatory effects of alkaline phosphatase in coronary artery bypass surgery with cardiopulmonary bypass. *Recent Pat Inflamm Allergy Drug Discov.* 2009;3(3):214-20.
- Kats S, Brands R, Hamad MA, Seinen W, Scharnhorst V, Wulkan RW, et al. Prophylactic treatment with alkaline phosphatase in cardiac surgery induces endogenous alkaline phosphatase release. *Int J Artif Organs.* 2012;35(2):144-51.
- Pilling D, Gomer RH. Regulatory pathways for fibrocyte differentiation. In: Bucala R, editor. *Fibrocytes: New Insights into Tissue Repair and Systemic Fibroses*: World Scientific Publishing Co. Pte. Ltd; 2007. p. 37-60.
- Pilling D, Buckley CD, Salmon M, Gomer RH. Inhibition of fibrocyte differentiation by serum amyloid P. *J Immunol.* 2003;171(10):5537-46.
- Pilling D, Roife D, Wang M, Ronkainen SD, Crawford JR, Travis EL, et al. Reduction of bleomycin-induced pulmonary fibrosis by serum amyloid P. *J Immunol.* 2007;179(6):4035-44.
- Moreira AP, Cavassani KA, Hullinger R, Rosada RS, Fong DJ, Murray L, et al. Serum amyloid P attenuates M2 macrophage activation and protects against fungal spore-induced allergic airway disease. *J Allergy Clin Immunol.* 2010;126(4):712-21.
- European Medicines Agency (EMA) – Guideline on similar biological medicinal products containing monoclonal antibodies; EMA/CHMP/BMWP/403543/2010. 2012.
- European Medicines Agency (EMA) – Guideline on similar biological medicinal products; CHMP/437/04 Rev 1. 2014.
- European Medicines Agency (EMA) – Guideline on similar biological medicinal products containing biotechnology-derived proteins as active substance; EMEA/CHMP/BMWP/42832/2005 Rev 1. 2014.
- US Food and Drug Administration (FDA) – Scientific Considerations in Demonstrating Biosimilarity to a Reference Product – Guidance for Industry. 2015.
- US Food and Drug Administration (FDA) – Quality Considerations in Demonstrating Biosimilarity of a Therapeutic Protein Product to a Reference Product – Guidance for Industry. 2015.

ABSTRACT

Preclinical development of new biological entities (NBEs) such as human protein therapeutics requires considerable expenditure of time and costs. Poor prediction of pharmacokinetics in humans further reduces net efficiency.

In this study, we show for the first time that pharmacokinetic data of NBEs in humans can be successfully obtained early in the drug development process by the use of microdosing in a small group of healthy subjects combined with ultra-sensitive accelerator mass spectrometry. After only minimal preclinical testing we performed a first-in-human phase 0/phase I trial with a human recombinant therapeutic protein (rescuing Alkaline Phosphatase, human recombinant placental alkaline phosphatase (hRESCAP®)) to assess its safety and kinetics.

Pharmacokinetic analysis showed dose linearity from microdose (53 µg) [¹⁴C]-hRESCAP to therapeutic doses (up to 5.3 mg) of the protein in healthy volunteers. This study demonstrates the value of a microdosing approach in a very small cohort for accelerating the clinical development of NBEs.

Introduction

New biological entities (NBEs) such as recombinant proteins, monoclonal antibodies and oligonucleotides are increasingly being developed for therapeutic and diagnostic purposes. Currently, NBEs make up 42% of the research pipelines of pharmaceutical companies, and 8% of currently marketed drugs are biotech products (1). Developing NBEs is particularly challenging as human biopharmaceuticals are often intrinsically immunologically incompatible with preclinical (animal) models (2, 3). Further, because of the lack of predictive preclinical models to study pharmacokinetic (PK) profiles, biologicals have a relatively high failure rate at late stages of drug development (4). Microdosing, a relatively new approach, is proposed to accelerate the overall drug development process. Although it is otherwise difficult, or impossible, to predict the PK of new drugs in humans, microdosing offers the superior advantage to obtain data with high statistical power, prior to a phase I study in a small group of volunteers and after limited preclinical safety testing (5-9). Thus, this approach is appealing to candidate drugs with a potentially undesirable PK profile, as these can be excluded before entering costly clinical trials.

In a phase 0 microdosing trial, extremely low doses of carbon-14 (¹⁴C) labelled compounds are administered to healthy volunteers (10, 11). Typically, a microdose would be <1% of the therapeutically active dose, ≤100 µg, or ≤30 nmol for proteins (10, 12, 13). The resulting minute drug concentrations in the body after microdoses are unlikely to elicit pharmacodynamic or toxicological effects and do not impose radiological risks. The detection of the extremely low amounts of carbon-14 labelled drugs in biological matrices is enabled by the highly sensitive analytical technique accelerator mass spectrometry (AMS) (14-16).

Until now, microdosing has been used only for small molecule drugs (7). The opinion prevails that microdosing cannot be applied to research on biologicals. This may be correct for biopharmaceuticals that target a specific tissue, resulting in a non-linear PK profile (8). However, for a (non)-endogenous NBE that resides in the systemic compartment, the PK is expected to show dose linearity.

Another advantage of microdosing is that the very small starting dose allows safe generation of safety and PK data in humans. In this view, the clinical trial, including the monoclonal antibody TGN1412, could have ended less disastrous than it did in 2006. In this particular study 0.1 mg/kg TGN1412 was administered (17), which, for the average person, would result in a dose of ~7 mg or 47 nmol. In the present study we show a microdose application starting with a 100-fold lower dose of an NBE.

Alkaline phosphatase (ALP) is an endogenous anti-inflammatory protein that is suggested to neutralize potentially harmful substrates such as damage-associated molecular pattern molecules, like extracellular nucleotides (18), pathogen-associated molecular pattern molecules, and lipopolysaccharides (19). A bovine homologue of ALP has previously been investigated for treatment of acute ischemia-mediated and hypoxia-mediated inflammatory responses during invasive surgery and sepsis, and was shown to be well tolerated in humans (20, 21). Because of its short plasma residence time, bovine ALP is not compatible with chronic disease management. The recent development of human recombinant ALP, human recombinant placental alkaline phosphatase (hRESCAP), which is expected to have a similar plasma residence time as the endogenous sialylated placental protein *in vivo*, may boost the treatment of an array of chronic inflammatory diseases. As ALP is endogenously expressed in humans at relatively high levels, dose linearity is expected. In this study, we report, to our knowledge for the first time, on a clinical microdosing study to determine the PK of a carbon-14 labelled hRESCAP. In phase 0 the PK of a single intravenous microdose of [¹⁴C]-hRESCAP were determined, whereas phase I focused on the safety, tolerability and PK at increasing doses. The current work also summarizes the required conditions for generalized execution of microdosing studies with biopharmaceuticals. A microdosing study using an NBE was never performed in humans before and these results may revolutionize the drug development of biotherapeutics.

Methods

ANIMAL STUDIES Mice animal studies were performed to determine the toxicity and investigate possible abnormalities in body or organ weight. No toxicity or abnormalities were observed (details: see Supplementary Material).

hRESCAP PRODUCTION hRESCAP is expressed in the human amnion-derived production CAP9 cell line (CEVEC Pharma, Köln, Germany). Good manufacturing practice production of hRESCAP was performed at the Genbet facilities (Oeiras, Portugal). Specific chemical and physical viral clearance studies, such as formaldehyde, diafiltration and nanofiltration, have been performed on the process that was used to inactivate putative extraneous viruses.

hRESCAP CHARACTERIZATION The sodium dodecyl sulfate-polyacrylamide gel electrophoresis and gel filtration chromatography were performed to determine

the molecular weight and purity for hRESCAP. The enzymatic activity of hRESCAP was tested *in vitro* (see below). Mass spectrometric analysis of the glycosylated protein and deglycosylated product indicated a G0-GlcNAc as the most prominent glycan structure, located at N271 (data not shown, Abundnz B.V., The Netherlands). No protein aggregation was determined for the bulk product and [¹⁴C]-hRESCAP by size-exclusion chromatography-ultraviolet (SEC-UV, Abundnz B.V., The Netherlands). hRESCAP was supplied as a clear to slightly opalescent, colourless, sterile, essentially pyrogen-free solution in a Hyclone bag. The protein concentration was determined using a Pierce BCA Protein Assay Kit (Pierce Biotechnology, Rockford, Illinois, USA). The mean protein concentration was 3.3 mg/mL. Stability studies on one batch of hRESCAP showed an initial loss of enzymatic activity from 1446 U/mg after production → 1064 U/mg after 2 months. The activity remained stable during the following months at 992 U/mg. The hRESCAP was stored in an aqueous buffer containing 10 mM Tris-HCl, 5 mM magnesium chloride, 0.1 mM zinc chloride and pH 8.3, at 2-8°C.

[¹⁴C]-hRESCAP SYNTHESIS AND QUALITY CONTROL A good manufacturing practice-produced and certified hRESCAP batch was radiolabelled with carbon-14 by reductive amination with [¹⁴C]-formaldehyde of lysine residues (see Supplementary Material). The product was characterized by radio-high performance liquid chromatography with a beta-flow-through detector, via comparison of retention times for the radiolabelled product and nonradioactive hRESCAP. The requirement for radiochemical purity of the batch was set at ≥95%. Furthermore, bacterial endotoxin content, filter integrity, and sterility were tested for each produced batch. Requirements for the enzymatic activity of the produced [¹⁴C]-hRESCAP batches were specified to be ≥70% of the original enzymatic activity. Protein concentrations of the batches were 8.8-11.4 µg/mL and the specific activities varied between 86 and 120 Bq/mL.

CLINICAL STUDY AND DATA ANALYSIS The clinical study with hRESCAP and [¹⁴C]-hRESCAP was designed as a two-phase study in healthy male volunteers (Figure 1). Blood samples were taken at regular time intervals after administration and one pre-dose sample was obtained for each volunteer.

DETERMINATION OF ENZYMATIC ACTIVITY The enzymatic activity of the plasma samples was determined using an Olympus AU 400 chemical analyser (Goffin Meyvis) at 410/480 nm. The instrument was calibrated using the system calibrator kit (66300 Goffin Meyvis) and deionized water as a blank. The method is based on

the recommendations of the “International Federation for Clinical Chemistry”. As a quality control the starting material hRESCAP was included.

AMS TOTAL COUNT ANALYSIS A novel AMS sample introduction method was used (15). Briefly, 1.5 µL plasma samples were transferred to tin foil cups, evaporated to dryness and combusted using an elemental analyser (Vario Micro, Elementar, Germany). The resulting CO₂ was captured on a zeolyte trap. CO₂ was released by heating of the trap and transferred to a vacuum syringe using helium. The resulting 6% v/v gas mixture of CO₂ with helium was infused at a pressure of 1 bar at 60 µL/min into the titanium target in the SO110 ion source of a 1 MV Tandetron AMS (High Voltage Engineering Europe B.V., The Netherlands) (22, 23). As the AMS solely counts [¹⁴C] atoms, the analysis is universal. No study, matrix or compound method development is required.

LIQUID CHROMATOGRAPHY ACCELERATOR MASS SPECTROMETRY (LC+AMS)

Enzymatically active hRESCAP was purified from plasma using a 4 mL high-performance liquid chromatography (HPLC) column (prepared in-house) containing mimetic ligand adsorbent for ALP (Prometic Life Sciences, Québec, Canada). The affinity chromatography specifically isolated enzymatically active ALP from plasma samples, including [¹⁴C]-hRESCAP (see Supplementary Material). Method validation was based on the European Bioanalysis Forum recommendation for AMS analysis (24). Calibration standards and quality controls were prepared in blank human pooled heparin plasma (Bioreclamation IVT, New York, USA). Activity levels ranged from 10-250 mBq/mL, and from 30-200 mBq/mL for the calibration standards and quality controls, respectively. All samples of two subjects, one receiving a microdose and one a high-dose, were analysed by LC+AMS. The LC+AMS data are in line with the total count and enzymatic activity analysis (>90% agreement between AUCs). As no additional advantage is provided by the LC+AMS data, the remaining subject samples were only analysed for total count and enzymatic activity.

AMS DATA PROCESSING For total control analysis, ratios were calibrated using the standard reference material oxalic acid II (OXII, SRM 4990c; National Institute of Standards and Technology, USA) (25). Anthracite was used as a zero-reference sample (Certified Reference Material, BCR-460 Coal). Australian National University sucrose (ANU sucrose, IAEA-CH-6, Reference Material 8542) was used for quality control (26). For LC+AMS data linear regression on calibration standards with weighting factor 1/x was applied.

PK MODELLING AND STATISTICS Subjects showed a nonzero background radioactivity and a baseline endogenous enzyme activity. Upon administration at time 0.5 h, the concentration-time curve exhibited three distinct elimination phases. This profile was described by a linear combination of three exponential terms (Eq. 1-4):

$$\tau = t - T_D \quad (1)$$

$$\phi = \ln(\lambda) \quad (2)$$

$$c = C_0 \quad \tau < 0 \quad (3)$$

$$c = C_0 + D/V_d \times \left\{ \begin{array}{l} \alpha_1 \times \exp[-\exp(\phi_1) \times \tau] + \\ \alpha_2 \times \exp[-\exp(\phi_2) \times \tau] + \\ \alpha_3 \times \exp[-\exp(\phi_3) \times \tau] \end{array} \right\} \quad \tau \geq 0 \quad (4)$$

where τ is the time after dosing T_D (0.5 h), ϕ are defined as the natural log of the elimination rate constants λ (h⁻¹), D is the administered dose (Bq or U), C_0 is the background radioactivity (mBq/mL) or baseline ALP activity (mU/mL), V_d is the apparent volume of distribution (L), and the multipliers α represent fixed but unknown proportions of the dose corresponding to the different protein fractions.

The natural logs ϕ of the elimination rate constants λ (Eq. 2) were estimated to enforce positive values without constraining the optimization problem. The exponential terms were ordered by their rate constants: $\phi_1 > \phi_2 > \phi_3$. The background was included in the model to account for between-subject and within-subject variation. For this purpose, placebo-treated subjects were also included in the dataset.

An equal volume of distribution V_d was assumed for all protein fractions. The multipliers α_1 , α_2 , and α_3 represent the fixed but unknown proportions of dose D corresponding to the different protein fractions, of which the first two were estimated and the last is set at $\alpha_3 = 1 - \alpha_1 - \alpha_2$.

Log-normal distributions about the means were considered appropriate. The log of the right hand side of Eq. 4 was fit to the log-transformed plasma concentration time data with the nonlinear mixed effects library *nlme* (27) in R (version 3.0.2.1), by the first order conditional estimation algorithm. Random effects were considered at the subject level in all coefficients, except for the background radioactivity.

To explicitly study dose-proportionality in PK across the doses administered the model was fit separately to the radioactivity *versus* time data and enzyme activity *versus* time data with and without dose as a covariate for all coefficients. To exclude a significant effect of the radiolabel on the PK of the protein, the model was fit to all data with and without method (enzyme activity or radioactivity) as a covariate for all parameters. The significance of each random effect term and covariate was evaluated by ANOVA.

Results

PRODUCTION AND ANALYSIS OF HRESCAP AND [¹⁴C]-HRESCAP A good manufacturing practice-compliant method to incorporate a [¹⁴C] label into hRESCAP was developed and various batches of [¹⁴C]-hRESCAP with 100% radiochemical purity were produced. On average, 0.4-0.6 [¹⁴C] atoms were present per hRESCAP dimer of ~110 kDa. [¹⁴C]-hRESCAP and hRESCAP were extensively characterized *in vitro* for: appearance, pH, radiochemical purity, chemical purity, radiochemical identity, glycosylation, stability, aggregation, enzymatic activity, and protein concentration (Supplementary Table S1). Both products were similar, if not identical, and met the predefined specifications. In addition, a 2-week repeated dose toxicity test in hRESCAP-tolerized mice was performed. Up to the highest dose tested (1 mg/kg or 750 U/mg daily for 14 days), there were no signs of toxicity observed. The collected data, combined with knowledge obtained from clinically tested bovine ALP (20, 21) resulted in approval from the Medical Ethics Review Board of the Foundation “Evaluation of Ethics in Biomedical Science”, Assen, The Netherlands. A clinical phase 0/phase I first-in-human study with [¹⁴C]-hRESCAP and hRESCAP was performed in accordance with the Declaration of Helsinki and Guideline for Good Clinical Practice.

STUDY DESIGN AND SUBJECT CHARACTERISTICS The clinical study with hRESCAP and [¹⁴C]-hRESCAP was designed as a two-phase study, starting with an open label, single dose study to assess the PK of a microdose of hRESCAP (phase 0), followed by a randomized, double-blind, placebo-controlled, parallel, single ascending dose first-in-human study to assess PK, safety, and tolerability of hRESCAP at various therapeutically relevant doses (phase I). A schematic overview of the study design is shown in Figure 1.

Fifteen (15; phase 0: n=3; phase I: n=12) healthy male volunteers, aged 18-44 years with a body mass index of 18.1-28 kg/m² and a body weight of 64.2-91.5 kg, were included. After providing informed consent, subjects were medically screened within 3 weeks before participation. Among others, exclusion criteria included history of allergy or other inflammatory indications, ALP levels in plasma of <30 U/L or >115 U/L (range of normal physiological concentrations) and clinically relevant abnormal laboratory results, electrocardiogram findings, vital signs, or physical findings that would interfere with the study objectives or subject safety.

PHASE 0 MICRODOSING STUDY WITH [¹⁴C]-HRESCAP After administration of a microdose of [¹⁴C]-hRESCAP to three healthy volunteers, blood samples were

collected at various time points up to 35 days after administration. A direct total ¹⁴C-count analysis was performed on 1.5 µL plasma samples using AMS. In addition, the ALP enzymatic activity of all plasma samples was determined. Because of the endogenous ALP plasma levels of the subjects, administration of a microdose (~44 U total) led to only slightly elevated ALP levels in plasma (Figure 2B, upper panels).

AMS analysis of the plasma samples showed a background radioactivity of 9.62-10.5 mBq/mL, originating from the natural presence of carbon-14. Upon administration of [¹⁴C]-hRESCAP the plasma concentration *versus* time curve exhibited three distinct elimination phases (Figure 2B, and Supplementary Figure S1), similar to the profile previously reported for bovine ALP, in humans and animals (21, 28). The inter-individual differences were negligible. A terminal half-life ($t_{1/2}$) of ~116 h (4.8 days) for hRESCAP was observed, which allowed continuation of the study to phase I (requirement to continue to phase I: $t_{1/2} \geq 2$ days; Figure 1).

PHASE I SINGLE ASCENDING DOSE STUDY OF HRESCAP SUPPLEMENTED WITH MICRODOSE [¹⁴C]-HRESCAP The single intravenous microdose was well tolerated in all healthy male subjects and did not result in clinically significant changes from pre-dose values. In phase I, increasing dosages of 361-5247 µg hRESCAP (~350-5300 enzymatic units, respectively), supplemented with 53 µg [¹⁴C]-hRESCAP (540-710 Bq), were administered. After administration increased ALP enzymatic activity levels in plasma were detected (Figure 2B), again displaying three-phase elimination kinetics. After registration of minor adverse effects (fatigue, headache) at the low dose, the medium dose was reduced by 50% to 1240 µg hRESCAP in total. Overall, the safety assessment showed that hRESCAP was well tolerated at all administered dosages. Administration of hRESCAP did not result in clinically significant changes in physiological parameters (data not shown).

PHARMACOKINETIC ANALYSIS Radioactivity and enzyme activity *versus* time data were first analysed by non-compartmental methods. PK parameters were derived for each subject, and then averaged for each dose group. The results are shown in Table 1. The plasma enzyme activity *versus* time showed an initial concentration (peak plasma concentration (C_{max})) above baseline of 1.5 U/mL and area under the curve (AUC_{0-inf}) above baseline of 66 h*U/mL at the highest dose of 5300 µg hRESCAP (5260 U), an (initial) volume of distribution of 3.1 L, and a $t_{1/2}$ of ~110 h. The dose-normalized parameters remain within a factor of 0.8-1.25, indicating dose-proportional kinetics. No striking differences between radioactivity and enzyme activity were observed. To further substantiate these findings and to

obtain a more detailed interpretation of the PK of hRESCAP, we analysed the data by nonlinear mixed effects modelling. The three-phase elimination was described by a tri-exponential model. In its common interpretation, the compound is dosed in a central compartment (plasma) and equilibrates with two peripheral compartments (extravascular spaces) at different rates. However, for hRESCAP, a more plausible explanation relates to the distinct degrees and patterns of glycosylation displaying different elimination kinetics. Protein analysis of produced hRESCAP showed two prominent peaks, the mass difference of which could be attributed to a glycan. Of the glycosylated hRESCAP, ~20% has a sialylated protein core. Animal studies with non-sialylated ALP demonstrated rapid plasma clearance that could be prevented by asialoprotein being supplemented as competitor for binding to asialoglycoprotein receptor (proprietary data). Human ALPs of different origin (liver, bone and placenta) show different sialylation patterns associated with different plasma residence times. Based on this, we expected that hRESCAP, appearing to be heterogeneous in its degree and pattern of sialylation in the protein analysis, would display a variation in the elimination rates.

The estimated coefficients of the best fit model to the separate and simultaneous data sets are given in Supplementary Tables S2 and S3. The individual and population predictions of plasma radioactivity and enzyme activity (simultaneously) are plotted in Figure 2. The obtained population mean coefficients are consistent with the results of the non-compartmental analysis. The obtained $t_{1/2}$ was 116 h. The population average volume of distribution was 3.2 L with some dependency on body weight, in line with human plasma volume. The within-subject coefficient of variation of background radioactivity and ALP activity in placebos were 1.7% in both cases, with no apparent trend in time (Figure 2). The respective protein fractions that showed different elimination kinetics made up ~40%, 40% and 20% of the dose, and their contributions to the AUC were calculated to be 1.1%, 17% and 82%, respectively (Supplementary Figure 1). The slowly eliminated fraction corresponds to ~20%, which is in line with the fraction of fully sialylated hRESCAP, supporting our interpretation of the observed kinetics.

The model fitted to the radioactivity and enzyme activity *versus* time data separately with and without dose as covariate showed a small but significant difference in the elimination rates λ_1 and λ_2 only for the enzyme activity data ($p=0.0011$ by analysis of variance (ANOVA)). The model fit to the datasets simultaneously with and without quantification method as covariate showed small but significant differences in the protein fraction q_1 and in λ_1 and λ_2 ($p<0.0001$). A possible explanation for the differences between radioactivity and enzyme activity may be that the radiolabels may not have been evenly distributed among the

different protein fractions. The impact of these differences on the dose-corrected AUCs is minor, because of the minimal contributions of these rates to the overall AUC (1.1% and 17%, respectively). This is illustrated in Figure 3, showing that predictions of the enzymatic activity in the phase I ascending dose study based on model fits of the microdose radioactivity data were accurate. Based on the fitted coefficients (Supplementary Table 2), a deviation between microdose and high dose AUC of 8% would be expected. Compared to prediction of human PK from animal data based on allometric scaling, in which predictions within a factor of two are commonly considered acceptable (29), this deviation can be considered very small.

Summarizing these results, the analysis shows that hRESCAP displays dose-proportional PK over the dose range tested, and that the microdose radioactivity levels in healthy volunteers could be used to accurately predict the enzyme activity levels at the intended therapeutic doses.

Discussion

Since the introduction of microdosing studies, there has been discussion on how predictive a microdose can be for the PK at therapeutic doses. Validation studies addressed this issue by selecting well-known small molecule drugs, as well as compounds that failed in traditional phase I clinical trials (9, 30). About 80% of these drugs showed dose-linear PK (9, 30). Consequently, microdosing proved to offer great potential to select the appropriate drug candidates. Although, currently, biologics make up an important part of the research pipelines in the pharmaceutical industry, here the application of microdosing considerably lags behind. Typically for proteins, concern exists about the predictive value of a microdose for the PK at therapeutic doses. Only a very limited number of protein microdosing studies have been performed (31, 32). These showed promising results, but none of these studies were performed in humans. As one of the major advantages of microdosing is the potential to directly obtain human data, an important application area of microdosing had until now been left unaddressed. However, it is important to realize that microdosing cannot automatically be applied to any biological directly. For proteins that show target-mediated disposition, microdosing data in combination with binding affinities determined *in vitro* and physiologically based PK modelling may allow the prediction of the PK at therapeutic levels from a microdose (33).

This first microdosing study with hRESCAP showed dose proportionality, in line with our expectations for this particular NBE, as the protein is endogenously present in the systemic circulation. In this study, microdosing immediately provides an added-value, and these results may encourage the exploration of a wider range of applications of microdosing with AMS to further assess clinical PK parameters at earlier stages of biopharmaceutical development. Additionally, this study demonstrates that a microdose can be used as a safe starting dose of biotherapeutics for first-in-human studies. This particular approach could have been helpful for the study, including the compound TGN1412. The microdose would have been about 100 times lower than was given in the study (17). After this conservative dosing regimen, consequences are minimized as these low drug concentrations will likely not induce toxicological effects, nor impose any radiological risks. Still, the pivotal information will become available relatively early, speeding up overall timelines in drug development.

Another advantage is that microdosing studies can be performed with a relatively low number of subjects (cost reduction of clinical studies). Our data showed almost negligible inter-individual differences in the PK (Figure 2A). In addition, the sensitive detection by AMS allows individuals to be their own controls (e.g. for baseline measurements before hRESCAP dosage), which improves statistical power of the data. The between-subject variation in ALP activity *versus* time was larger than in radioactivity (Figure 2B), but also limited in this study. This may be due to ALP being an endogenous protein and inclusion of subjects with baseline ALP within normal range.

To obtain approval from the regulatory authorities for a microdosing study with a biotherapeutic, limited preclinical studies are required (14-day single dose study one species, rodent, and structure-activity relationships (SAR) assessment) (10). A clear difference with traditional small molecule microdosing studies lies in the incorporation of the carbon-14 label into the molecule of interest, reductive amination *versus* chemical derivatization, respectively. Although the labelling approach is generally applicable for proteins, the product characterization strategy after labelling will be protein-specific. Comprehensive analysis of hRESCAP before and after labelling showed no differences illustrating the feasibility of this approach.

In summary, microdosing holds the promise that selected compounds may be developed more rationally and faster, by the early availability of human PK data. Important concomitant advantages will be significant reductions in costs of drug development and the use of laboratory animals.

FIGURE 1 Study design of the phase 0/phase I first-in-human study with [¹⁴C]-human recombinant placental alkaline phosphatase (hRESCAP).

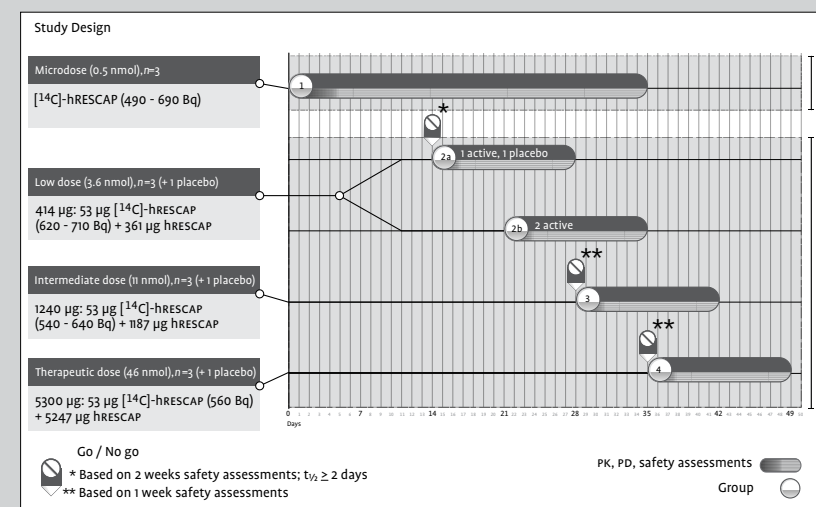


FIGURE 2 Plasma concentration time in individual healthy volunteers after intravenous administration of a microdose of 53 µg [¹⁴C]-human recombinant placental alkaline phosphatase (hRESCAP, 45 U, ~592 Bq) alone (first row of panels), or in combination with increasing doses of unlabelled hRESCAP (subsequent rows of panels, respectively 414, 1240 and 5300 µg or 391, 1224 and 5260 U, in total). The fourth column of panels shows the placebos. Symbols indicate the observed radioactivity in mBq/mL (A) or alkaline phosphatase (ALP) activity in mU/mL (B), solid and dashed curves show the individual and population average simulations by a fitted nonlinear mixed effects model.

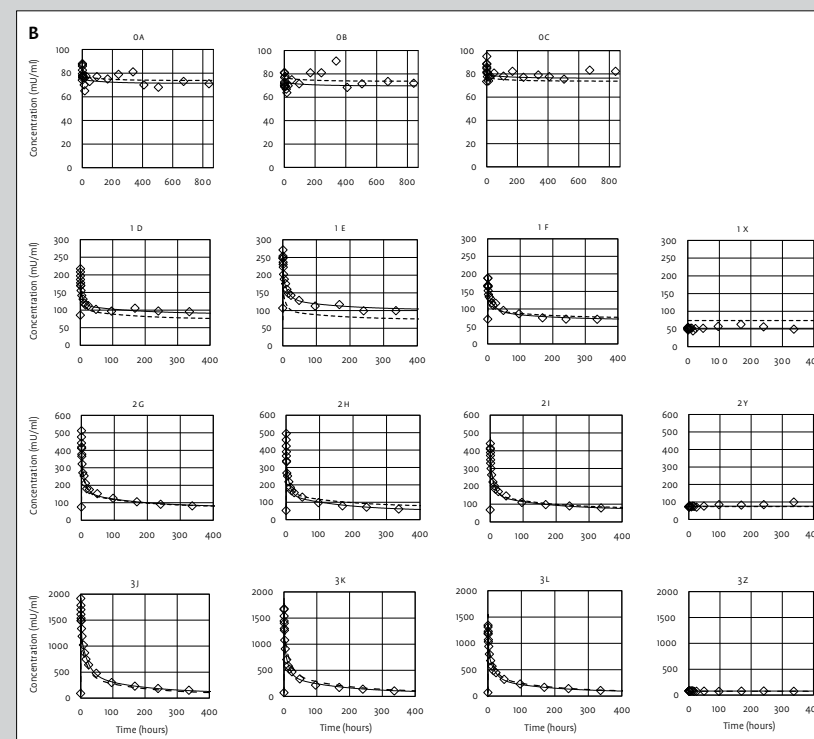
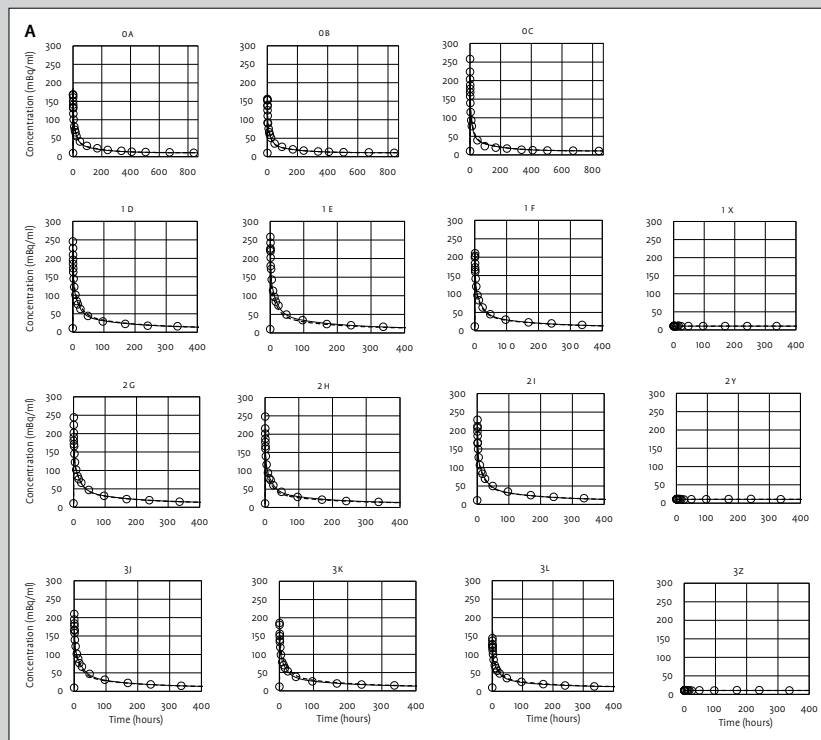


FIGURE 3 A. Observed plasma radioactivity (mean with standard deviation as error bars, in mBq/mL) after a microdose of 557.9 Bq [¹⁴C]-human recombinant placental alkaline phosphatase (hRESCAP, symbols) and fitted population average (curve). B. Observed plasma alkaline phosphatase (ALP) activity (mean with standard deviation as error bars, in mU/mL) after a dose of 391 U (upper panel; 414 µg), 1224 U (middle panel; 1240 µg) and 5260 U (lower panel; 5300 µg). The dotted curve represents model predictions based on the model fit of the microdose radioactivity.

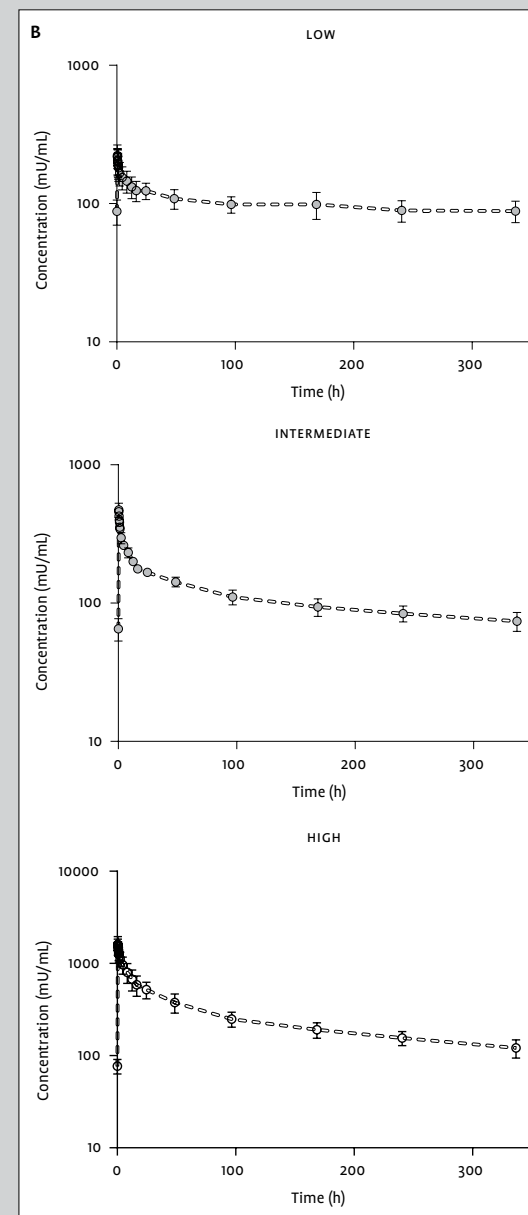
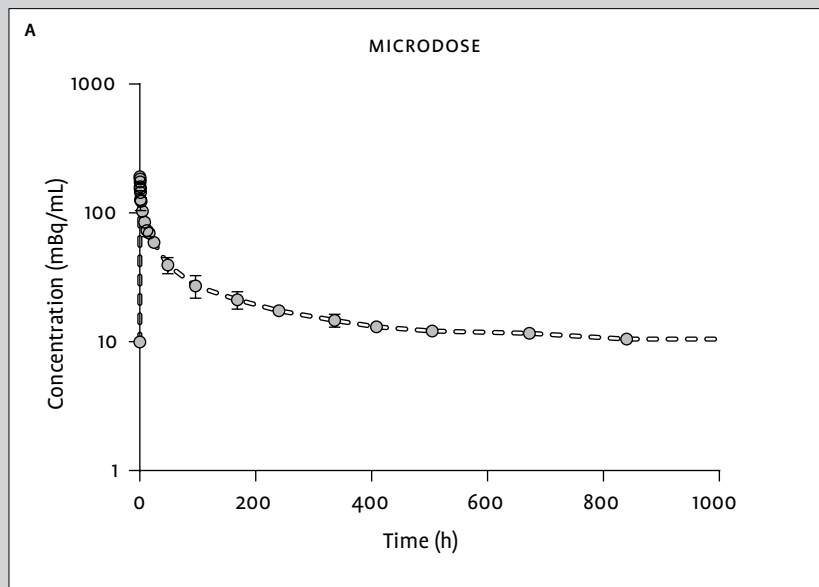


TABLE 1 Summary of pharmacokinetics of hRESCAP, established by non-compartmental analysis unless reported otherwise.

	Microdose	Low	Intermediate	High
Radioactivity (Bq)	556	649	606	558
Background (mBq/mL)	10.0 (4.7)	11.1 (6.0)	11.0 (1.2)	10.3 (8.0)
C _{max} (mBq/mL) ¹	194 (9.6)	208 (12)	226 (13)	180 (20)
C _{max} /Dose	0.35 (9.6)	0.32 (12)	0.37 (13)	0.32 (20)
V _d (L)	2.9 (9.6)	3.1 (12)	2.7 (13)	3.1 (20)
AUC ₀₋₃₃₆ (h*mBq/mL) ¹	6457 (22)	6518 (18)	6820 (5.1)	6225 (21)
AUC _{0-inf} (h*mBq/mL) ¹	7834 (27)	7401 (19)	7630 (6.3)	6984 (23)
AUC ₀₋₃₃₆ /Dose	11 (22)	11 (18)	12 (5.1)	11 (21)
AUC _{0-inf} /Dose	13 (27)	13 (19)	13 (6.3)	12 (23)
t _{1/2} (h)	136 (17)	118 (1.7)	117 (6.6)	119 (6.0)
Enzyme activity (U)	45	391	1224	5260
Baseline (mU/mL)	72.7 (2.6)	90.2 (25)	65.2 (18)	77.2 (18)
C _{max} (mU/mL) ¹	15.3 (35)	127 (6.3)	407 (14.0)	1516 (23)
C _{max} /Dose	0.35 (35)	0.33 (6.3)	0.33 (14)	0.29 (23)
V _d (L)	2.9 (35)	3.0 (6.3)	3.0 (14)	3.4 (23)
AUC ₀₋₃₃₆ (h*mU/mL) ¹	475 ²	3842 (29)	14473 (1.1)	59570 (21)
AUC _{0-inf} (h*mU/mL) ¹	531 ²	4536 (41)	15737 (3.2)	65913 (22)
AUC ₀₋₃₃₆ /Dose	10.7 ²	10 (29)	12 (1.1)	11 (21)
AUC _{0-inf} /Dose	11.9 ²	12 (41)	13 (3.2)	13 (22)
t _{1/2} (h)	108 ²	108 ²	104 (19)	121 (7.2)

1. Maximum concentration (C_{max}) and area under the curves (AUCs) reported are the areas above background radioactivity or baseline alkaline phosphatase (ALP). 2. Estimates based on the model fit are given, as the variation was too high to establish these values reliably by non-compartmental methods. Values reported represent means and coefficients of variation (between brackets) of three subjects in each dose group. V_d: Volume of distribution; t_{1/2}: terminal half-life.

SUPPLEMENTARY MATERIAL

Methods

ANIMAL STUDIES Mice were housed and handled according to guidelines of Utrecht University (Utrecht, The Netherlands), and complying with Dutch and European legislation. Approval of the local Institutional Animal Care and Use Committee was obtained prior to the start of the studies. Female Balb/c mice were obtained from Charles River Laboratories (Wilmington, Massachusetts, USA). All animals were between 5-7 weeks at the start of the experiment (tolerization). Mice were tolerized to human proteins prior to repeated dose toxicity studies. Specifically, mice were daily exposed to ad libitum supplies of supernatants of CAP9 cells expressing hRESCAP, mixed with water for a period of 3 weeks. Next, daily doses of hRESCAP of 0 (placebo), 150 and 750 U/kg body weight were administered interperitoneal for 14 days (*n*=10 mice per group). At day 15, blood was collected by cardiac puncture under isoflurane anaesthesia and mice were killed by cervical dislocation. Gross necropsy was performed and organs were weighed. Blood was sampled in heparine coated vials and analysed with a laser-based haematology analyser (Advia 2120i, Siemens Medical Solutions Diagnostics GmbH, Erfurt, Germany) at the University Veterinary Diagnostic Laboratory (UVDL), Utrecht University (Utrecht, The Netherlands). Another part of the blood samples was centrifuged, and plasma was analysed for activity of aspartate aminotransferase (ASAT), alanine aminotransferase (ALAT), gamma glutamyl transferase (GGT) and alkaline phosphatase (AP) at the UVDL by a UniCel DxC-600 analyser (Beckman-Coulter Inc. USA).

No toxicity signs or abnormalities in body or organ weight were observed in any of the different treatment groups. Also, no significant differences were observed between the placebo and the low and high dose groups in the haematological data (not shown). GGT activity was below the detection limit of 5 U/L in all samples. In transaminase activity of ALAT and ASAT no significant differences between test and control groups were observed. As expected, the AP activity was significantly and dose-related increased in the groups of mice daily treated with 150 and 750 IU/kg body weight.

REDUCTIVE AMINATION To 925 µL of a 0.2 M borate (Na₂B₄O₇-10H₂O, Sigma-Aldrich, St. Louis, MO) buffer 125 µL of hRESCAP solution (1.4 mg/mL) was added while keeping the reaction mixture at 0°C. Subsequently, 60 µL [¹⁴C]-formaldehyde

(0.01% in water; ARC, St. Louis, Missouri, USA) was added, and the reaction was started by addition of 100 μL of a 1 M sodium cyanoborohydride (NaCNBH_3 ; Sigma-Aldrich, St. Louis, Missouri, USA), under continuous shaking. After 10, respectively 40 minutes, 100 μL portions of 1 M NaCNBH_3 were added. After another incubation of 1 hour the reaction was quenched by the addition of 100 μL glycine (10% solution in water). After 10 minutes, the reaction mixture was diluted to a volume of 2.5 mL with a 0.9% sodiumchloride solution (Fresenius Kabi, Zeist, The Netherlands) and purified with a PD-10 column (GE Healthcare, Little Chalfont, United Kingdom). Subsequently, the protein containing fraction (2.5 mL) was further diluted with 15 mL saline. Of this solution, 15 mL was filtrated using a 0.2 μm sterile GV filter (Millipore, Billerica, Massachusetts, USA) and directly collected into a closed container system. The remaining solution was used for quality control of the produced batch.

LC+AMS 25 μL plasma was diluted to 175 μL with Tricine pH 5.5. The total volume (200 μL) was injected on the HPLC (Surveyor). Chromatographic conditions are specified in Supplementary Table S4. The fraction in which enzymatically active ALP eluted had a total volume of 7.5 mL. 1.5 mL of this fraction was washed twice with 1.5 mL MilliQ using Amicon filter devices with 10 kDa cut off (EMD Millipore, Billerica, Massachusetts, USA). The sample was evaporated to dryness and re-dissolved in 50 μL MilliQ after which it was subsequently transferred to a tin foil cup. Again the sample was evaporated to dryness and analysed by automated CO_2 combustion AMS analysis.

FIGURE S1 Deconvolution of the plasma radioactivity-time curve into three distinct elimination phases of HRESCAP (as shown in Figure 2 on page 28).

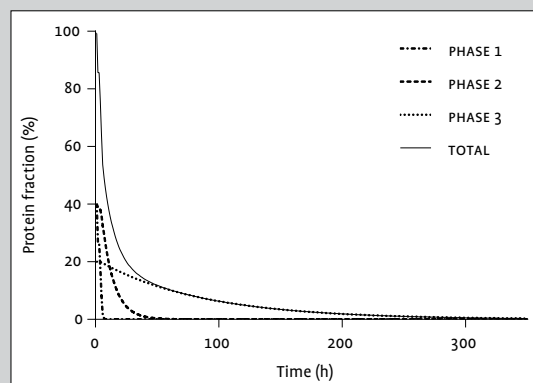


TABLE S1 Parameters, including specification criteria for [^{14}C]-HRESCAP. All produced batches met the predefined criteria.

Parameter	Specification
Appearance	Clear
pH	3.5-6.5
Radiochemical purity (HPLC)	$\geq 95\%$
Chemical purity (HPLC)	OK
Radiochemical identity (HPLC)	OK
Enzymatic Activity	$\geq 70\%$
Protein Concentration	7-13 $\mu\text{g}/\text{mL}$
Aggregation (SEC-UV)	0%
Stability (SEC-UV)	OK

HPLC: high-performance liquid chromatography; SEC-UV: size-exclusion chromatography-ultraviolet.

TABLE S2 Parameter estimates corresponding to the separate best fit models of radioactivity versus time and enzyme activity versus time. Values represent estimated population means (fixed effects); between brackets the between-subject coefficients of variation are given for parameters showing significant random effects.

Parameter	Radioactivity vs. time	Enzyme activity vs. time
C_0 (mBq/mL; mU/mL)	10.5	73.9 (17)
V_d (intercept) (L)	3.15 (10)	3.34 (15)
$\sim \text{BW}$	0.026 $\times\{\text{BW}-78.3\}$	0.043 $\times\{\text{BW}-78.3\}$
Q_1	0.41	0.36
λ_1 (intercept) (h^{-1})	0.92	2.0
$\sim \text{Dose}$	-	-0.00019 $\times\text{D}$
Q_2	0.42	0.41
λ_2 (intercept) (h^{-1})	0.056 (4.5)	0.11 (13)
$\sim \text{Dose}$	-	-0.00011 $\times\text{D}$
Q_3	0.17	0.23
λ_3 (h^{-1})	0.0060 (1.9)	0.0064

Q_i : fixed but unknown proportions of the dose corresponding to the different protein fractions; BW: body weight; C_0 : background radioactivity; λ : elimination rate constant; V_d : volume of distribution; vs.: versus.

TABLE S3 Parameter estimates corresponding to the simultaneous fit of radioactivity versus time and enzyme activity versus time. Values represent estimated population means (fixed effects); between brackets the between-subject coefficients of variation are given for parameters showing significant random effects. The parameters in the middle column did not differ significantly between the two methods.

Parameter	Radioactivity vs. time	Enzyme activity vs. time
C ₀ (mBq/mL; mU/mL)	10.5	73.8 (18)
V _d (intercept) (L)	3.20 (11)	0.028×{BW-78.3}
~ BW		
α ₁	0.42	0.38
λ ₁ (intercept) (h ⁻¹)	0.80	1.92 (66)
~ Dose	-	-0.00016×D
α ₂	0.41	
λ ₂ (intercept) (h ⁻¹)	0.052 (3.7)	0.10 (14)
~ Dose	-	-0.00011×D
α ₃	0.17	0.21
λ ₃ (h ⁻¹)	0.0060	

α: fixed but unknown proportions of the dose corresponding to the different protein fractions; BW: body weight; C₀: background radioactivity; λ: elimination rate constant; V_d: volume of distribution; vs.: versus.

TABLE S4 Chromatographic conditions.

Time (min)	Solvent A (%)	Solvent B (%)	Solvent C (%)	Solvent D (%)	Flow rate (mL/min)
0	100	0	0	0	0.75
20	100	0	0	0	0.75
20.10	0	0	0	100	0.75
30	0	0	0	100	0.75
30.10	0	100	0	0	0.75
45	0	100	0	0	0.75
45.10	0	0	100	0	0.75
75	0	0	100	0	0.75
75.10	100	0	0	0	0.75
105	100	0	0	0	0.75

Solvent A: 10 mM Trizine pH 5.2-5.8; Solvent B: 10 mM K₂HPO₄ pH 8.5; Solvent C: 0.5 M NaOH; Solvent D: MilliQ.

REFERENCE LIST

- Pharma E. The NASDAQ Biotech Index Up Close, Surveying Tomorrow's BioPharma Landscape. 2012.
- Bugelski PJ, Treacy G. Predictive power of preclinical studies in animals for the immunogenicity of recombinant therapeutic proteins in humans. *Curr Opin Mol Ther.* 2004;6(1):10-6.
- Wierda D, Smith HW, Zwickl CM. Immunogenicity of biopharmaceuticals in laboratory animals. *Toxicology.* 2001;158(1-2):71-4.
- Ledford H. Translational research: 4 ways to fix the clinical trial. *Nature.* 2011;477(7366):526-8.
- Bae SK, Shon JH. Microdosing studies using accelerated mass spectrometry as exploratory investigational new drug trials. *Arch Pharm Res.* 2011;34(11):1789-98.
- Garner RC, Lappin G. The phase 0 microdosing concept. *Br J Clin Pharmacol.* 2006;61(4):367-70.
- Henderson PT, Pan CX. Human microdosing for the prediction of patient response. *Bioanalysis.* 2010;2(3):373-6.
- Johnson G. Using microdosing to enhance development. *Genetic Engineering and Biotechnology News.* 2008;28(19).
- Lappin G, Kuhn W, Jochemsen R, Kneer J, Chaudhary A, Oosterhuis B, et al. Use of microdosing to predict pharmacokinetics at the therapeutic dose: experience with 5 drugs. *Clin Pharmacol Ther.* 2006;80(3):203-15.
- European Medicines Agency (EMA) – Position Paper on nonclinical safety studies to support clinical trials with a single microdose – CPMP/SWP/2599/02/ Rev1. 2004.
- US Food and Drug Administration (FDA) – Guidance for Industry, Investigators and Reviewers – Exploratory IND Studies. 2006.
- European Medicines Agency (EMA) – Guideline on Strategies to Identify and Mitigate Risks for First-in-Human Clinical Trials with Investigation Medicinal Products – EMEA/CHMP/SWP/28367/07. 2007.
- European Medicines Agency (EMA) – Note for Guidance on Non-Clinical Safety Studies for the Conduct of Human Clinical Trials and Marketing Authorization for Pharmaceuticals – CPMP/ICH/286/95. 2008.
- Salehpour M, Possnert G, Bryhni H. Subattomole sensitivity in biological accelerator mass spectrometry. *Anal Chem.* 2008;80(10):3515-21.
- van Duijn E, Sandman H, Grossouw D, Mocking JA, Coulier L, Vaes WH. Automated combustion accelerator mass spectrometry for the analysis of biomedical samples in the low attomole range. *Anal Chem.* 2014;86(15):7635-41.
- Vogel JS, Grant PG, Buchholz BA, Dingley K, Turteltaub KW. Attomole quantitation of protein separations with accelerator mass spectrometry. *Electrophoresis.* 2001;22(10):2037-45.
- Muller PY, Brennan FR. Safety assessment and dose selection for first-in-human clinical trials with immunomodulatory monoclonal antibodies. *Clin Pharmacol Ther.* 2009;85(3):247-58.
- Rezende AA, Pizauro JM, Ciancaglini P, Leone FA. Phosphodiesterase activity is a novel property of alkaline phosphatase from osseous plate. *Biochem J.* 1994;301 (Pt 2):517-22.
- Poelstra K, Bakker WW, Klok PA, Hardonk MJ, Meijer DK. A physiologic function for alkaline phosphatase: endotoxin detoxification. *Lab Invest.* 1997;76(3):319-27.
- Kats S, Brands R, Hamad MA, Seinen W, Scharnhorst V, Wulkan RW, et al. Prophylactic treatment with alkaline phosphatase in cardiac surgery induces endogenous alkaline phosphatase release. *Int J Artif Organs.* 2012;35(2):144-51.
- Kats S, Brands R, Seinen W, de Jager W, Bekker MW, Hamad MA, et al. Anti-inflammatory effects of alkaline phosphatase in coronary artery bypass surgery with cardiopulmonary bypass. *Recent Pat Inflamm Allergy Drug Discov.* 2009;3(3):214-20.
- Keck BD, Ognibene T, Vogel JS. Analytical validation of accelerator mass spectrometry for pharmaceutical development. *Bioanalysis.* 2010;2(3):469-85.
- Klein M, Vaes WHJ, Fabrick B, Sandman H, Mous DJW, Gott dang A. The 1 MV multi-element AMS system for biomedical applications at the Netherlands Organization for Applied Scientific Research (TNO). *Nuclear Instruments and Methods in Physics Research B.* 2013;294:14-7.
- Higton D, Young G, Timmerman P, Abbott R, Knutsson M, Svensson LD. European Bioanalysis Forum recommendation: scientific validation of quantification by accelerator mass spectrometry. *Bioanalysis.* 2012;4(22):2669-79.
- Stuiver M. Business meeting – International Agreements and the Use of the New Oxalic Acid Standard. *Radiocarbon.* 1983;25(2):793-5.
- Xu XM, Kosh MS, Druffel-Rodriguez KC, Trumbore SE, Southon JR. Is the consensus value of Anu sucrose (IAEA C-6) too high? *Radiocarbon.* 2010;52(3):866-74.
- Pinheiro J, Bates D, DebRoy S, Sarkar D, Team. *TRDC. NLME: Linear and nonlinear mixed effects models.* R Foundation for Statistical Computing version 3 1-100. 2011.

- 28 Beumer C, Wulferink M, Raaben W, Fiechter D, Brands R, Seinen W. Calf intestinal alkaline phosphatase, a novel therapeutic drug for lipopolysaccharide (LPS)-mediated diseases, attenuates LPS toxicity in mice and piglets. *J Pharmacol Exp Ther*. 2003;307(2):737-44.
- 29 European Microdosing AMS Partnership Programme (EUMAPP). Outcomes from EUMAPP – A study comparing *in vitro*, *in silico*, microdose and pharmacological dose pharmacokinetics. 2012 2012.
- 30 Lappin G, Shishikura Y, Jochemsen R, Weaver RJ, Gesson C, Brian HJ, et al. Comparative pharmacokinetics between a microdose and therapeutic dose for clarithromycin, sumatriptan, propafenone, paracetamol (acetaminophen), and phenobarbital in human volunteers. *Eur J Pharm Sci*. 2011;43(3):141-50.
- 31 Lamers RJ, de Jong AF, Lopez-Gutierrez JM, Gomez-Guzman J. Iodine-129 microdosing for protein and peptide drug development: erythropoietin as a case study. *Bioanalysis*. 2013;5(1):53-63.
- 32 Salehpour M, Ekblom J, Sabetsky V, Hakansson K, Possnert G. Accelerator mass spectrometry offers new opportunities for microdosing of peptide and protein pharmaceuticals. *Rapid Commun Mass Spectrom*. 2010;24(10):1481-9.
- 33 Sugiyama Y, Yamashita S. Impact of microdosing clinical study -- why necessary and how useful? *Adv Drug Deliv Rev*. 2011;63(7):494-502.

CHAPTER 3

Recombinant human serum amyloid p in healthy volunteers and patients with pulmonary fibrosis

Pulmonary Pharmacology & Therapeutics, 2013 Dec, 26(6):672-676

M.R. Dillingh, B. van den Blink, M. Moerland, M.G.J. van Dongen, M. Levi, A. Kleinjan, M.S. Wijnsbeek, M.L. Luper Jr., D.M. Harper, J.A. Getsy, H.C. Hoogsteden, J. Burggraaf

ABSTRACT

PRM-151, recombinant human pentraxin-2 also referred to as serum amyloid P (SAP), is under development for treatment of fibrosis. A first-in-human trial was performed to assess the safety, tolerability, and pharmacokinetics of single ascending intravenous doses of PRM-151 administered to healthy subjects, using a randomized, blinded, placebo controlled study design. Each cohort included three healthy subjects (PRM-151:placebo; 2:1). SAP levels were assessed using a validated enzyme linked immunoassay method, non-discriminating between endogenous and exogenous SAP. At a dose level of 10 mg/kg, at which a physiologic plasma level of SAP was reached, two additional healthy volunteers and three pulmonary fibrosis (PF) patients were enrolled enabling comparison of the pharmacokinetic SAP profile between healthy volunteers and PF patients. In addition, the percentage of fibrocytes (CD45+/Procollagen-1+ cells) in whole blood samples was assessed to demonstrate biological activity of PRM-151 in the target population.

PRM-151 administration was generally well tolerated. In two pulmonary fibrosis patients non-specific, transient skin reactions (urticaria and erythema) were observed. PRM-151 administration resulted in a 6- to 13-fold increase in mean baseline plasma SAP levels at dose levels of 5, 10, and 20 mg/kg. The estimated terminal half-life ($t_{1/2}$) of PRM-151 in healthy volunteers was 30 h. Pharmacokinetic profiles were comparable between healthy volunteers and PF patients. PRM-151 administration resulted in a 30-50% decrease in fibrocyte numbers 24 h post-dose. This suggests that administration of PRM-151 may be associated with a reduction of fibrocytes in PF patients, a population for which current pharmacotherapeutic options are limited. The pharmacological action of PRM-151 should be confirmed in future research.

Introduction

Idiopathic pulmonary fibrosis (IPF) is the most common idiopathic interstitial pneumonia (IIP) (1). It is a chronic, progressive, irreversible and lethal disease that generally occurs in middle-aged and elderly adults. IPF is a disease of unknown cause although recurrent epithelial injury and aberrant wound healing are thought to lead to fibrosis. Symptoms of IPF include chronic and progressive exertional dyspnoea, cough, a poor quality of life and eventually death. Therapeutic options are limited for all forms of pulmonary fibrosis (2), and the only treatment proven effective in prolonging survival is lung transplantation with a post-transplantation 5-year survival for IPF patients of approximately 44% (3). Efficacious therapy for pulmonary fibrosis remains elusive (4), and particularly pharmacotherapeutic options are limited.

In IPF, monocyte-derived cells play a central role in the fibrotic scarring process, as they take part in the production of (excess) collagen and cytokines such as platelet derived growth factor (PDGF), transforming growth factor- β (TGF- β), interleukin-1 (IL-1), monocyte chemoattractant protein-1 (MCP-1) and tumour necrosis factor- α (TNF- α) (5-7). The fibrocyte is a unique mesenchymal progenitor cell that differentiates from monocytes, and may be an important source of (myo) fibroblasts during tissue repair and tissue remodelling (8-10). Elevated levels of fibrocytes are associated with increased fibrosis and adverse clinical outcomes. The mean survival of IPF patients with fibrocyte counts exceeding 5% of total blood leukocytes was 7.5 months compared with 27 months for IPF patients with lower fibrocyte counts (11). Therefore, the fibrocyte may be a target for therapy in IPF, with fibrocyte counts as possible biomarker (10, 12).

The differentiation of circulating monocytes into fibrocytes (13-15) and pro-fibrotic (M2) macrophages (16) is controlled by serum amyloid P (SAP, also called pentraxin-2, PTX-2), a naturally occurring protein that circulates in the bloodstream with a crucial role in regulating wound healing (17). It has been shown that maintaining an elevated level of SAP in blood or locally at a site of injury can prevent excess scarring and the progression of fibrosis. Indeed, exogenous administration of SAP has been shown to reduce fibrosis in various animal fibrosis models such as in rodent models of ischemia reperfusion injury (18), bleomycin-induced lung fibrosis and lung fibrosis mediated by TGF- β overexpression (19), by decreasing the numbers of fibrocytes and pro-fibrotic M2-macrophages (15, 19, 20). The decreased accumulation of fibrocytes by SAP might be due to reduced leukocyte recruitment via lowering the levels of inflammatory cytokines (15).

In patients with IPF, the SAP level has been implicated to correlate with lung function (19). Furthermore, SAP directly inhibited M2-macrophage differentiation of monocytes into a pro-fibrotic phenotype (19). Taken together, these data suggest that the targeting of pro-fibrotic macrophages and fibrocytes by SAP-directed therapies might be a reasonable approach to the treatment of IPF. PRM-151, the recombinant form of human SAP (rhSAP), is such a compound that could potentially be used to prevent, treat, and reduce fibrosis. Preclinical data using human serum-derived SAP and PRM-151 demonstrated a potent anti-fibrotic activity of SAP in models of lung injury, skin injury, kidney injury and radiation-induced injury (15-21). We performed a first-in-human (FIH) trial to provide an initial assessment of the safety, tolerability, and pharmacokinetics (PK) of PRM-151 after administration of single intravenous doses. Importantly, a rational study design was chosen, consisting of 1) an efficient single ascending dose part in small cohorts of healthy subjects to assess the safety, tolerability, and pharmacokinetics of PRM-151, aiming to cover a range of PRM-151 doses resulting in plasma SAP levels with expected anti-fibrotic activity, and 2) an expanded cohort at a PRM-151 dose level that resulted in a desired SAP plasma level in the first study part. In this second study part two additional healthy volunteers and three pulmonary fibrosis (PF) patients were included, which not only allowed an initial comparison of the compound's pharmacokinetic and safety profile between healthy subjects and fibrosis patients, but also allowed the selection of a suitable biomarker for initial demonstration of biological activity of PRM-151 in PF patients. Especially the latter is of crucial importance for modern drug development, as the availability of such a pharmacodynamic measure will enable a more rational and efficient future development of the compound in the target population.

Methods

SUBJECTS Single ascending doses of PRM-151 were administered as an intravenous infusion to 26 healthy volunteers. In addition, three PF patients (one female, two males) were enrolled to compare pharmacokinetics of PRM-151 between healthy volunteers and the target population. One patient had a diagnosis of IPF according to the current European Respiratory Society/American Thoracic Society consensus statement (22) and two other (related) patients were diagnosed with Familial Interstitial Pneumonia. In the PF patients, fibrocytes were assessed as a pharmacodynamic parameter to demonstrate biological activity of PRM-151 early in the clinical development.

The healthy volunteers were aged 18-53 years (inclusive) and the PF patients were aged 29-72 years (inclusive), all subjects with a body mass index of 18-33 kg/m² and a body weight \geq 50 kg. The use of any over-the-counter drugs, including herbal supplements (except for the occasional use of paracetamol and vitamins \leq 100% of the recommended daily allowance) within 72 h before study day 1 was prohibited.

After signing an informed consent, subjects were medically screened within 3 weeks before test article administration. Exclusion criteria for healthy volunteers included history of amyloidosis, any active inflammatory condition and screening electrocardiogram (ECG) conduction intervals that were not within the gender specific normal range (QTc male <430 ms and females <450 ms). Exclusion criteria for PF patients included forced vital capacity (FVC) <45% predicted and history of amyloidosis, connective tissue disorder, chronic obstructive pulmonary disease (COPD), cystic fibrosis, tuberculosis or sarcoidosis. The study was conducted in accordance with the Declaration of Helsinki and Guideline for Good Clinical Practice, and was approved by the Ethics Review Board of the Leiden University Medical Centre, The Netherlands.

STUDY DESIGN This was a randomized, blinded, placebo controlled, inpatient/outpatient, sequential-group study of ascending single doses of 0.1, 0.25, 0.5, 1, 2, 5, 10, and 20 mg/kg PRM-151 (or placebo), administered to healthy subjects as a continuous intravenous infusion over 30 min under fasting conditions. Each cohort included three healthy subjects. Within each cohort, two subjects received PRM-151 and one subject received placebo. The subjects included in the expansion cohort (two healthy subjects, three patients) received a single continuous intravenous infusion of 10 mg/kg PRM-151 over 30 min under fasting conditions in an open label, inpatient/outpatient portion of the study. The starting dose for this FIH study was selected according to the US Food and Drug Administration (FDA) guidelines and based on the no-observed-adverse-effect level (NOAEL) in rats and cynomolgus monkeys. The selected PRM-151 dose range was based on the pharmacokinetic behaviour of PRM-151 as observed in preclinical models and an anticipated therapeutic PRM-151 dose that would result in a systemic SAP level of at least twice the normal circulating level, expected to result in anti-fibrotic activity as based on animal studies.

PHARMACOKINETIC ANALYSIS The concentrations of PRM-151 in plasma were determined using a validated enzyme linked immunoassay (ELISA) method (Charles River Laboratories). This validated analytical method did not differentiate

between PRM-151 and endogenous human SAP. As a result, plasma concentrations measured in day 1 pre-dose (0 h) samples were a measure of baseline endogenous SAP levels and all the plasma concentrations obtained post-dose (at 0.5, 0.75, 1, 1.5, 2, 3, 4, 6, 8, 12, 16, 24, 30, 36, 48, 72, 96 h) measured endogenous SAP plus PRM-151 levels. For pharmacokinetic analysis, the baseline SAP concentration was subtracted from all post-dose concentrations to generate baseline-corrected PRM-151 plasma concentrations. Baseline-corrected PRM-151 values that were negative were assumed to be zero. A non-compartmental analysis PK method was used to analyse the baseline-corrected plasma concentrations of PRM-151.

PHARMACODYNAMIC ANALYSIS The pharmacodynamic effect of PRM-151 was investigated in three PF patients by assessing the percentage of fibrocytes (CD45+/Procollagen-1+ cells) in whole blood samples collected before, 24 h and 3 weeks after the administration of PRM-151. Briefly, Ficoll isolated peripheral blood mononuclear cells (PBMCs) were stored at -150°C until use. After thawing, cells were washed twice, resuspended in RPMI 1640 culture medium, supplemented with 10% fetal calf serum (FCS), 50 µg/mL gentamycin (GIBCO) and cultured with lipopolysaccharide (LPS, 1 µg/mL Sigma O26:b6) for 48 h at 37°C and 5% CO₂. Cells were then stained with biotinylated anti-CD45 and streptavidin APC-CY7/efluor-780 (eBioscience). After paraformaldehyde fixation and saponin permeabilization, intracellular staining was performed with anti-Rat Procollagen-1 (Millipore) and Goat anti Rat Qdot® 605 (Molecular Probes Life Technologies). Fixable Aqua Dead Cell Stain kit (Invitrogen, Molecular Probes) was used as a live/dead marker. Flow cytometry was performed using the LSRII Becton Dickinson fluorescence activated cell sorter (FACS) machine with DIVA™ software, analysis was performed with Flowjo Software.

Results

SAFETY Only mild and transient adverse events (AEs) were observed and these were equally distributed between PRM-151 and placebo treatment. In one of the PF patients, three circumscribed non-specific urticarial lesions were observed during drug administration. The urticaria resolved spontaneously within 2 h upon stopping the infusion. There were no signs of anaphylaxis or dyspnoea or changes in blood pressure, heart rate, saturation or taste. A second PF patient experienced a non-specific skin erythema 5 days after dosing, which resolved spontaneously.

PHARMACOKINETIC RESULTS, HEALTHY VOLUNTEERS AND PF PATIENTS The mean baseline plasma concentration of SAP in the healthy volunteers was 20.4 ± 6.7 µg/mL. Based on the observations in healthy volunteers (periodic sampling of plasma SAP concentrations over a 24 h period prior to dosing, and subjects receiving placebo treatment), there was no indication for a significant diurnal rhythm in endogenous plasma SAP concentrations. Administration of PRM-151 doses of 2, 5, 10, and 20 mg/kg resulted in a distinct increase over baseline SAP levels, lasting up to 24 h (2 mg/kg) and 72 h (5, 10 and 20 mg/kg) after administration of study medication. At a dose level of 20 mg/kg, maximal plasma SAP concentration was approximately 13 times higher than the measured mean baseline concentration. The mean baseline plasma SAP concentration in PF patients was 15.0 ± 7.5 µg/mL. Pharmacokinetic profiles of healthy volunteers and PF patients receiving 10 mg/kg SAP were comparable (Figure 1). However, it should be noted that patient sample number was small and individual SAP concentration-time profiles were variable between patients (data not shown). As a result, no reliable t_{1/2} of PRM-151 could be estimated in PF patients. Calculated pharmacokinetic parameters corrected for individual baseline SAP levels for healthy volunteers (three highest dose levels) and PF patients (10 mg/kg) are provided in Table 1. At a comparable dose level, the mean maximum concentration (C_{max}, µg/mL) of PRM-151 was similar between the two study populations (healthy volunteers, 145 ± 24.8 versus PF patients, 115 ± 31.1). The estimated t_{1/2} of PRM-151 in healthy volunteers was 30 h.

PHARMACODYNAMIC RESULTS Fibrocytes (CD45+/procollagen-1+ cells) were identified in PBMCs collected from the PF patients (Figure 2). Before administration of PRM-151, 1.5-3.3% of all PBMCs consisted of CD45+/procollagen-1+ cells. At 24 h after PRM-151 administration, the percentage of fibrocytes was diminished in all three PF patients by 30-50%. At day 22, the number of fibrocytes was still reduced in two subjects, whereas for the third subject the number returned to baseline levels.

Discussion

PRM-151, recombinant human SAP, is being developed as a novel anti-fibrotic agent. PRM-151 could attenuate monocyte differentiation into M2-macrophages and fibrocytes, and thus be a potential treatment for a variety of fibrotic diseases such as pulmonary fibrosis, scleroderma, cirrhosis, and cardiac fibrosis.

We performed an FIH dose escalation study to provide an initial evaluation of PRM-151 tolerability, safety and pharmacokinetics in healthy volunteers. Importantly, we also included a small cohort of pulmonary fibrosis patients to allow comparison of PRM-151 pharmacokinetics between healthy volunteers and patients, and early assessment of biological activity of PRM-151 in the target population.

Single intravenous doses of PRM-151 (10 mg/kg PRM-151 administered in PF patients, and up to 20 mg/kg in healthy volunteers) were well tolerated. Study drug administration did not raise any serious safety concerns and did not result in any clinically significant changes in blood or urinary laboratory parameters, nor in vital signs or ECG recordings. All reported adverse events were mild and transient and did not require medical intervention. The most common adverse events were fatigue and headache. Adverse events were equally distributed between PRM-151 and placebo treated patients, suggesting that these adverse events were not related to test article. Neither the nature nor the frequency of reported AEs increased with increasing doses of PRM-151. In one PF patient, a mild allergic reaction (urticaria) developed which resolved spontaneously.

The pharmacokinetics of PRM-151 was well-comparable between healthy volunteers and PF patients. The mean baseline plasma concentrations of SAP measured in the healthy volunteers and PF patients included in this study were 20.4 ± 6.7 $\mu\text{g/mL}$ and 15.0 ± 7.5 $\mu\text{g/mL}$, respectively. These values are consistent with SAP levels reported in literature (19, 23). Interestingly, Murray et al. demonstrated a reduction of plasma SAP levels in IPF patients correlated with disease severity (19), underlining the potency of circulating SAP levels as a therapeutic target. In our study, administration of 5, 10 and 20 mg/kg PRM-151 to healthy subjects resulted in peak plasma concentrations that were almost 6-13 times higher than the mean baseline plasma SAP levels. Administration of 10 mg/kg PRM-151 to PF patients resulted in a 9-fold increase in mean baseline SAP level, indicating that circulating SAP levels can successfully be raised by PRM-151 treatment.

Next, we explored whether an increase in circulating SAP could influence the prevalence of monocyte-derived cell types that play a key role in fibrosis, or their soluble markers. SAP inhibits the differentiation of monocytes into M2-macrophages and fibrocytes (13-16). In three PF patients, we investigated the effect of PRM-151 treatment on the proportion of fibrocytes, as assessed by FACS analysis (CD45+/procollagen-1+ cells). Before PRM-151 treatment, we observed PBMC fibrocyte proportions of 1.5-3.3%. This is in line with results reported in literature for patients with stable IPF: in 51 patients, an average fibrocyte count of $2.72 \pm 0.34\%$ was observed (11). The same research group reported an average fibrocyte count of $1.0 \pm 0.12\%$ in a control group of seven healthy volunteers. Administration of

PRM-151 resulted in a 30-50% reduction in the percentage of fibrocytes (24 h post-dose). We cannot exclude the possibility that the presence of LPS in the culture medium may have influenced our results, however, an earlier report did not show significant effects of *Escherichia coli*-derived LPS on fibrocyte differentiation in a PBMC culture (24). Although the number of subjects was small, these results indicate a potential beneficial effect of PRM-151 in patients with elevated numbers of fibrocytes.

The minimum target therapeutic dose of PRM-151 to induce anti-fibrotic activity was estimated to be approximately double the normal circulating concentration, based on preclinical animal studies. This indicates that the selected dose level of 10 mg/kg in our study, resulting in a 9-fold increase of mean baseline SAP level and the associated decrease in fibrocyte number, might be unnecessarily high to induce the intended pharmacological effect. This should be confirmed or invalidated in future clinical studies.

In conclusion, we demonstrated that single intravenous doses of PRM-151 were generally well tolerated in healthy volunteers and a small group of PF patients. The administration of PRM-151 resulted in a 6- to 13-fold increase in circulating SAP levels at the highest dose levels tested. Circulating SAP levels remained elevated for a considerable period of time. Pharmacokinetic behaviour of PRM-151 did not differ between PF patients and healthy volunteers. Importantly, our data suggest that administration of PRM-151 may be associated with a reduction of fibrocytes in PF patients. Given the fact that the patient number was small, it is important that the pharmacological action of PRM-151 is confirmed in a multiple ascending dose study in IPF patients in the near future.

FIGURE 1 Mean plasma concentration-time profiles in healthy volunteers (A; n=5) and pulmonary fibrosis patients (B; n=3), with standard deviation as error bars. SAP: serum amyloid P.

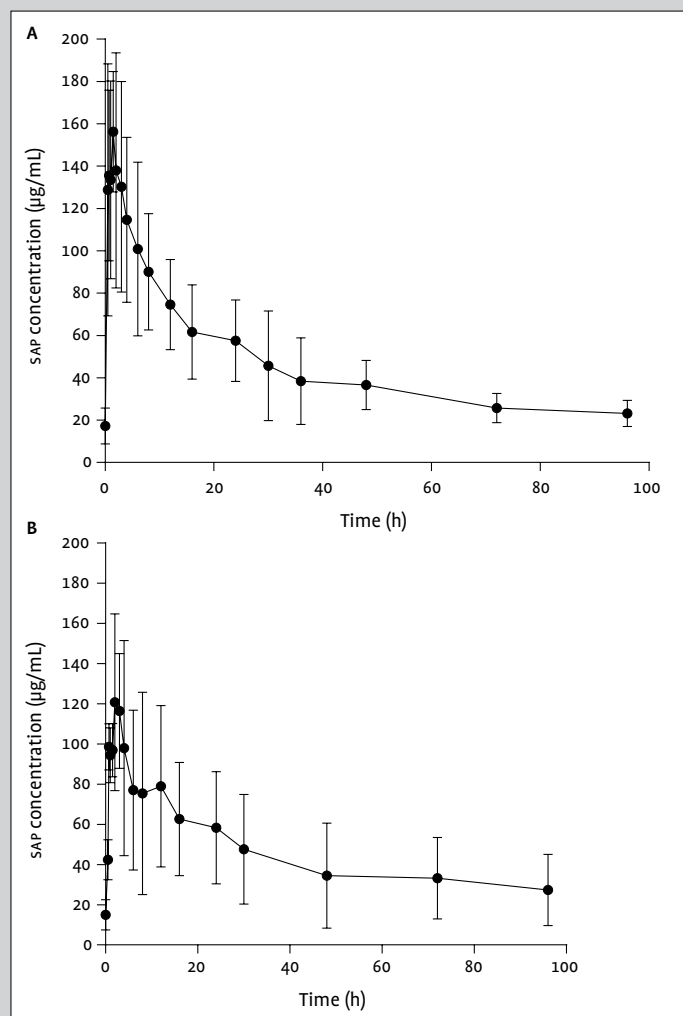


FIGURE 2 Effect of PRM-151 on fibrocytes in pulmonary fibrosis patients.

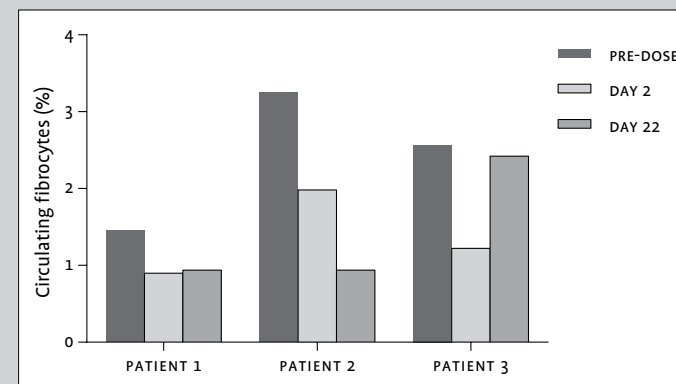


TABLE 1 Pharmacokinetic parameters in healthy volunteers and pulmonary fibrosis patients.

Pharmacokinetic parameter	Healthy volunteers			PF patients n=3
	5 mg/kg n=2	10 mg/kg n=4	20 mg/kg n=2	
t_{max} (h)	0.75 ± 0.354	1.25 ± 0.645	1.25 ± 0.354	1.50 ± 0.500
C_{max} (µg/mL)	89.6 ± 22	145 ± 24.8	243 ± 60.2	115 ± 31.1
$t_{1/2}$ (h)	ND	29.7 ± 7.66	20.3 ± 18.42	ND
AUC_t (µg*h/mL)	1721 ± 378	2672 ± 1128	5547 ± 1301	2943 ± 2025

Data are presented as mean ± standard deviation. AUC: area under the curve; C_{max} : maximum concentration; ND: not determined; PF: pulmonary fibrosis; $t_{1/2}$: terminal half-life; t_{max} : time at observed maximum concentration.

Recombinant human pentraxin-2 therapy in patients with idiopathic pulmonary fibrosis: safety, pharmacokinetics and exploratory efficacy

European Respiratory Journal, 2016 Mar, 47(3):889-897

B. van den Blink, M.R. Dillingh, L.C. Ginns, L.D. Morrison, M. Moerland, M.S. Wijsenbeek, E.G. Trehu, B.J. Bartholmai, J. Burggraaf

REFERENCE LIST

- 1 Swigris JJ, Stewart AL, Gould MK, Wilson SR. Patients' perspectives on how idiopathic pulmonary fibrosis affects the quality of their lives. *Health Qual Life Outcomes*. 2005;3:61.
- 2 Nathan SD, Shlobin OA, Weir N, Ahmad S, Kaldjob JM, Battle E, et al. Long-term course and prognosis of idiopathic pulmonary fibrosis in the new millennium. *Chest*. 2011;140(1):221-9.
- 3 King TE, Jr., Pardo A, Selman M. Idiopathic pulmonary fibrosis. *Lancet*. 2011;378(9807):1949-61.
- 4 Adkins JM, Collard HR. Idiopathic pulmonary fibrosis. *Semin Respir Crit Care Med*. 2012;33(5):433-9.
- 5 Kelly M, Kolb M, Bonniaud P, Gauldie J. Re-evaluation of fibrogenic cytokines in lung fibrosis. *Curr Pharm Des*. 2003;9(1):39-49.
- 6 Zhang K, Phan SH. Cytokines and pulmonary fibrosis. *Biol Signals*. 1996;5(4):232-9.
- 7 Gauldie J, Jordana M, Cox G. Cytokines and pulmonary fibrosis. *Thorax*. 1993;48(9):931-5.
- 8 Mehrad B, Burdick MD, Zisman DA, Keane MP, Belperio JA, Strieter RM. Circulating peripheral blood fibrocytes in human fibrotic interstitial lung disease. *Biochem Biophys Res Commun*. 2007;353(1):104-8.
- 9 Phillips RJ, Burdick MD, Hong K, Lutz MA, Murray LA, Xue YY, et al. Circulating fibrocytes traffic to the lungs in response to CXCL12 and mediate fibrosis. *J Clin Invest*. 2004;114(3):438-46.
- 10 van den Blink B, Wijsenbeek MS, Hoogsteden HC. Serum biomarkers in idiopathic pulmonary fibrosis. *Pulm Pharmacol Ther*. 2010;23(6):515-20.
- 11 Moeller A, Gilpin SE, Ask K, Cox G, Cook D, Gauldie J, et al. Circulating fibrocytes are an indicator of poor prognosis in idiopathic pulmonary fibrosis. *Am J Respir Crit Care Med*. 2009;179(7):588-94.
- 12 Keeley EC, Mehrad B, Strieter RM. The role of fibrocytes in fibrotic diseases of the lungs and heart. *Fibrogenesis Tissue Repair*. 2011;4:2.
- 13 Pilling D, Gomer RH. Regulatory pathways for fibrocyte differentiation. In: Bucala R, editor. *Fibrocytes: New Insights into Tissue Repair and Systemic Fibroses*: World Scientific Publishing Co. Pte. Ltd; 2007. p. 37-60.
- 14 Pilling D, Buckley CD, Salmon M, Gomer RH. Inhibition of fibrocyte differentiation by serum amyloid P. *J Immunol*. 2003;171(10):5537-46.
- 15 Pilling D, Roife D, Wang M, Ronkainen SD, Crawford JR, Travis EL, et al. Reduction of bleomycin-induced pulmonary fibrosis by serum amyloid P. *J Immunol*. 2007;179(6):4035-44.
- 16 Moreira AP, Cavassani KA, Hullinger R, Rosada RS, Fong DJ, Murray L, et al. Serum amyloid P attenuates M2 macrophage activation and protects against fungal spore-induced allergic airway disease. *J Allergy Clin Immunol*. 2010;126(4):712-21.
- 17 Naik-Mathuria B, Pilling D, Crawford JR, Gay AN, Smith CW, Gomer RH, et al. Serum amyloid P inhibits dermal wound healing. *Wound Repair Regen*. 2008;16(2):266-73.
- 18 Haudek SB, Xia Y, Huebener P, Lee JM, Carlson S, Crawford JR, et al. Bone marrow-derived fibroblast precursors mediate ischemic cardiomyopathy in mice. *Proc Natl Acad Sci U S A*. 2006;103(48):18284-9.
- 19 Murray LA, Chen Q, Kramer MS, Hesson DP, Argenti RL, Peng X, et al. TGF-beta driven lung fibrosis is macrophage dependent and blocked by Serum amyloid P. *Int J Biochem Cell Biol*. 2011;43(1):154-62.
- 20 Murray LA, Rosada R, Moreira AP, Joshi A, Kramer MS, Hesson DP, et al. Serum amyloid P therapeutically attenuates murine bleomycin-induced pulmonary fibrosis via its effects on macrophages. *PLoS One*. 2010;5(3):e9683.
- 21 Murray LA, Kramer MS, Hesson DP, Watkins BA, Fey EG, Argenti RL, et al. Serum amyloid P ameliorates radiation-induced oral mucositis and fibrosis. *Fibrogenesis Tissue Repair*. 2010;3:11.
- 22 Raghu G, Collard HR, Egan JJ, Martinez FJ, Behr J, Brown KK, et al. An official ATS/ERS/RS/ALAT statement: idiopathic pulmonary fibrosis: evidence-based guidelines for diagnosis and management. *Am J Respir Crit Care Med*. 2011;183(6):788-824.
- 23 Nelson SR, Tennent GA, Sethi D, Gower PE, Ballardie FW, Amatayakul-Chantler S, et al. Serum amyloid P component in chronic renal failure and dialysis. *Clin Chim Acta*. 1991;200(2-3):191-9.
- 24 Maharjan AS, Pilling D, Gomer RH. Toll-like receptor 2 agonists inhibit human fibrocyte differentiation. *Fibrogenesis Tissue Repair*. 2010;3:23.

ABSTRACT

Abnormal fibrogenic repair response upon alveolar injury is believed to play an important role in the pathogenesis of idiopathic pulmonary fibrosis (IPF). PRM-151 (recombinant human pentraxin-2, also known as serum amyloid P), has been shown to reduce fibrosis in preclinical lung fibrosis models, and was well tolerated with a favourable pharmacokinetic profile in an earlier single-dose phase I study.

A randomised, double-blind, placebo-controlled, multiple ascending dose trial was performed to assess the tolerability and pharmacokinetic and pharmacodynamic characteristics of multiple doses of PRM-151 in IPF patients.

Subjects in three successive cohorts (1, 5, or 10 mg/kg *versus* placebo) received intravenous study drug on days 1, 3, 5, 8 and 15, and were followed-up to day 57.

PRM-151 was well tolerated at all dose levels, with no serious adverse reactions. Administration of PRM-151 resulted in 2- to 8-fold dose-dependent increases in circulating pentraxin-2 levels. Forced vital capacity and 6-min walk test showed trends towards improvement in the combined PRM-151 dose groups. On high-resolution computed tomography scans, stable or improved lung volume unoccupied by interstitial lung abnormality was noted in some PRM-151 subjects compared to placebo subjects on day 57. The efficacy of PRM-151 in IPF remains to be investigated in dedicated future trials.

Introduction

Idiopathic pulmonary fibrosis (IPF) is a debilitating and fatal disease with a median survival time of 3 years upon diagnosis. Patients with IPF suffer from cough, progressive dyspnoea on exertion and lung function decline. Recent positive results in investigational drug trials have shown that IPF is amenable to therapy and reduction in lung function decline is attainable (1, 2). However, patients using these new drugs still suffer from progressive disease and only lung transplantation offers a curative option to a limited number of patients, indicating the necessity for additional therapies (3, 4).

Although the pathogenesis of IPF has not been fully elucidated, an aberrant fibrogenic repair response upon alveolar injury seems to play a central role (5). Improving normal wound healing and repair is therefore of great interest in IPF. The endogenous blood plasma protein pentraxin (PTX)-2, also known as serum amyloid P, is believed to play a crucial role in regulating wound healing and fibrosis (6). PTX-2 is closely related to PTX-1 (C-reactive protein); both are short pentraxins synthesised by the liver. PTX-2 is constitutively synthesised at steady-state levels, while PTX-1 is an acute-phase protein that can respond to inflammatory signalling by rapid increase in synthesis and circulating levels. A third member of the pentraxin family is PTX-3, which is also an acute-phase protein with a significant role in the orchestration of tissue repair and remodelling (7).

PTX-2 has been shown to accumulate at sites of fibrosis in animal models (8). PTX-2 inhibits differentiation of monocytes into pro-inflammatory and profibrotic macrophages and fibrocytes, while promoting their differentiation into regulatory macrophages (9). This in turn promotes epithelial healing and resolution of inflammation and scarring. The constitutive level of production and consumption of PTX-2 at fibrotic sites is thought to result in the lower circulating levels of PTX-2 in fibrotic disease, as seen in IPF (8), end-stage renal disease (8) and non-alcoholic steatohepatitis (10).

PRM-151 is recombinant human PTX-2, produced in a Chinese hamster ovary cell expression system, which has been shown to reduce fibrosis in preclinical models of transforming growth factor- β 1 (TGF- β 1)- and bleomycin-induced lung fibrosis, with durable effects up to 30 days after dosing (9, 11, 12). The first clinical study with PRM-151, in which single intravenous doses varying from 0.1 to 20 mg/kg were administered to healthy volunteers and a small cohort of pulmonary fibrosis patients, demonstrated that PRM-151 was well tolerated and that the compound displayed a favourable pharmacokinetic profile (13).

The current study was designed to assess the safety and tolerability of multiple escalating intravenous doses of PRM-151, to determine its pharmacokinetic behaviour, and to explore its pharmacodynamic effects, including functional measures such as pulmonary function tests, 6-min walking distance, patient-reported outcomes, and plasma biomarkers relevant for the pathophysiology of pulmonary fibrosis. After study completion, a retrospective analysis of data from high-resolution computed tomography (HRCT) scans was performed using a quantitative imaging modality. Some of the results of these studies have been previously reported in the form of an abstract (14).

Methods

STUDY DESIGN The study was a randomised, placebo-controlled, double-blind, sequential-group study of ascending multiple doses of PRM-151. The study was conducted in accordance with the Declaration of Helsinki and Good Clinical Practice guidelines, and was approved by local ethical review boards. Three study centres (two in the USA and one in the Netherlands) enrolled a total of 21 patients. All subjects provided written informed consent prior to enrolment.

Subjects were enrolled in three successive cohorts, each to include seven subjects, randomly assigned to receive either placebo ($n=2$) or PRM-151 (1, 5 or 10 mg/kg; $n=5$ per successive dose level). Each subject participated in the study for ~13 weeks, which included a screening evaluation within 35 days before the first test article administration and a study period of 8 weeks entailing 2 brief inpatient periods and 11 outpatient visits that could be conducted at home at the subject's request. The test article was administered on days 1, 3, 5, 8 and 15 as an intravenous infusion over 30 min, under fasting conditions. The decision to progress to the next dose level was made following review of the blinded safety data up to day 6 for at least four subjects.

MAIN SUBJECT INCLUSION AND EXCLUSION CRITERIA Participants were to be males or females of non-childbearing potential, aged 40-80 years, with a body mass index of 18-33 kg/m² and a body weight ≥ 45 kg. All subjects had a diagnosis of IPF as determined by a definite or possible usual interstitial pneumonia (UIP) pattern on HRCT as described in the current American Thoracic Society (ATS)/European Respiratory Society/Japanese Respiratory Society/Latin American Thoracic Association statement (4), or by a surgical lung biopsy consistent with IPF. Other idiopathic interstitial pneumonias or interstitial lung diseases

associated with environmental exposure, medication or systemic disease were excluded. Other inclusion criteria included forced vital capacity (FVC) $\geq 45\%$ predicted, diffusing capacity of the lung for carbon monoxide (DLCO) 35-80%, and a resting oxygen saturation on oxygen $\geq 88\%$. The use of cyclophosphamide, systemic steroids, immunosuppressives or any investigational drug within 35 days before test article administration was prohibited.

SAFETY ANALYSIS Safety was evaluated from reported clinical adverse events, scheduled physical examinations, vital signs, 12-lead electrocardiograms (ECGs), HRCT findings and clinical laboratory test results. Serum levels of antibodies to PTX-2 were measured to evaluate for immune response on day 1 (pre-dose) and on days 29 and 57. All subjects were carefully observed for symptoms of infusion reaction, including allergic reactions or hypersensitivity (e.g. urticaria and pruritus).

PHARMACOKINETIC ANALYSIS Blood samples were obtained pre-dose and at multiple time points on days 1 through 57 for pharmacokinetic analysis. Plasma PRM-151 concentrations were determined using a validated enzyme-linked immunosorbent assay (ELISA) method (Intertek Pharmaceutical Services, San Diego, California, USA). Non-compartmental pharmacokinetic analysis was performed for PRM-151 using Phoenix® WinNonlin® (version 6.3; Certara, Mountain View, California, USA) and SigmaPlot® (version 11; Systat Software, San Jose, California, USA). Because the bioanalytical method did not differentiate between PRM-151 and endogenous human PTX-2, baseline PTX-2 concentration was subtracted from all post-dose concentrations to generate baseline-corrected PRM-151 plasma concentrations. Baseline-corrected PRM-151 values that were negative were assumed to be zero.

EFFICACY ENDPOINTS The pharmacodynamic effects of PRM-151 were assessed using functional tests and measurement of relevant plasma biomarkers. Pulmonary function was assessed using pulmonary function tests (FVC, FVC % predicted (PRED), forced expiratory volume in 1 s (FEV₁) and DLCO) at screening and on days 1, 15 and 57. A 6-min walk test (6MWT) was performed at screening and on days 16 and 57 according to the 2002 ATS standards. Subjects were also asked to complete the St George's Respiratory Questionnaire (SGRQ) on days 1, 16, 22 and 57. EDTA blood samples were collected over the course of the study period for assessment of a variety of blood biomarkers (including multiple matrix metalloproteinases, cytokines and chemoattractants) using either a custom glass slide array (53 biomarkers analysed by RayBiotech, Norcross, Georgia, USA) or an ELISA

(4 biomarkers analysed by Promedior, Lexington, Massachusetts, USA). Because of the limited sample size, only exploratory analyses were planned, allowing the identification of gross trends across treatment groups.

Non-contrast HRCT scans with contiguous reconstruction, performed according to local institutional protocols, were obtained at screening (4-5 weeks prior to day 1) and at day 57. For each subject, the HRCT scan data with the highest contiguous reconstruction technique that were most similar at both time points were utilised for analysis. A retrospective exploratory quantitative analysis was performed centrally using CALIPER (computer-aided lung informatics for pathology evaluation and rating) software (developed by Mayo Clinic, Rochester, Minnesota, USA and licensed to Imbio, Minneapolis, Minnesota, USA). Lung texture analysis using CALIPER classifies each voxel of lung parenchyma based on morphology and density characteristics into one of five subtypes: normal; ground glass; reticular; honeycombing; and mild, moderate or severe low attenuation areas. In analysis of the extent of disease in this study, areas of ground glass, reticular and honeycombing subtypes were combined as interstitial lung abnormalities (ILA) and normal or mild low attenuation areas were considered non-ILA parenchyma (normal or mild low-attenuation areas representing hyperinflated tissue not involved by interstitial lung disease features). Previous studies have shown that CALIPER results are comparable to but more reproducible than radiologist assessment (15), they correlate with FVC % PRED, DLCO and 6MWT (16), and changes in ILA features over time are predictive of mortality in IPF (17). CALIPER results were reported as change from screening to day 57 in percentage of total lung volume occupied by ILA and non-ILA features.

Results

DEMOGRAPHICS In total, 21 subjects were enrolled: eight subjects in cohort 1 (1 mg/kg), seven subjects in cohort 2 (5 mg/kg) and six subjects in cohort 3 (10 mg/kg). All cohorts included two subjects treated with a placebo solution. In the first cohort, treatment was terminated for one subject due to observed adverse events (see later). This subject was replaced by another subject treated at the same dose level. In the last cohort, only six subjects were enrolled (PRM-151: $n=4$; placebo: $n=2$) due to limited supply of study medication. Demographics are presented in Table 1. In four subjects, all aged >65 years, a diagnosis of IPF was made based on possible UIP on HRCT without histology, in an appropriate clinical setting. Although according to current consensus a diagnosis of "unclassifiable idiopathic

interstitial pneumonia" may be considered in these patients (18), several studies indicate that the diagnostic likelihood of IPF in such a setting is very high (~95%) (19, 20). Another subject did not have definite UIP on HRCT but was diagnosed with familial IPF; histology following subsequent lung transplantation showed a definite UIP pattern.

SAFETY No infusion reactions, dose-limiting toxicity or serious adverse events were observed. In addition, no antibodies to PRM-151 were detected. In the PRM-151-treated subjects, the most common treatment-emergent adverse events recorded during the study were cough ($n=7$; 47%), productive cough ($n=4$; 27%), fatigue ($n=3$; 20%) and headache ($n=3$; 20%). The incidence of these events was comparable in the placebo group (cough 33% ($n=2$); productive cough 33% ($n=2$); fatigue 17% ($n=1$) and headache 17% ($n=1$)) (Table 2). Neither the nature nor the frequency of these reported adverse events increased with ascending PRM-151 dose levels. One subject in the 1 mg/kg dose group experienced an episode of moderate hypotension and dizziness just before administration of the third dose of PRM-151. These symptoms were considered possibly related to PRM-151 administration, and resulted in the discontinuation of PRM-151 treatment for that subject.

PHARMACOKINETICS The mean \pm standard error of the mean baseline plasma concentration of PTX-2 was 41.2 ± 3.4 $\mu\text{g/mL}$ in the 6 placebo-treated subjects and 32.6 ± 1.2 $\mu\text{g/mL}$ in the 15 PRM-151-treated subjects. Administration of 1, 5 and 10 mg/kg PRM-151 to IPF patients resulted in peak plasma concentrations that were 2-, 5- and 8-fold elevated compared to the mean baseline plasma PTX-2 levels (Figure 1A and B). Because of minimal circadian variability in endogenous PTX-2 (as evidenced by the values measured over time in the placebo-treated subjects (not shown)), non-compartmental analysis of PRM-151 pharmacokinetics was performed after subtraction of each individual subject's endogenous baseline PTX-2 level from levels at later time points. PRM-151 exposure (maximum concentration (C_{max}) and area under the curve (AUC) over 48 h) increased linearly with increasing doses (Figure 1C and D). C_{max} was observed after 1-2 h. The median observed half-life on day 15 was 32.8 h, but was highly variable between individual subjects, ranging from 11 to 110 h. PRM-151 did not accumulate in plasma when administered on a weekly basis (Figure 1A and B).

EFFICACY ENDPOINTS Mean baseline pulmonary function measures (FVC, FVC % PRED, DLCO and FEV1) were lower in the placebo group compared to the PRM-151 groups (Table 3). In the placebo group, FVC, FVC % PRED, and FEV1 were

all decreased on day 57 compared to baseline, indicative of a worsening of pulmonary function. In all PRM-151-treated groups, increased pulmonary function measures were observed compared to baseline levels, although the magnitude of increase in FVC, FVC % PRED, and FEV1 was modest, and the differences between groups were not statistically significant. Relative increases of $\geq 5\%$ in FVC % PRED between baseline and day 57 occurred in six PRM-151-treated subjects (5% increase in three subjects and 10% increase in three subjects) and in none of the placebo-treated subjects (Figure 2). A relative decline of $\geq 5\%$ from baseline FVC % PRED was observed in two PRM-151-treated subjects and two placebo subjects (Figure 2). No indication of PRM-151 dose level dependency on lung function tests was observed, and there was no apparent correlation between change in FVC % PRED and C_{max} or AUC of PRM-151. PRM-151 treatment did not have an effect on DLCO.

Mean distance walked in the 6MWT decreased slightly over time in the placebo group and the lowest PRM-151 dose group (1 mg/kg), and the mean distance walked improved in the two higher PRM-151 dose groups (Table 3). None of these differences were statistically significant. No PRM-151 effect was observed on SGRQ outcome (not shown).

Plasma vascular endothelial growth factor (VEGF) levels progressively increased over time in the placebo-treated subjects; the levels remained stable in the PRM-151-treated subjects. Other plasma biomarkers potentially related to fibrosis or the biology of PTX-2, including matrix metalloproteinase-7 (MMP-7), intercellular adhesion molecule-1 (ICAM-1), interleukin (IL)-8, vascular cell adhesion molecule-1 (VCAM-1), and S100A12 did not show differences between PRM-151 and placebo groups (Supplementary Table S1).

Baseline quantitative imaging data were analysed in 16 subjects who had ≤ 36 days between screening HRCT and day 1 pulmonary function tests. There was a strong negative correlation between screening FVC % PRED and percentage of lung volume identified as non-ILA using CALIPER ($r = -0.7$; Figure 3), which demonstrates the potential value of quantitative imaging as biomarker in clinical trials in IPF. Non-ILA lung volume decreased in all placebo subjects and was stable or increased in five PRM-151-treated subjects, all of whom had stable or increased FVC % PRED (Supplementary Table S2). There was no clear correlation between the magnitude of change in FVC % PRED and percentage non-ILA lung volume (not shown). HRCT analysis was limited in four subjects by poor inspiratory effort on the day 57 scan. Non-ILA determination was possibly limited by the technical limitations of the retrospective analysis of the HRCT data, including differences in HRCT protocols used at the different study sites.

Discussion

This study demonstrated that PRM-151, administered as five intravenous infusions over 15 days at doses ranging from 1 to 10 mg/kg, was well tolerated in patients with IPF, and did not raise any safety concerns. One subject receiving 1 mg/kg PRM-151 experienced an episode of moderate hypotension and dizziness, which resulted in treatment termination prior to the third dose. This event was considered possibly to be related to PRM-151 administration. The most frequently reported adverse events (cough, productive cough, fatigue and headache) were equally distributed between PRM-151- and placebo-treated subjects, suggesting that these events were not related to the test article and that some (such as cough) were a natural part of the disease. Neither the nature nor the frequency of these adverse events increased with ascending PRM-151 dose levels. Importantly, no allergic or anaphylactic signs were observed.

At 10 mg/kg, the highest dose level tested, administration of PRM-151 resulted in an 8-fold increase in circulating PTX-2 levels, which remained elevated for ≥ 2 days. These data confirm the earlier observations on PRM-151 kinetics in IPF patients (13). There were no indications for accumulation of PRM-151 in plasma when administered at the selected dosing regimen. The inter-individual variability observed in half-life was substantial, which may relate to the small and heterogeneous study population (e.g. sex and disease state). A population pharmacokinetic approach may be suitable for identification of key covariates determining the pharmacokinetic behaviour of PRM-151, which may be supportive for further clinical development of the compound.

Based on preclinical experiments in animal models, PRM-151 was expected to exert pharmacological activity at the dose levels explored in this clinical study. In mouse and rat models of lung fibrosis, purified mouse and rat PTX-2 were effective at dose levels of 2.5 mg/kg and 1.6 mg/kg, respectively, while human PTX-2 was routinely effective at 2-10 mg/kg in the mouse models of lung fibrosis (no lower doses were evaluated) (9, 11, 12, 21). Although the physiological validity and translatability of animal fibrosis models to human IPF can be argued (22), these animal study results indicate sufficient PRM-151 exposure for intended pharmacological effect at the dose levels of 1-10 mg/kg selected in our clinical study. PTX-2 acts as a ligand for Fc γ receptors expressed on monocytes and macrophages, stimulating their differentiation into restorative regulatory macrophages with their local production of IL-10 (8). Therefore, the optimal dose regimen of PRM-151 may require a threshold dosing interval to effectively modulate tissue-resident monocyte/macrophage populations. Although our study was not designed to demonstrate

clinical efficacy of PRM-151, potential trends in clinical effects of PRM-151 were explored that could guide further clinical development of the compound. Some trends towards improvement in multiple pulmonary function measures (FVC, FVC % PRED, FEV₁ and 6-min walking distance) and increases in normal lung volume by quantitative imaging on day 57 were observed. We cannot exclude the possibility that the observed trend for PRM-151 effects was related to differences in disease severity between placebo and PRM-151 treatment groups, despite randomisation and the double-blind nature of the study. Plasma biomarkers (MMP-7, IL-10, ICAM-1, IL-8, VCAM-1 and S100A12), validated to indicate disease prognosis, did not show differences between PRM-151 and placebo groups (23). Since the sample size in the clinical study was small, and the treatment duration was relatively short, no firm conclusions can be drawn on clinical efficacy endpoints. Evaluation of cellular biomarkers at the site of disease, such as alveolar macrophages, would have been valuable for assessment of the biological effect of PRM-151. The repeated investigations necessary to obtain such biomarkers in a study population burdened by considerable disease were deemed unfeasible for this study. However, it should be noted that such an approach is being employed in an IPF trial (clinicaltrials.gov NCT01371305).

In summary, five intravenous doses of PRM-151 over 2 weeks were generally well tolerated in IPF patients. Administration of PRM-151 resulted in a substantial increase in circulating PTX-2 levels. Some clinical efficacy markers showed trends towards improvement in the PRM-151 dose groups. However, efficacy of PRM-151 in IPF will be investigated in a dedicated future trial, which will prospectively evaluate both changes in lung function and tissue abnormalities by quantitative image analysis of HRCT.

FIGURE 1A&B Mean plasma concentration of pentraxin-2 (PTX-2) versus time. Time course over A: 48 h following the first dose of PRM-151 on day 1; B: 170 h following the last dose of PRM-151 on day 15. Lower limit of quantification 4.0 ng/mL. Individual subject values for C. maximum concentration (C_{max}) and D. area under the curve at 48 h (AUC_{0-48h}) versus PRM-151 dose following day 1 and day 15 administrations. All values are based on baseline-corrected PTX-2 plasma concentrations.

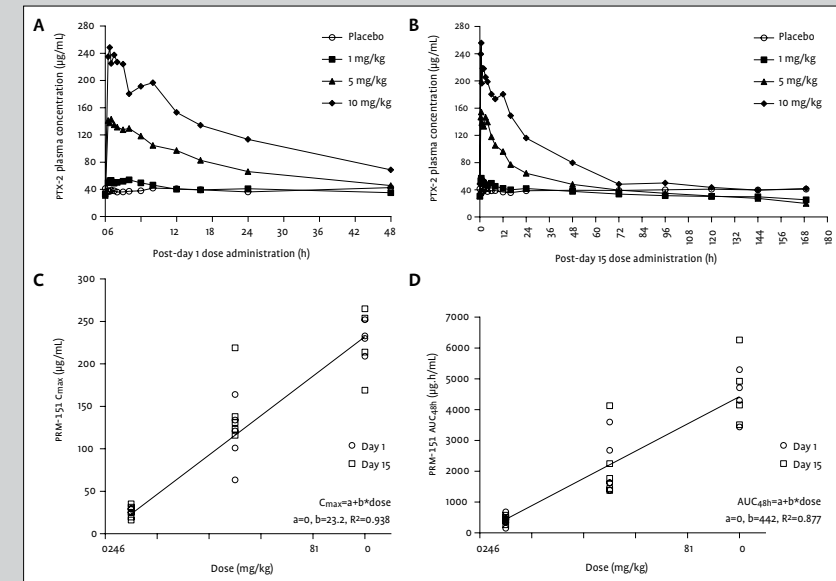


FIGURE 2 Individual subject values of relative change in forced vital capacity (FVC)% predicted from baseline to day 57. CFB: change from baseline.

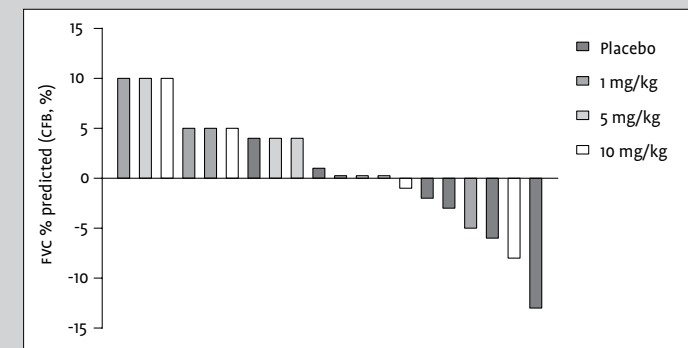


FIGURE 3 Correlation between screening values of percentage of lung volume identified as interstitial lung abnormality (ILA) and forced vital capacity (FVC) % predicted.

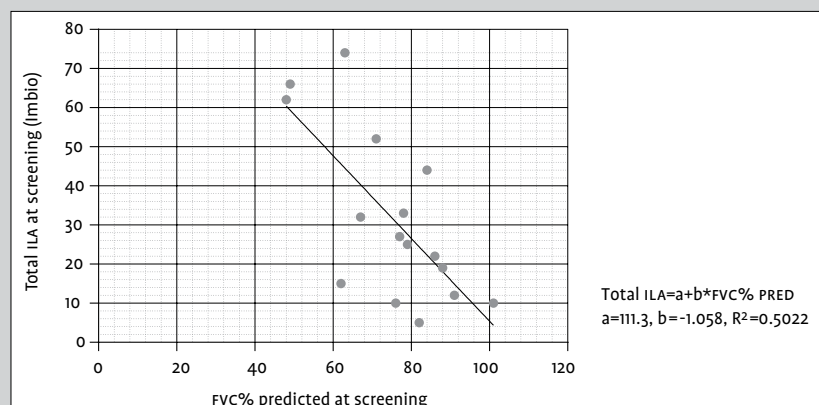


TABLE 1 Patient characteristics.

	Placebo	PRM-151			
		1 mg/kg	5 mg/kg	10 mg/kg	All doses
Subjects	6	6	5	4	14
Age (years)	65.5 ± 12.9	63.7 ± 8.5	70.6 ± 8.3	66.5 ± 5.7	66.7 ± 7.8
Male	4 (67)	5 (83)	4 (80)	4 (100)	13 (87)
Race					
White	5 (83)	6 (100)	5 (100)	4 (100)	15 (100)
African American	1 (17)	0 (0)	0 (0)	0 (0)	0 (0)
BMI (kg/m ²)	28.7 ± 3.1	28.6 ± 2.3	28.6 ± 4.6	28.9 ± 2.7	28.7 ± 3.1
Oxygen	4 (67)	0(0)	1(20)	0(0)	1 (7)
UIP on HRCT					
No	2 (33)	3 (50)	0 (0)	0 (0)	3 (20)
Possible	1 (17)	1 (17)	2 (40)	2 (50)	5 (33)
Definite	3 (50)	2 (33)	3 (60)	2 (50)	7 (47)
UIP upon lung biopsy	2 (33)	3 (50)	1 (20)	0 (0)	4 (27)

Data are presented as n, mean ± standard deviation or n (%). BMI: body mass index; UIP: usual interstitial pneumonia; HRCT: high-resolution computed tomography.

TABLE 2 Adverse Events.

	Placebo	PRM-151			All doses	All
		1 mg/kg	5 mg/kg	10 mg/kg		
Subjects	6	6	5	4	15	21
Cough	2 (33)	4 (67)	3 (60)	0 (0)	7 (47)	9 (43)
Productive cough	2 (33)	1 (17)	2 (40)	1 (25)	4 (27)	6 (29)
Fatigue	1 (17)	0 (0)	2 (40)	1 (25)	3 (20)	4 (19)
Headache	1 (17)	2 (33)	0 (0)	1 (25)	3 (20)	4 (19)
Dyspnoea	2 (33)	2 (33)	0 (0)	0 (0)	2 (13)	4 (19)
Dizziness	1 (17)	1 (17)	1 (20)	0 (0)	2 (13)	3 (14)
Pruritus	1 (17)	1 (17)	1 (20)	0 (0)	2 (13)	3 (14)
Haematoma	1 (17)	2 (33)	0 (0)	0 (0)	2 (13)	3 (14)
Dyspnoea exertional	2 (33)	1 (17)	0 (0)	0 (0)	1 (7)	3 (14)
Nasopharyngitis	2 (33)	1 (17)	0 (0)	0 (0)	1 (7)	3 (14)
Back pain	2 (33)	0 (0)	1 (20)	0 (0)	1 (7)	3 (14)
Dysphonia	0 (0)	2 (33)	0 (0)	0 (0)	2 (13)	2 (10)
Hypotension	0 (0)	1 (17)	0 (0)	1 (25)	2 (13)	2 (10)
Lymphadenopathy	1 (17)	1 (17)	0 (0)	0 (0)	1 (7)	2 (10)
Catheter site haematoma	1 (17)	1 (17)	0 (0)	0 (0)	1 (7)	2 (10)
Malaise	1 (17)	1 (17)	0 (0)	0 (0)	1 (7)	2 (10)
Hypertension	1 (17)	1 (17)	0 (0)	0 (0)	1 (7)	2 (10)
Non-cardiac chest pain	2 (33)	0 (0)	0 (0)	0 (0)	0 (0)	2 (10)
Vomiting	2 (33)	0 (0)	0 (0)	0 (0)	0 (0)	2 (10)

Data are presented as n or n (%). Events reported by at least 2 (10%) out of the 21 subjects are listed.

Treatment-emergent adverse events were defined as events occurring from the first day of dosing to the end of study (day 57 or early termination day).

TABLE 3 Pulmonary function tests and 6-min walking distance (6MWD): baseline values and change from baseline on day 57.

	Placebo	PRM-151			
	6	1 mg/kg	5 mg/kg	10 mg/kg	All doses
Subjects	6	5	5	4	14
FVC (L)					
Baseline	2.15 ± 0.64	2.96 ± 0.85	2.78 ± 0.73	2.97 ± 0.71	2.90 ± 0.71
Day 57 change from baseline	-0.063 ± 0.116	0.058 ± 0.164	0.060 ± 0.074	0.078 ± 0.210	0.064 ± 0.142
FVC % PRED					
Baseline	63.2 ± 16.7	82.4 ± 15.5	80.0 ± 7.8	72.8 ± 14.3	78.8 ± 12.5
Day 57 change from baseline	-1.5 ± 3.3	2.4 ± 4.6	2.8 ± 3.0	1.8 ± 5.3	2.4 ± 4.0
DLCO (%)					
Baseline	35.2 ± 8.4	41.2 ± 10.5	52.8 ± 9.8	46.0 ± 7.2	46.7 ± 10.1
Day 57 change from baseline	-2.3 ± 2.1	0.2 ± 3.3	-4.0 ± 6.8	-1.5 ± 3.8	-1.8 ± 4.9
FEV1 (%)					
Baseline	68.8 ± 17.7	85.8 ± 16.8	87.0 ± 11.9	73.0 ± 12.1	82.6 ± 14.3
Day 57 change from baseline	-1.7 ± 4.3	2.6 ± 4.3	2.4 ± 1.1	0.3 ± 3.8	1.9 ± 3.2
6MWD (m)					
Baseline	458 ± 73	457 ± 157	470 ± 101	439 ± 63	456 ± 109
Day 57 change from baseline	-11 ± 51	-11 ± 63	6 ± 43	35 ± 45	8 ± 51

Data are presented as *n* or mean ± standard deviation. FVC: forced vital capacity; FVC % PRED: forced vital capacity percentage predicted; DLCO: diffusing capacity of the lung for carbon monoxide; FEV1: forced expiratory volume in 1 s.

TABLE S1 Plasma biomarkers at baseline, day 15 and day 57.

Cytokine	Unit	Placebo			PRM-151								
		Baseline	Day 15		Day 57		Baseline		Day 15		Day 57		
			mean	SD	mean	SD	mean	SD	mean	SD	mean	SD	mean
MCP-1	ng/ml	1524	793	1493	848	2176	1283	1509	455	1688	539	2097	1450
Eotaxin	µg/ml	653	761	369	159	567	499	362	106	421	101	547	326
TARC	ng/ml	471	447	246	141	595	590	236	219	249	216	580	931
PARC	ng/ml	556	638	335	141	442	279	280	80	284	64	462	570
MIP-3β	ng/ml	2352	4217	1570	2304	2889	4932	575	338	684	379	930	1118
CCL21/6CKINE	ng/ml	703	466	449	159	670	492	433	211	414	169	743	928
MDC	ng/ml	73	36	78	51	72	33	42	24	63	45	46	24
TECK	ng/ml	283	172	300	226	353	277	206	76	236	87	503	973
ENA-78	ng/ml	534	275	552	257	889	577	501	299	585	387	922	832
IL-8	ng/ml	1176	290	1081	175	1351	522	931	268	951	183	1148	400
MIG	ng/ml	2093	2034	1430	764	1957	1273	1381	1010	1385	938	1726	1706
IP-10	ng/ml	803	671	577	377	958	790	458	237	478	163	657	556
I-TAC	ng/ml	227	97	198	72	239	81	163	79	177	65	191	76
SDF-1	ng/ml	417	571	301	317	260	280	166	97	157	82	309	535
SDF-1β	ng/ml	571	582	432	395	502	472	272	98	299	94	558	799
BLC	ng/ml	415	342	337	292	516	557	241	84	249	69	423	534
Fractalkine	ng/ml	199	266	154	105	229	342	113	98	107	86	160	304
BMP-7	ng/ml	557	357	477	329	943	1285	369	126	339	101	704	1164
CRP	ng/ml	21119	6217	15377	6343	21561	6917	22271	7963	18604	4030	23579	7735
FAS	ng/ml	1971	628	1855	1180	2350	1134	1825	512	1761	550	2445	1946
ICAM-1	ng/ml	8314	6793	6784	4594	7349	4861	10725	13894	9455	11562	9639	11334
VCAM-1	ng/ml	3103	2831	2512	1696	3426	2354	3697	1626	4181	1413	4247	1923
IFN-γ	ng/ml	943	368	910	482	1099	807	673	218	694	185	961	663
IGF-1	ng/ml	700	1006	542	591	511	565	273	95	306	105	474	607
IL-4	ng/ml	398	293	390	367	482	487	235	56	255	63	463	673
IL-6	ng/ml	562	206	609	277	872	812	429	147	498	116	788	792
IL-10	ng/ml	494	92	484	169	611	483	373	133	431	120	590	329
IL-12p40	ng/ml	474	378	498	445	972	1484	297	80	323	113	547	837
IL-12p70	ng/ml	452	456	422	279	582	670	258	75	280	74	599	1055
IL-13	ng/ml	548	269	740	663	776	696	398	124	458	124	724	754
IL-1RA	ng/ml	223	92	210	95	230	90	191	95	202	101	208	102
MMP-1	ng/ml	256	274	243	232	453	710	129	48	146	70	383	836
MMP-3	ng/ml	4540	2201	4012	3021	5207	1566	6842	5039	7000	4025	7545	4409
MMP-7	ng/ml	22	19	20	15	25	13	12	9	13	10	21	14
MMP-8	ng/ml	2161	3321	1548	1928	2139	1645	952	500	1108	494	1035	510
MMP-9	ng/ml	21585	18362	19214	11266	17765	13730	16093	7543	20570	12127	13228	8464
Oncostatin	ng/ml	207	62	177	61	235	88	147	75	140	64	183	88
Osteopontin	ng/ml	93	52	96	91	110	60	76	62	85	53	91	65
PAI-1	ng/ml	1623	1631	1853	2047	2774	2677	2324	2140	2536	2372	2712	2342
PDGF-AA	ng/ml	754	728	771	518	2153	3603	627	685	1825	3377	1850	1835
PDGF-BB	ng/ml	3226	3625	2770	1862	9494	13744	2945	3488	3189	2966	6090	5690
RAGE	ng/ml	633	372	646	358	781	587	881	539	949	582	958	636
TGF-β1	ng/ml	800	233	844	315	936	386	663	201	657	137	984	906
TGF-β2	ng/ml	132	17	128	28	152	33	114	44	122	40	138	54
TGF-β3	ng/ml	177	330	149	166	217	352	72	73	83	69	193	455
TIE-1	ng/ml	326	345	299	250	323	261	188	59	214	75	370	602
TIE-2	ng/ml	247	223	247	219	224	184	161	88	176	80	392	868
TIMP-1	ng/ml	27771	20486	23840	16762	27238	21023	19052	10386	25048	13800	17699	11525
TIMP-2	ng/ml	4005	2416	4441	2389	3822	1833	5686	2534	5912	2354	5191	1850
TIMP-4	ng/ml	2576	2725	2006	1252	2047	1455	2099	673	2004	604	2302	1045
TNF-α	ng/ml	789	212	994	533	1224	1069	627	202	623	171	967	834
STNF RI	ng/ml	1193	938	1275	854	1508	1185	1330	662	1453	500	1696	974
VEGF	ng/ml	65	27	70	18	123	86	59	39	45	19	57	25
MMP-13	ng/ml	901	533	789	556	1295	1021	1626	4136	1554	3757	1700	3943
SP-D	ng/ml	64	83	63	77	78	95	60	32	60	34	63	38
Haptoglobin	ng/ml	2510000	1470000	2710000	1390000	3560000	2950000	2730000	1320000	2740000	1120000	3500000	1280000
S100A12	ng/ml	153	153	92	59	115	69	61	41	57	39	82	67

TABLE S2 Individual subject data comparing absolute change in forced vital capacity % predicted (FVC % PRED) versus change in total lung volume free of interstitial lung abnormalities (ILA; non-ILA) on day 57.

	Placebo										PRM-151									
	1 mg/kg					5 mg/kg					10 mg/kg									
Subject number	123	125	202	207	211	203	204	205	210	122	124	206	208	209	126	128	129			
FVC % PRED (change from screening)	-5	-1	-4	-2	-12	+13	+9	+1	-3	+12	-1	+8	+4	+2	0	+6	+2			
FVC % PRED (change from baseline)	-1	+1	-4	-2	-6	+5	+8	+3	0	+4	0	+3	0	+7	-4	+4	+8			
Non-ILA (% change from screening)	-23	-3	-30	-2	-13	5	-4	-9	0	-42	-24	24	16	5	-1	-1	-4			

REFERENCE LIST

- King TE, Jr., Bradford WZ, Castro-Bernardini S, Fagan EA, Glasspole I, Glassberg MK, et al. A phase 3 trial of pirfenidone in patients with idiopathic pulmonary fibrosis. *N Engl J Med*. 2014;370(22):2083-92.
- Richeldi L, du Bois RM, Raghu G, Azuma A, Brown KK, Costabel U, et al. Efficacy and safety of nintedanib in idiopathic pulmonary fibrosis. *N Engl J Med*. 2014;370(22):2071-82.
- King TE, Jr., Brown KK, Raghu G, du Bois RM, Lynch DA, Martinez F, et al. BUILD-3: a randomized, controlled trial of bosentan in idiopathic pulmonary fibrosis. *Am J Respir Crit Care Med*. 2011;184(1):92-9.
- Raghu G, Collard HR, Egan JJ, Martinez FJ, Behr J, Brown KK, et al. An official ATS/ERS/JRS/ALAT statement: idiopathic pulmonary fibrosis: evidence-based guidelines for diagnosis and management. *Am J Respir Crit Care Med*. 2011;183(6):788-824.
- Wolters PJ, Collard HR, Jones KD. Pathogenesis of idiopathic pulmonary fibrosis. *Annu Rev Pathol*. 2014;9:157-79.
- Cox N, Pilling D, Gomer RH. Serum amyloid P: a systemic regulator of the innate immune response. *J Leukoc Biol*. 2014;96(5):739-43.
- Doni A, Musso T, Morone D, Bastone A, Zambelli V, Sironi M, et al. An acidic microenvironment sets the humoral pattern recognition molecule PTX3 in a tissue repair mode. *J Exp Med*. 2015;212(6):905-25.
- Castano AP, Lin SL, Surowy T, Nowlin BT, Turlapati SA, Patel T, et al. Serum amyloid P inhibits fibrosis through Fc gamma R-dependent monocyte-macrophage regulation *in vivo*. *Sci Transl Med*. 2009;1(5):5ra13.
- Pilling D, Roife D, Wang M, Ronkainen SD, Crawford JR, Travis EL, et al. Reduction of bleomycin-induced pulmonary fibrosis by serum amyloid P. *J Immunol*. 2007;179(6):4035-44.
- Verna EC, Patel J, Bettencourt R, Nguyen P, Hernandez C, Valasek MA, et al. Novel association between serum pentraxin-2 levels and advanced fibrosis in well-characterised patients with non-alcoholic fatty liver disease. *Aliment Pharmacol Ther*. 2015;42(5):582-90.
- Murray LA, Rosada R, Moreira AP, Joshi A, Kramer MS, Hesson DP, et al. Serum amyloid P therapeutically attenuates murine bleomycin-induced pulmonary fibrosis via its effects on macrophages. *PLoS One*. 2010;5(3):e9683.
- Murray LA, Chen Q, Kramer MS, Hesson DP, Argenti RL, Peng X, et al. TGF-beta driven lung fibrosis is macrophage dependent and blocked by Serum amyloid P. *Int J Biochem Cell Biol*. 2011;43(1):154-62.
- Dilling MR, van den Blink B, Moerland M, van Dongen MG, Levi M, Kleinjan A, et al. Recombinant human serum amyloid P in healthy volunteers and patients with pulmonary fibrosis. *Pulm Pharmacol Ther*. 2013;26(6):672-6.
- van den Blink B, Burggraaf J, Morrison LB, Wijsenbeek MS, Moerland M, Dilling MR, et al. A phase I study of PRM-151 in patients with Idiopathic Pulmonary Fibrosis. American Thoracic Society (ATS) International Conference, May 17-22, 2013, Philadelphia, PA, USA (Abstract 5707). 2013.
- Zavaletta VA, Bartholmai BJ, Robb RA. High resolution multidetector CT-aided tissue analysis and quantification of lung fibrosis. *Acad Radiol*. 2007;14(7):772-87.
- Raghuath S, Rajagopalan S, Karwoski RA, Maldonado F, Peikert T, Moua T, et al. Quantitative stratification of diffuse parenchymal lung diseases. *PLoS One*. 2014;9(3):e93229.
- Maldonado F, Moua T, Rajagopalan S, Karwoski RA, Raghuath S, Decker PA, et al. Automated quantification of radiological patterns predicts survival in idiopathic pulmonary fibrosis. *Eur Respir J*. 2014;43(1):204-12.
- Travis WD, Costabel U, Hansell DM, King TE, Jr., Lynch DA, Nicholson AG, et al. An official American Thoracic Society/European Respiratory Society statement: Update of the international multidisciplinary classification of the idiopathic interstitial pneumonias. *Am J Respir Crit Care Med*. 2013;188(6):733-48.
- Fell CD, Martinez FJ, Liu LX, Murray S, Han MK, Kazerooni EA, et al. Clinical predictors of a diagnosis of idiopathic pulmonary fibrosis. *Am J Respir Crit Care Med*. 2010;181(8):832-7.
- Raghu G, Chen SY, Yeh WS, Maroni B, Li Q, Lee YC, et al. Idiopathic pulmonary fibrosis in US Medicare beneficiaries aged 65 years and older: incidence, prevalence, and survival, 2001-11. *Lancet Respir Med*. 2014;2(7):566-72.
- Pilling D, Buckley CD, Salmon M, Gomer RH. Inhibition of fibrocyte differentiation by serum amyloid P. *J Immunol*. 2003;171(10):5537-46.
- Moore B, Lawson WE, Oury TD, Sisson TH, Raghavendran K, Hogoaboam CM. Animal models of fibrotic lung disease. *Am J Respir Cell Mol Biol*. 2013;49(2):167-79.
- Richards TJ, Kaminski N, Baribaud F, Flavin S, Brodmerkel C, Horowitz D, et al. Peripheral blood proteins predict mortality in idiopathic pulmonary fibrosis. *Am J Respir Crit Care Med*. 2012;185(1):67-76.

CHAPTER 5

**Characterization of
inflammation and immune
cell modulation induced by
low-dose LPS administration
to healthy volunteers**

Journal of Inflammation, 2014, 11(28)

M.R. Dillingh*, E.P. van Poelgeest*, K.E. Malone, E.M. Kemper, E.S.G. Stroes,
M. Moerland, J. Burggraaf (*authors contributed equally)

ABSTRACT

Human *in vivo* models of systemic inflammation are used to study the physiological mechanisms of inflammation and the effect of drugs and nutrition on the immune response. Although *in vivo* lipopolysaccharide (LPS) challenges have been applied as methodological tool in clinical pharmacology studies, detailed information is desired on dose-response relationships, especially regarding LPS hyporesponsiveness observed after low-dose *in vivo* LPS administration. A study was performed to assess the *in vivo* inflammatory effects of low intravenous LPS doses, and to explore the duration of the induced LPS hyporesponsiveness assessed by subsequent *ex vivo* LPS challenges.

This was a randomized, double-blind, placebo-controlled study with single ascending low doses of LPS (0.5, 1 and 2 ng/kg body weight) administered to healthy male volunteers (three cohorts of eight subjects, LPS: placebo; 6:2). The *in vivo* inflammatory response was assessed by measurement of cytokines and CRP. *Ex vivo* LPS challenges were performed (at -2, 6, 12, 24, 48 and 72 h relative to *in vivo* LPS administration) to estimate the duration and magnitude of LPS hyporesponsiveness by assessment of cytokine release (TNF- α , IL-1 β , IL-6, IL-8).

LPS administration dose-dependently increased body temperature (+1.5°C for 2 ng/kg LPS), heart rate (+28 BPM for 2 ng/kg LPS), CRP and circulating cytokines which showed clearly distinctive increases from placebo already at the lowest LPS dose level tested (0.5 ng/kg, contrast for timeframe 0-6 h: TNF- α +413%, IL-6 +288%, IL-8 +254%; all $p \leq 0.0001$). *In vivo* LPS administration dose-dependently induced a period of hyporesponsiveness in the *ex vivo* LPS-induced cytokine release (IL-1 β , IL-6 and TNF- α), with maximal hyporesponsiveness observed at 6 h, lasting no longer than 12 h. For IL-6 and IL-8, indications for immune cell priming were observed.

We demonstrated that an *in vivo* LPS challenge, with LPS doses as low as 0.5 ng/kg, elicits a cytokine response that is clearly distinctive from baseline cytokine levels. This study expanded the knowledge about the dose-effect relationship of LPS-induced hyporesponsiveness. As such, the low-dose LPS challenge has been demonstrated to be a feasible methodological tool for future clinical studies exploring pharmacological or nutritional immune-modulating effects.

Introduction

Human models of systemic inflammation have been developed with the purpose to explore the molecular mechanisms and physiological significance of the systemic inflammatory response encountered in acute as well as chronic inflammatory conditions, such as sepsis, trauma, type 2 diabetes, atherosclerosis, and Alzheimer's disease, in a controlled, standardized experimental setting. A better understanding of the underlying molecular and pathophysiological mechanisms could lead to optimized prevention and treatment of these disorders, associated with morbidity and mortality (1). In addition, human models of systemic inflammation can be applied in clinical pharmacology studies to assess the effects of specific interventions (medicinal or non-medicinal) on the inflammatory response in non-diseased populations.

Human endotoxaemia is often used as a model of systemic inflammation. In this experimental setting, purified lipopolysaccharide (LPS, also referred to as endotoxin) from the cell membrane of *Escherichia coli* (*E. coli*) or other Gram-negative bacteria is administered intravenously to healthy volunteers resulting in flu-like symptoms, increased production of C-reactive protein (CRP) and increased concentrations of pro- and anti-inflammatory cytokines. Since the effects of *E. coli* are highly reproducible, this is the predominant bacterial source used (1). LPS induces an inflammatory response via stimulation of Toll-like receptors (TLRs), basic signaling receptors of the innate immune system activated by tissue damage or by molecules associated with pathogen-associated molecular patterns (PAMPs) on invading microorganisms. LPS is known to activate multiple intracellular pathways (e.g. the MyD88-dependent and TIR domain-containing adapter inducing interferon- β (TRIF)-dependent pathways) (2, 3).

The human endotoxaemia model has been studied extensively, and commonly applies relatively high LPS doses (2-4 ng/kg body weight) (1, 4-8). However, an endotoxaemia model applying such relatively high LPS doses is not preferred as methodological tool in clinical pharmacology studies since the elicited immune response is so strong that potential effects of immune-modulating interventions may not be observed, other homeostatic mechanisms may be temporarily impaired, and, importantly, the elicited immune response at these LPS doses is not free of risk for the volunteer. Studies applying lower LPS doses have been performed (9, 10), but thorough characterization of a human endotoxaemia model at lower LPS dose levels is desired. In the current study, 0.5 ng/kg was selected as the lowest LPS dose to be administered intravenously because an LPS dose of 0.2 ng/kg was shown previously to elicit no cytokine response *in vivo* (11). We performed

a study to characterize the LPS dose relationship of the human inflammatory response at low LPS doses (0.5, 1 and 2 ng/kg) administered to healthy volunteers. Furthermore, we explored the effects of such an *in vivo* LPS challenge on the inflammatory response induced by subsequent *ex vivo* LPS challenges. It has been described that an *in vivo* LPS challenge induces hyporesponsiveness to following *in vivo* or *ex vivo* LPS challenges. The biochemical mechanisms accounting for this hyporesponsiveness have been demonstrated to involve negative regulators such as interleukin-1 receptor-associated kinase-M (IRAK-M), suppressor of cytokine signalling-1 (SOCS-1), SH2 domain-containing inositol 5'-phosphatase (SHIP), ST2 and interleukin (IL)-10 (2, 3, 12-18) and downregulation of CD14 (19).

It has been reported that *ex vivo* LPS hyporesponsiveness following an *in vivo* LPS challenge was resolved after 1 week (4). However, the exact time course of this phenomenon and relation to LPS dose level is unclear. Since such information could be important for (repeated) application of *in vivo* and *ex vivo* LPS challenges in clinical pharmacology studies, characterization of this hyporesponsiveness was an objective of our study.

Methods

SUBJECTS Twenty-four (24) healthy male volunteers, aged 18-28 years (inclusive) with a body mass index of 18-25 kg/m² and a body weight \geq 56 kg, participated in this study. After providing informed consent, subjects were medically screened within 3 weeks prior to participation. Exclusion criteria included history of sepsis, cardiovascular disease, previous syncope or malignancy, haemorrhagic diathesis, any active inflammatory or infectious disease, renal impairment, diabetes mellitus, thyroid dysfunction, and prior exposure to endotoxin in an experimental setting within 4 weeks of the anticipated exposure. Any use of medication that in the opinion of the investigator would complicate or compromise the study or interfere with the study objectives was not permitted during the study. The study was conducted in accordance with the Declaration of Helsinki and Guideline for Good Clinical Practice, and was approved by the Medical Ethics Review Board of the Academic Medical Center, Amsterdam, The Netherlands.

STUDY DESIGN This was a randomized, blinded, placebo controlled study of ascending single doses of 0.5, 1 and 2 ng/kg LPS (U.S. Reference *E. coli* endotoxin CC-RE-Lot 3 (O113:H, 10:K negative, National Institute of Health, Bethesda, Maryland, USA, approximately 10 EU/ng); or placebo), administered to healthy

male subjects as an intravenous bolus over 2 min. Each cohort included eight healthy subjects, of which six subjects received LPS and two placebo (sodium chloride 0.9%). Subjects were pre-hydrated with 1500 mL glucose/saline (2.5% glucose/0.45% sodium chloride) 2 h prior to LPS (/placebo) administration, followed by an intravenous drip of 150 mL/h for a period of 6 h. After LPS/placebo administration, subjects were confined to the clinical research unit for 24 h.

SAFETY MONITORING Safety monitoring was performed by adverse events monitoring, physical examination, assessment of electrocardiogram (ECG) and vital signs, and laboratory evaluations (routine haematology, chemistry, coagulation, and semi-quantitative dipstick urinalysis). In case of clinically significant findings in dipstick analysis, a microscopic investigation of the urine was performed. For subject safety, maximally two subjects were treated within 1 day, with a lag time of at least 40 min between subjects. All blinded safety data collected up to at least 24 h after LPS/placebo administration were reviewed before the decision was made to escalate the LPS dose level and proceed with the next cohort.

INFLAMMATORY MARKERS The systemic inflammatory response was assessed by frequent measurement of CRP and a panel of cytokines (IL-1 β , IL-6, IL-8 and tumour necrosis factor- α (TNF- α)) using a human ultra-sensitive 4-plex (Meso Scale Discovery (MSD)). CRP levels were measured as part of the standard chemistry panel. Samples for cytokine analysis were collected in sodium heparin (Greiner) tubes. In addition, the effect of an *in vivo* LPS challenge on cytokine release (IL-1 β , IL-6, IL-8, TNF- α) induced by an *ex vivo* LPS challenge was studied. Blood samples were collected in sodium heparin tubes (Greiner) before and 6, 12, 24, 48 and 72 h after the *in vivo* LPS administration. Whole blood cultures were prepared with a 1:1 dilution with RPMI 1640 medium and incubated with LPS (*E. coli* O111:B4, manufactured by Sigma-Aldrich, Saint Louis, Missouri, USA, catalog number L-3012, approximately 10 EU/ng) for 24 h at 37°C, 5% CO₂. Cultures were centrifuged and supernatants were used for cytokine assessment using the earlier mentioned cytokine 4-plex with a 20-fold dilution. Whole blood cultures were performed by Good Biomarker Sciences, Leiden, The Netherlands.

STATISTICAL ANALYSIS Statistical analysis was performed for circulating inflammatory markers and *ex vivo*-induced cytokines, which were log-transformed prior to analysis. These repeatedly measured parameters were analysed with a mixed model of variance with treatment, time, and treatment by time as fixed factors and subject as random factor and the baseline measurement as covariate. A variance

components (co)variance structure was used to model the within-subject errors, the Kenward-Roger approximation to estimate denominator degrees of freedom and the restricted maximum likelihood method to estimate model parameters. Contrasts were calculated within the model for each parameter over the following time profiles: baseline to 6 h post-dose for circulating cytokines; baseline to 24 h post-dose for CRP; and at 6 h post-dose for *ex vivo*-induced cytokines. The general treatment effect and specific contrasts were reported with the estimated difference, the 95% confidence interval (CI), the least square mean (LSM) estimates and the *p*-value. Graphs of the LSM estimates over time by treatment present 95% CI as error bars and change from baseline LSM estimates. All analyses were performed using SAS® For Windows Version 9.1.3 (SAS Institute, Cary, North Carolina, USA).

Results

SAFETY MONITORING Single intravenous low doses of LPS were well tolerated in healthy male subjects. Observed adverse events (AEs) were of mild severity and self-limiting without therapeutic intervention. The most frequent occurring AEs, probably or possibly related to treatment, were headache, observed in 66.7% of the LPS-treated subjects and 33.3% of the placebo-treated subjects and feeling cold, observed in 44.4% of the LPS-treated subjects and none of the placebo-treated subjects. No clinically relevant changes or unexpected treatment-related trends were observed in supine systolic and diastolic blood pressure, body temperature, or ECG-derived parameters following administration of LPS (Figure 1). LPS dose-dependently increased body temperature and heart rate, with a maximal increase amounting approximately 1.5°C and 28 ± 13.2 bpm for the highest LPS dose tested, observed at 3-4 h after LPS administration.

LPS administration resulted in a dose-dependent decrease in monocyte count (maximal change from baseline -1.9 ± 2.3, -4.8 ± 3.6 and -7.7 ± 1.5% at 6 h post-LPS for doses of 0.5, 1 and 2 ng/kg, respectively), returning to baseline levels within 12 to 24 h post-LPS (data not shown). In addition, LPS administration resulted in decreased blood platelet count levels (minimal change from baseline of -15 ± 9.4, -28 ± 14.4, and -31 ± 9.1*10⁹/L at 4 h post-dose, data not shown) and an increase in neutrophil count (maximum change from baseline 25.8 ± 3.5, 40.4 ± 9.5, and 42.9 ± 6.2% at 4 h post-LPS for doses of 0.5, 1 and 2 ng/kg, respectively) and leukocyte count (maximum change from baseline 4.0 ± 1.3, 4.4 ± 1.2, 6.3 ± 1.4*10⁹/L at 4-6 h post-LPS), returning to baseline at 12-24 h post-dose (data not shown). Eosinophil, erythrocyte, lymphocyte, and basophil counts and haematocrit and haemoglobin

slightly decreased after LPS administration, with maximal changes observed 4 h after LPS administration (data not shown).

Activated partial thromboplastin time (APTT) was variable over the day, ranging from -0.7 to +0.9 s around a baseline of 29.3 ± 1.8 s. LPS administration resulted in a decrease in APTT, with an estimated difference of -2.0 s (*p*=0.0151) at 1 ng/kg LPS and a maximal mean decrease from baseline of -3.9 s at 4 h post-LPS (Figure 2). Although the decrease in APTT upon administration of 2 ng/kg LPS was comparable in size, this difference did not reach a level of statistical significance (*p*=0.1233). An effect of LPS administration on prothrombin time (PT) was not observed (data not shown).

CIRCULATING INFLAMMATORY MARKERS CRP levels were low in the placebo-treated group (data not shown; baseline concentration 0.85 ± 1.08 mg/L, with a minimal variability over time of maximally 0.30 ± 0.55 mg/L). LPS administration dose-dependently increased CRP, maximal levels observed 24 h post-dose (11.31 ± 6.73, 15.15 ± 3.93, and 18.42 ± 5.15 mg/L for LPS doses of 0.5, 1 and 2 ng/kg, respectively, Figure 3A; all contrasts presented for the complete time profile up to 24 h post-dose, *versus* placebo, *p*<0.0001). In the placebo-treated group, circulating cytokine levels were minimal (Figure 3B-D). LPS administration resulted in a dose-dependent increase in TNF-α, IL-6, and IL-8, with maximal levels amounting 221.9 ± 61.2, 314.8 ± 130.9 and 329.4 ± 84.4 pg/mL, respectively. Maximal concentrations were reached at 1.5-3 h after LPS administration. For all LPS dose levels tested, contrasts for cytokine release *versus* placebo (time interval 0-6 h post-dose) reached a distinct level of significance (*p*<0.0001). In a considerable number of samples, IL-1β levels were below the limit of quantification (LOQ, 0.6 pg/mL, data not shown). In general, higher levels of IL-1β were observed with increasing LPS doses. For all subjects in the 2 ng/kg dose group, IL-1β levels above LOQ could be detected 3-6 h post-LPS, ranging from 0.7 to 2.6 pg/mL. No statistical analysis was performed for IL-1β.

EX-VIVO LPS-INDUCED CYTOKINE RELEASE *Ex vivo* LPS-induced IL-1β, IL-6, IL-8 and TNF-α release was variable over time, as observed in the placebo-treated subjects (Figure 4). *In vivo* LPS administration dose-dependently decreased *ex vivo* LPS-induced TNF-α release at the highest two dose levels tested in the first hours after the *in vivo* LPS challenge (Figure 4A). Maximal mean reduction was observed at 6 h post-dose with an estimated difference (95% CI) of -66.4% (-81.4 to -39.0%) and -74.7% (-86.0 to -54.3%) for 1 and 2 ng/kg, respectively, which differed significantly from placebo (Table 1, *p*=0.0005 and *p*<0.0001 for 1 and 2 ng/kg, respectively).

Subsequently, TNF- α release increased and exceeded levels as observed for the placebo group at 12 h post-LPS. *Ex vivo* LPS-induced IL-1 β release basically mirrored the patterns observed for TNF- α release, with a maximal mean reduction at 6 h post-LPS with an estimated difference (95% CI) of -65.8% (-79.5 to -43.1%) and -84.7% (-90.8 to -74.5%; Figure 4B and Table 1; $p < 0.0001$ and $p < 0.0001$ versus placebo for 1 and 2 ng/kg, respectively), and a return to placebo levels at approximately 12 h post-dose. An *in vivo* LPS challenge at 1 and 2 ng/kg significantly inhibited the *ex vivo* LPS-induced release of IL-6 lasting for approximately 12 h post-LPS and a maximal effect at 6 h with an estimated difference (95% CI) of -31.3% (-50.8 to -4.0%) and -41.3% (-58.1 to -17.8%; Figure 4C and Table 1; $p = 0.0283$ and $p = 0.0024$ versus placebo for 1 and 2 ng/kg, respectively). Remarkably, *ex vivo* IL-6 release increased after the *in vivo* administration of 0.5 ng/kg LPS, peaking at 6 h post-LPS and almost significantly exceeding cytokine levels observed for placebo-treated subjects with an estimated difference (95% CI) of 34.8% (-3.1 to 87.5% (Figure 4C and Table 1; $p = 0.0754$ versus placebo). A same response was observed for *ex vivo* IL-8 release: *in vivo* administration of LPS resulted in an increased IL-8 response to an *ex vivo* LPS challenge for the two lowest LPS doses tested with an estimated difference (95% CI) of 55.1% (-6.6 to 157.5%) and 19.2% (-28.8 to 99.5%; Figure 4D and Table 1; at 6 h, $p = 0.0879$ and $p = 0.4961$ versus placebo, for 0.5 and 1 ng/kg, respectively), but not for the 2 ng/kg dose. The observed increases in IL-8 release were followed by a strong decrease up to 12 h post-dose, which was consistent for all LPS doses tested (Figure 4D).

Discussion

Human endotoxaemia has been applied frequently as a controlled and standardized model of systemic inflammation providing mechanistic insight in molecular and physiological inflammatory pathways. The *in vivo* LPS challenge can also be applied as methodological tool in clinical pharmacology studies to assess the effects of specific interventions (medicinal or non-medicinal) on the inflammatory response in healthy volunteers. This experimental model has been studied extensively, and commonly applies relatively high LPS doses (2-4 ng/kg body weight) (1, 4-8). However, such relatively high LPS doses are not preferred for reasons mentioned, and characterization of a human endotoxaemia model applying lower LPS dose levels is desired. Therefore, we performed a study to characterize the human inflammatory response induced by low LPS doses administered to healthy volunteers. In addition, we explored the effects of an *in vivo* LPS

challenge on the inflammatory response induced by subsequent *ex vivo* LPS challenges. Although it is known from literature that an *in vivo* LPS challenge induces hyporesponsiveness to subsequent *in vivo* or *ex vivo* LPS challenges (2, 3, 12-18), the exact time course of this phenomenon and relation to LPS dose level is unclear.

Administration of low LPS doses (0.5-2 ng/kg) to healthy volunteers was well tolerated and safe; all reported AEs were of mild severity and self-limiting, and no unexpected treatment-related trends in vital signs or ECG recordings nor in urinary or blood laboratory parameters were measured. LPS administration dose-dependently increased body temperature and heart rate with maximum levels observed at 3-4 h post-dose (change to baseline of approximately 1.5°C and 28 \pm 13.2 bpm). Observed changes in haematology parameters were expected as a result of LPS treatment (5, 8, 20, 21) and subject hydration from 2 h pre-dose till 6 h post-dose. Furthermore, LPS administration temporarily inhibited APTT, with a maximal decrease from baseline of approximately 3-4 s at 4 h post-LPS, in line with previously reported LPS effects on coagulation (22, 23). There is a close interaction between coagulation and inflammation pathways (24, 25). Stimulation of monocytes with endotoxin results in an increased expression of tissue factor, the main initiator of coagulation (23, 26, 27). Based on this observation an increase in PT levels was expected via the extrinsic pathway, however, this could not be confirmed by the results from our study due to a high variability over the 24 h time profile. Cytokines such as IL-6 and TNF- α are the main mediators of inflammation-induced coagulation (28, 29). Whereas changes in temperature and heart rate after an *in vivo* LPS challenge could serve as a pharmacodynamic readout measure for pharmacological or dietary interventions, APTT effect size and contrast versus placebo of an *in vivo* LPS challenge were limited.

In vivo LPS administration dose-dependently increased circulating CRP and cytokine levels (TNF- α , IL-6 and IL-8). Maximal CRP levels were observed 24 h post-LPS and maximal cytokine levels were observed 1.5-3 h post-LPS. A single intravenous dose of LPS as low as 0.5 ng/kg induced a distinct inflammatory response in the healthy volunteers.

A power calculation was performed which showed that in a parallel study design, at an LPS dose level of 0.5 ng/kg, a sample size of eight subjects per treatment group would provide 80% power to detect a 28% inhibition in the LPS-induced TNF- α response, at a two-sided significance level of 0.05. Under the same conditions, it would be possible to demonstrate an inhibition of the LPS-induced cytokine response of 53% and 49% for IL-6 and CRP, respectively. Given the fact that the inter-subject variability on log scale is well comparable between different LPS doses, this power calculation also applies for LPS doses of 1 and 2 ng/kg.

Circulating IL-1 β levels were low and for the majority of the samples tested the level was below LOQ (0.6 pg/mL). However, in the highest LPS dose group tested, an increase in circulating IL-1 β levels could be demonstrated at 3-6 h post-LPS, with observed IL-1 β levels ranging from 0.7 to 2.6 pg/mL. This is in contrast with IL-1 β release following an *ex vivo* LPS challenge of whole blood cultures, which caused the release of substantial amounts of IL-1 β . Reports from other human endotoxaemia experiments also note IL-1 β responses are very low or lacking, despite high circulating levels of IL-6 and TNF- α (30-35). Interestingly, even in cases of severe sepsis, IL-1 β can be detected in only a small fraction of patients and corresponds weakly with disease severity (36). However it can be acutely induced in response to certain surgical procedures, and is implicated in many chronic inflammatory conditions, such as diabetes, cardiovascular disease, and rheumatoid arthritis. Since IL-1 β expression is limited to inflammasome activation and requires multiple signals (37, 38), this suggests that low-dose human endotoxaemia may be insufficient to induce systemic IL-1 β . LPS stimulation in whole blood cultures also induces cell death, which may facilitate inflammasome activation and induce substantial IL-1 β release as seen in our *ex vivo* LPS experiment.

In vivo LPS administration induced LPS hyporesponsiveness as evidenced by *ex vivo* cytokine release of IL-1 β , IL-6 and TNF- α . This hyporesponsiveness was LPS dose-dependent. Although the kinetics of endotoxin hyporesponsiveness have been described previously, the exact time course of the hyporesponsiveness is not well documented (4). Here we demonstrate that LPS-induced hyporesponsiveness of specific cytokines reached a maximum at 6 h after the *in vivo* LPS challenge, and lasted no longer than 12 h. Interestingly, it has been reported that attenuated cytokine responses *in vivo* persisted for at least 2 weeks (4). This indicates that there is a significant discrepancy between the LPS hyporesponsiveness measured after an *in vivo* LPS challenge, for which the tissue-resident macrophages, migrating leukocytes and endothelial cells are implicated to be the main sources of cytokine production, and an *ex vivo* LPS challenge, for which only the circulating leukocytes are the source of cytokine release and there is no active clearance of endotoxin since the system is closed (4, 39). The fact that the estimated duration of the derangement of the immune system induced by an *in vivo* LPS challenge is dependent on the selected methodology (assessment by *ex vivo* LPS challenge or *in vivo* LPS challenge) should be carefully taken into account when designing future clinical pharmacology studies applying *in vivo/ex vivo* LPS challenges, and this process should be driven by the nature and mechanism of action of the investigational product.

Interestingly, patterns for *ex vivo* LPS-induced IL-8 release (at all *in vivo* LPS doses tested) and IL-6 release (at the lowest *in vivo* LPS dose tested) differed from the patterns observed for IL-1 β and TNF- α : a preceding *in vivo* LPS challenge caused an increased cytokine release after an *ex vivo* LPS challenge, rather than an inhibition of cytokine release. It may be well possible that immune cells were primed by the low-dose *in vivo* LPS challenge, resulting in an augmented IL-8 and IL-6 responses after *ex vivo* LPS stimulation. Priming of innate immune cells by low endotoxin levels has been described before, and allows the immune system to elicit a strong inflammatory response against potential pathogens (2). Although priming of the murine immune system has been explored rather extensively, the underlying mechanisms in human immunology are poorly understood. Pre-treatment of murine macrophage cells with very low doses of LPS results in an augmented cytokine production after subsequent LPS stimulation, which is LPS concentration-dependent (40-42). In general it should be noted that humans are much more sensitive to LPS than mice, indicating the relative poor feasibility of murine models to support human endotoxin responses (43). The fact that, dependent on the *in vivo* LPS dose applied and specific cytokine measured, either LPS hyporesponsiveness or LPS priming is observed in a relatively narrow LPS dose range (0.5-2 ng/kg) indicates that a delicate balance exists between endotoxin hyporesponsiveness and endotoxin priming, which is still to be characterized in more detail.

It should be noted that sample collection tubes used for *ex vivo* LPS challenges contained an endotoxin-like contamination. Although the exact level of contamination could not be expressed in relative endotoxin units, additional experiments indicated that the contamination was TLR4-specific. As a consequence of this contamination, *ex vivo* LPS challenges were performed at an endotoxin level resulting in a maximal TLR4-mediated response (EC_{100}) rather than the anticipated sub-maximal response level (EC_{80}), which was believed not to affect study outcomes.

Conclusion

Overall, our experiments demonstrate that human endotoxaemia induced by commonly applied relatively high LPS doses (exceeding 2 ng/kg) can be avoided: application of LPS doses as low as 0.5 ng/kg result in significant responses in routine safety markers (e.g. temperature, blood pressure and heart rate) and

circulating cytokine levels that can function as pharmacodynamic markers. As such, the low-dose LPS challenge has been demonstrated to be a feasible methodological tool for future clinical studies exploring pharmacological or nutritional immune-modulating effects. An *in vivo* LPS challenge induced immune cell hyporesponsiveness or immune cell priming (dependent on *in vivo* LPS dose and cytokine readout), determined by repeated *ex vivo* LPS challenges, but the duration of these effects was limited. These results indicate that a combination of *in vivo* LPS administration and repeated *ex vivo* LPS challenges can be applied in clinical pharmacology studies.

FIGURE 1 Vital signs: temperature (°C, A), heart rate (bpm, B), systolic blood pressure (mmHg, C), diastolic blood pressure (mmHg, D), change from baseline with standard deviation as error bars.

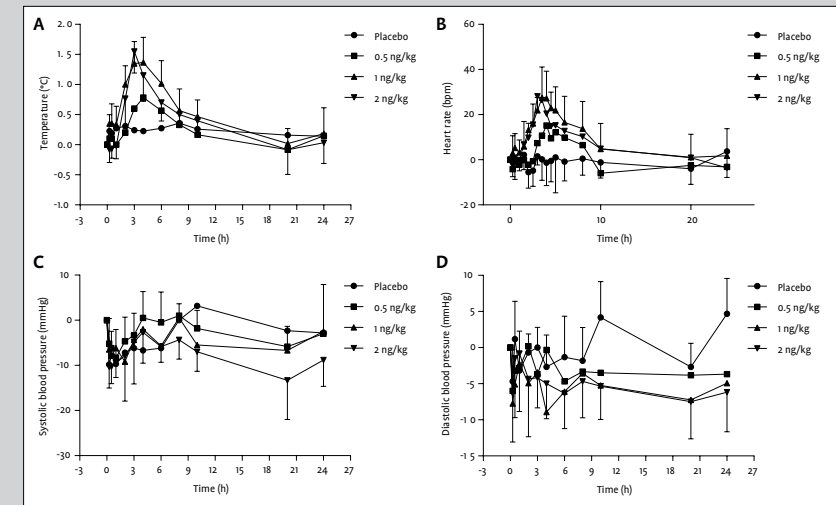


FIGURE 2 Activated partial thromboplastin time (APTT) least square mean change from baseline profile, with 95% confidence interval as error bars.

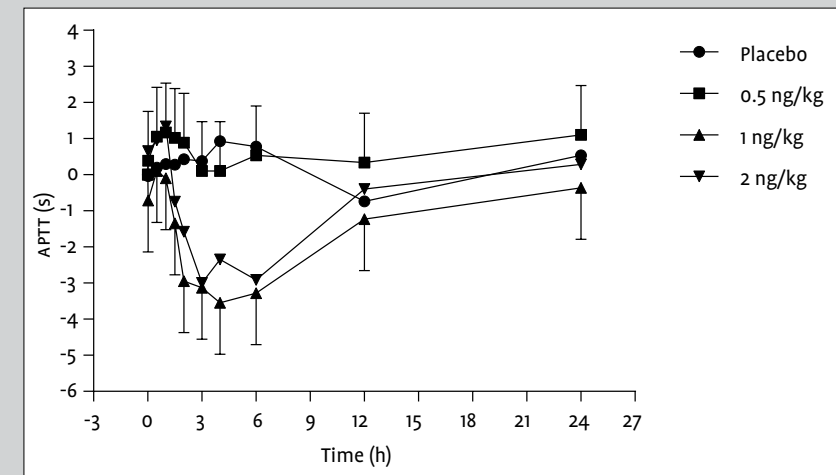


FIGURE 3 C-reactive protein (CRP, A) time profile graph, with standard deviation as error bars; tumour necrosis factor- α (TNF- α , B), interleukin (IL)-6 (C), IL-8 (D) time profile graphs up to 6 h, with standard deviation as error bars.

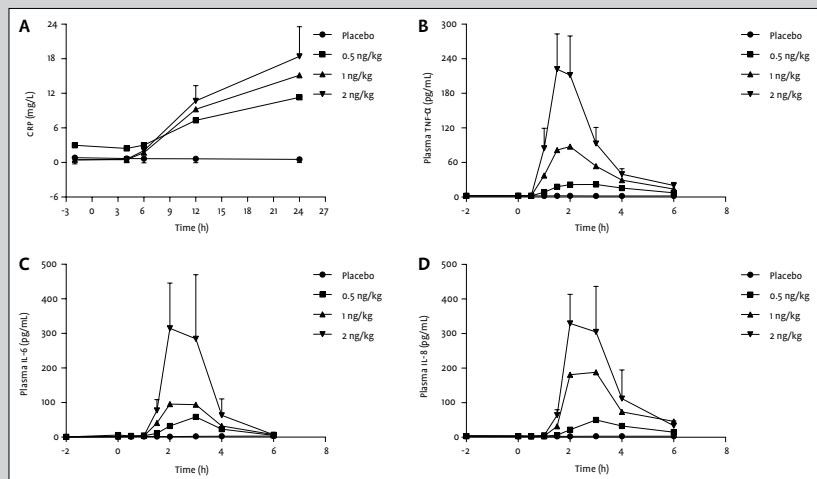


FIGURE 4 Tumour necrosis factor- α (TNF- α , A), interleukin (IL)-1 β (B), IL-6 (C), IL-8 (D) after *ex vivo* lipopolysaccharide (LPS) challenge (10 EU/ng, 24 h incubation) least square mean change from baseline profile, with 95% confidence interval as error bars, *in vivo* LPS challenge at t=0.

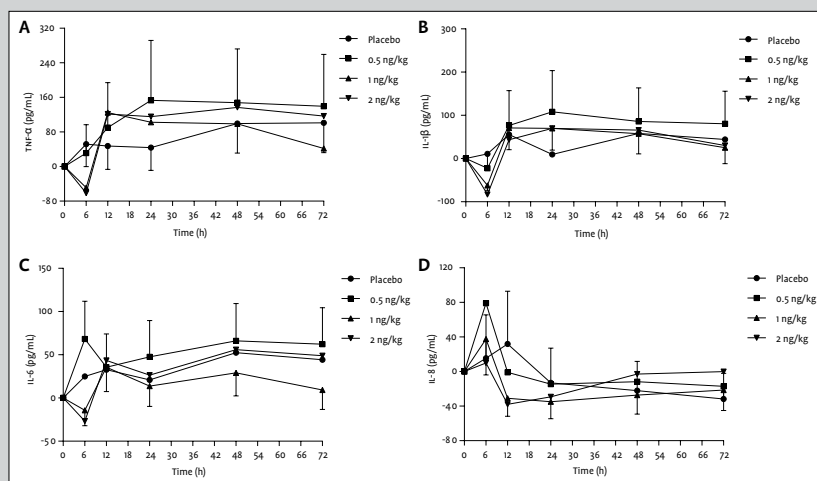


TABLE 1 Contrasts of analysis of covariance at 6 h post-dose after *ex vivo* lipopolysaccharide challenge.

	0.5 ng/kg vs. placebo		1 ng/kg vs. placebo		2 ng/kg vs. placebo	
	Estimated difference (%)	p-value	Estimated difference (%)	p-value	Estimated difference (%)	p-value
TNF- α	-13.6	0.6256	-66.4	0.0005	-74.7	<0.0001
IL-1 β	-30.0	0.1606	-65.8	<0.0001	-84.7	<0.0001
IL-6	34.8	0.0754	-31.3	0.0283	-41.3	0.0024
IL-8	55.1	0.0879	19.2	0.4961	-4.8	0.8475

IL: interleukin; TNF- α : tumour necrosis factor- α ; vs.: versus.

REFERENCE LIST

- 1 Andreassen AS, Krabbe KS, Krogh-Madsen R, Taudorf S, Pedersen BK, Moller K. Human endotoxemia as a model of systemic inflammation. *Curr Med Chem.* 2008;15(17):1697-705.
- 2 Fu Y, Glaros T, Zhu M, Wang P, Wu Z, Tyson JJ, et al. Network topologies and dynamics leading to endotoxin tolerance and priming in innate immune cells. *PLoS Comput Biol.* 2012;8(5):e1002526.
- 3 Fujihara M, Muroi M, Tanamoto K, Suzuki T, Azuma H, Ikeda H. Molecular mechanisms of macrophage activation and deactivation by lipopolysaccharide: roles of the receptor complex. *Pharmacol Ther.* 2003;100(2):171-94.
- 4 Kox M, de Kleijn S, Pompe JC, Ramakers BP, Netea MG, van der Hoeven JG, et al. Differential *ex vivo* and *in vivo* endotoxin tolerance kinetics following human endotoxemia. *Crit Care Med.* 2011;39(8):1866-70.
- 5 Draisma A, Pickkers P, Bouw MP, van der Hoeven JG. Development of endotoxin tolerance in humans *in vivo*. *Crit Care Med.* 2009;37(4):1261-7.
- 6 van der Poll T, Coyle SM, Moldawer LL, Lowry SF. Changes in endotoxin-induced cytokine production by whole blood after *in vivo* exposure of normal humans to endotoxin. *J Infect Dis.* 1996;174(6):1356-60.
- 7 de Vos AF, Pater JM, van den Pangaart PS, de Kruij MD, van 't Veer C, van der Poll T. *In vivo* lipopolysaccharide exposure of human blood leukocytes induces cross-tolerance to multiple TLR ligands. *J Immunol.* 2009;183(1):533-42.
- 8 van Eijk LT, van der Pluijm RW, Ramakers BP, Dorresteyn MJ, van der Hoeven JG, Kox M, et al. Body mass index is not associated with cytokine induction during experimental human endotoxemia. *Innate Immun.* 2013;20(1):61-7.
- 9 Ferguson JF, Mulvey CK, Patel PN, Shah RY, Doveikis J, Zhang W, et al. Omega-3 PUFA supplementation and the response to evoked endotoxemia in healthy volunteers. *Mol Nutr Food Res.* 2013;58(3):601-13.
- 10 Nieuwdorp M, Meuwese MC, Mooij HL, van Lieshout MH, Hayden A, Levi M, et al. Tumor necrosis factor- α inhibition protects against endotoxin-induced endothelial glycocalyx perturbation. *Atherosclerosis.* 2009;202(1):296-303.
- 11 Draisma A, de Goeij M, Wouters CW, Riksen NP, Oyen WJ, Rongen GA, et al. Endotoxin tolerance does not limit mild ischemia-reperfusion injury in humans *in vivo*. *Innate Immun.* 2009;15(6):360-7.
- 12 Morris M, Li L. Molecular mechanisms and pathological consequences of endotoxin tolerance and priming. *Arch Immunol Ther Exp (Warsz).* 2012;60(1):13-8.
- 13 Kobayashi K, Hernandez LD, Galan JE, Janeway CA, Jr., Medzhitov R, Flavell RA. IRAK-M is a negative regulator of Toll-like receptor signaling. *Cell.* 2002;110(2):191-202.
- 14 Sly LM, Rauh MJ, Kalesnikoff J, Song CH, Krystal G. LPS-induced upregulation of SHIP is essential for endotoxin tolerance. *Immunity.* 2004;21(2):227-39.
- 15 Chang J, Kunkel SL, Chang CH. Negative regulation of MyD88-dependent signaling by IL-10 in dendritic cells. *Proc Natl Acad Sci U S A.* 2009;106(43):18327-32.
- 16 Brint EK, Xu D, Liu H, Dunne A, McKenzie AN, O'Neill LA, et al. ST2 is an inhibitor of interleukin 1 receptor and Toll-like receptor 4 signaling and maintains endotoxin tolerance. *Nat Immunol.* 2004;5(4):373-9.
- 17 Nakagawa R, Naka T, Tsutsui H, Fujimoto M, Kimura A, Abe T, et al. SOCS-1 participates in negative regulation of LPS responses. *Immunity.* 2002;17(5):677-87.
- 18 Kinjyo I, Hanada T, Inagaki-Ohara K, Mori H, Aki D, Ohishi M, et al. SOCS1/AB is a negative regulator of LPS-induced macrophage activation. *Immunity.* 2002;17(5):583-91.
- 19 Schaaf B, Luitjens K, Goldmann T, van Bremen T, Sayk F, Dodt C, et al. Mortality in human sepsis is associated with downregulation of Toll-like receptor 2 and CD14 expression on blood monocytes. *Diagn Pathol.* 2009;4:12.
- 20 van 't Veer C, van den Pangaart PS, van Zoelen MA, de Kruij M, Birjmohun RS, Stroes ES, et al. Induction of IRAK-M is associated with lipopolysaccharide tolerance in a human endotoxemia model. *J Immunol.* 2007;179(10):7110-20.
- 21 Sivapalaratnam S, Farrugia R, Nieuwdorp M, Langford CF, van Beem RT, Maiwald S, et al. Identification of candidate genes linking systemic inflammation to atherosclerosis; results of a human *in vivo* LPS infusion study. *BMC Med Genomics.* 2011;4:64.
- 22 Ungerstedt JS, Soop A, Sollevi A, Blomback M. Bedside monitoring of coagulation activation after challenging healthy volunteers with intravenous endotoxin. *Thromb Res.* 2003;111(6):329-34.
- 23 de Jonge E, Dekkers PE, Creasey AA, Hack CE, Paulson SK, Karim A, et al. Tissue factor pathway inhibitor dose-dependently inhibits coagulation activation without influencing the fibrinolytic and cytokine response during human endotoxemia. *Blood.* 2000;95(4):1124-9.
- 24 Levi M, van der Poll T, Buller HR. Bidirectional relation between inflammation and coagulation. *Circulation.* 2004;109(22):2698-704.
- 25 Esmon CT. The interactions between inflammation and coagulation. *Br J Haematol.* 2005;131(4):417-30.
- 26 Levi M, van der Poll T, ten Cate H. Tissue factor in infection and severe inflammation. *Semin Thromb Hemost.* 2006;32(1):33-9.
- 27 Franco RF, de Jonge E, Dekkers PE, Timmerman JJ, Spek CA, van Deventer SJ, et al. The *in vivo* kinetics of tissue factor messenger RNA expression during human endotoxemia: relationship with activation of coagulation. *Blood.* 2000;96(2):554-9.
- 28 Stouthard JM, Levi M, Hack CE, Veenhof CH, Romijn HA, Sauerwein HP, et al. Interleukin-6 stimulates coagulation, not fibrinolysis, in humans. *Thromb Haemost.* 1996;76(5):738-42.
- 29 van der Poll T, Buller HR, ten Cate H, Wortel CH, Bauer KA, van Deventer SJ, et al. Activation of coagulation after administration of tumor necrosis factor to normal subjects. *N Engl J Med.* 1990;322(23):1622-7.
- 30 van Deventer SJ, Buller HR, ten Cate JW, Aarden LA, Hack CE, Sturk A. Experimental endotoxemia in humans: analysis of cytokine release and coagulation, fibrinolytic, and complement pathways. *Blood.* 1990;76(12):2520-6.
- 31 van Eijk LT, Dorresteyn MJ, Smits P, van der Hoeven JG, Netea MG, Pickkers P. Gender differences in the innate immune response and vascular reactivity following the administration of endotoxin to human volunteers. *Crit Care Med.* 2007;35(6):1464-9.
- 32 Coyle SM, Calvano SE, Lowry SF. Gender influences *in vivo* human responses to endotoxin. *Shock.* 2006;26(6):538-43.
- 33 Michie HR, Manogue KR, Spriggs DR, Revhaug A, O'Dwyer S, Dinarello CA, et al. Detection of circulating tumor necrosis factor after endotoxin administration. *N Engl J Med.* 1988;318(23):1481-6.
- 34 Van Zee KJ, Coyle SM, Calvano SE, Oldenburg HS, Stiles DM, Pribble J, et al. Influence of IL-1 receptor blockade on the human response to endotoxemia. *J Immunol.* 1995;154(3):1499-507.
- 35 Dorresteyn MJ, van Eijk LT, Netea MG, Smits P, van der Hoeven JG, Pickkers P. Iso-osmolar prehydration shifts the cytokine response towards a more anti-inflammatory balance in human endotoxemia. *J Endotoxin Res.* 2005;11(5):287-93.
- 36 Blackwell TS, Christman JW. Sepsis and cytokines: current status. *Br J Anaesth.* 1996;77(1):110-7.
- 37 Netea MG, Nold-Petry CA, Nold MF, Joosten LA, Opitz B, van der Meer JH, et al. Differential requirement for the activation of the inflammasome for processing and release of IL-1 β in monocytes and macrophages. *Blood.* 2009;113(10):2324-35.
- 38 Martinon F, Burns K, Tschopp J. The inflammasome: a molecular platform triggering activation of inflammatory caspases and processing of proIL-1 β . *Mol Cell.* 2002;10(2):417-26.
- 39 Dorresteyn MJ, Draisma A, van der Hoeven JG, Pickkers P. Lipopolysaccharide-stimulated whole blood cytokine production does not predict the inflammatory response in human endotoxemia. *Innate Immun.* 2010;16(4):248-53.
- 40 West MA, Koons A. Endotoxin tolerance in sepsis: concentration-dependent augmentation or inhibition of LPS-stimulated macrophage TNF secretion by LPS pretreatment. *J Trauma.* 2008;65(4):893-8.
- 41 Hirohashi N, Morrison DC. Low-dose lipopolysaccharide (LPS) pretreatment of mouse macrophages modulates LPS-dependent interleukin-6 production *in vitro*. *Infect Immun.* 1996;64(3):1011-5.
- 42 Deng H, Maitra U, Morris M, Li L. Molecular mechanism responsible for the priming of macrophage activation. *J Biol Chem.* 2013;288(6):3897-906.
- 43 Munford RS. Murine responses to endotoxin: another dirty little secret? *J Infect Dis.* 2010;201(2):175-7.

CHAPTER 6

**Clinical evaluation of
Humira® biosimilar ONS-3010
in healthy volunteers:
focus on pharmacokinetics and
pharmacodynamics**

Frontiers in Immunology, 2016 Nov, 7(508)6

M.R. Dillingh, J.A.A. Reijers, K.E. Malone, J. Burggraaf,
K. Bahrt, L. Yamashita, C. Rehrig, M. Moerland

ABSTRACT

ONS-3010 is being developed by Oncobiologics Inc. (Cranbury, New Jersey, USA) as a biosimilar of Humira®. This randomized, double blind, single-centre phase I study (Eudract registration # 2013-003551-38) was performed to demonstrate pharmacokinetic biosimilarity between two reference products (Humira® EU and US) and ONS-3010 in healthy volunteers, and to compare the safety and immunogenicity profiles. In addition, the intended pharmacological activity was assessed and compared by application of a whole blood challenge.

Hundred-ninety-eight (198) healthy volunteers received a single 40 mg subcutaneous dose of ONS-3010, Humira® EU or US. The pharmacodynamic effects were assessed by lipopolysaccharide (LPS)/aluminium hydroxide whole blood challenges ($n=36$; $n=12$ per treatment arm; male:female, 1:1).

Equivalence was demonstrated on the pharmacokinetic endpoints (AUC_{0-inf} , C_{max} and AUC_{0-last}) based on bounds of 80-125% for the ratio of the geometric means (ONS-3010/Humira®). The immunogenicity profiles were comparable between treatment groups and there were no indications for differences in routine safety parameters. Administration of adalimumab resulted in the observation of dramatically reduced TNF- α levels upon stimulation with LPS/aluminium hydroxide (>99%), with no differences between the three treatment groups in terms of magnitude or duration. Adalimumab also resulted in a reduction of LPS/aluminium hydroxide-induced IL-8 release (maximally 30%), suggested to have a causal relationship with the anti-TNF- α treatment. LPS/aluminium hydroxide-induced release of IL-1 β and IL-6 was not inhibited by anti-TNF- α treatment.

Taken together, these data are promising for the further clinical development of ONS-3010, demonstrate the relevance of the LPS/aluminium challenge to monitor Humira® effects, and emphasize the value of whole blood challenges for monitoring of proximal drug effects in healthy volunteers, and potentially in the target population.

Introduction

Biotherapeutic adalimumab (Humira®, AbbVie Inc, North Chicago, Illinois, USA) is a recombinant human IgG1 monoclonal antibody binding tumour necrosis factor- α (TNF- α), which is one of the earliest and most potent cytokines mediating inflammatory responses (1). TNF- α is produced primarily by activated macrophages but also by CD4+ lymphocytes, natural killer (NK) cells, neutrophils, mast cells, eosinophils, and neurons. Binding of TNF- α to its receptor, TNF receptor type 1 (TNFR1) or TNF receptor type 2 (TNFR2), results in downstream activation of caspase, nuclear factor- κ -B (NF κ B), c-Jun N-terminal kinase (JNK) or mitogen-activated protein kinase (MAPK) pathways (2). TNF- α is an autocrine stimulator as well as a potent paracrine inducer of interleukin (IL)-1, IL-6, IL-8 and other inflammatory cytokines (3). Blockage of TNF- α therefore not only results in inhibition of direct TNF effects but also has a more general effect on inflammation (3, 4). Inactivation of TNF- α has proven to be important in downregulating the inflammatory and immune reactions associated with rheumatoid arthritis and other autoimmune conditions (3, 5-10). Adalimumab binds specifically to TNF- α , blocks its interaction with TNFR1 and TNFR2 and lyses surface TNF- α -expressing cells *in vitro* in the presence of complement. Adalimumab also modulates biological responses induced or regulated by TNF- α , including changes in the levels of adhesion molecules responsible for leukocyte migration (11).

The development of products that are designed as a biosimilar of the original licensed product has gained interest over recent years because of expiring patents of originator's biotherapeutic products. This is also the case for Humira®: the patent is expected to expire in December 2016 in the US and in April 2018 in the EU. Per US Food and Drug Administration (FDA) and European Medicines Agency (EMA) guidelines, demonstration of biosimilarity between test and reference biotherapeutics comprises quality characteristics, pharmacokinetic (PK) properties, biological activity, safety and efficacy (12-16). Although the FDA and EMA recommend to include pharmacodynamic (PD) endpoints in biosimilarity studies whenever feasible, no guidance is provided on the clinical development phase in which PD endpoints may be included. Assessing PD effects only in advanced phases of clinical development bears the risk of late discovery of non-biosimilarity, as was the case for Alpheon, recombinant human interferon (IFN)- α -2a (17). The addition of PD endpoints in early biosimilarity studies could add valuable information for the evaluation of overall comparability of products.

ONS-3010 is being developed by Oncobiologics Inc. (Cranbury, New Jersey, USA) as a biosimilar of Humira®. A phase I clinical study was performed to demonstrate

PK biosimilarity between two reference products (the EU and US approved forms of Humira®) and ONS-3010 in healthy volunteers, and to compare the safety and immunogenicity profile of ONS-3010 with the two registered forms of Humira®. In addition, the intended pharmacological activity of the three products was assessed and compared by application of a whole blood challenge. In this model, robust activation of Toll-like receptor 4 (TLR4)-driven NFKB signaling and the NALP3/NLRP3 inflammasome pathway is induced in circulating immune cells by incubation of freshly isolated whole blood with lipopolysaccharide (LPS) and aluminium hydroxide (18-22). NFKB signaling generates an inflammatory response characterized by TNF- α , IL-6, IL-8, IL-1 β and IFN- γ release (23), whereas inflammasome activation results in further enhancement of IL-1 β responses and secretion of IL-18 and IL-33 (21, 24, 25). TLR4 and inflammasome pathways are implicated in the pathogenesis of autoimmune diseases such as rheumatoid arthritis (26-28), and TNF- α blockade specifically alters these responses by its effect on NFKB, playing a key role in NLRP3 priming (26, 29). Application of LPS/aluminium hydroxide whole blood challenges in this healthy volunteer trial not only allowed early assessment of the intended PD activity of ONS-3010 in comparison with the two reference products, but also provided mechanistic insight into the secondary effects of TNF- α blockade.

Methods

STUDY DESIGN The bioequivalence study was a randomized, double blind, single-centre phase I study with three treatment arms: ONS-3010 (Oncobiologics Inc, Cranbury, New Jersey, USA) and reference products Humira® EU (AbbVie, Berkshire, UK) and Humira® US (AbbVie, North Chicago, USA, Eudract registration # 2013-003551-38). The study was performed in a total number of 198 volunteers, who were deemed healthy, and screened negative for (latent) tuberculosis, acute infectious disease, malignancy, and autoimmune disorders. All women of child bearing potential and all males had to practice effective contraception during the study and had to be willing and able to continue contraception for at least 5 months after dose administration of study treatment to be able to participate in the study. In addition, the subjects had to have a negative screening result for Hepatitis B/C and HIV and smoking was prohibited during the complete study period. Sixty-six (66) subjects per treatment arm received a single subcutaneous dose of 40 mg TNF- α antibody according to a randomization schedule which was stratified for gender. Pharmacokinetic, immunogenicity and safety analyses were conducted for all 198 study participants. The PD effects of these three TNF- α

blockers were assessed by LPS/aluminium hydroxide whole blood challenges, for which 36 subjects were randomly selected from the three treatment arms (six male and six female subjects per arm). Before the LPS/aluminium hydroxide whole blood challenges were implemented as a PD bioassay in the clinical study, the effect of TNF- α blockade on the LPS/aluminium hydroxide-induced inflammatory response was explored in an *in vitro* experiment (see below).

The phase I clinical trial was conducted in accordance with the Declaration of Helsinki and Guideline for Good Clinical Practice, and was approved by the Independent Ethics Committee of the Foundation 'Evaluation of Ethics in Biomedical Research', Assen, The Netherlands.

PHARMACOKINETIC ANALYSIS Plasma concentrations of adalimumab (ONS-3010, Humira® EU or Humira® US) following a single 40 mg subcutaneous dose administration were assessed in blood samples collected in 4 mL SST™ Gel and Clot Activator tubes (Becton Dickinson), from day 1 (pre-dose) up to day 71 (post-dose). An electrochemiluminescence assay (Meso Scale Discovery (MSD)) was developed and validated to measure the concentration of adalimumab in human serum. Data values below the limit of quantification (BLOQ, 250 ng/mL) were set to 125 ng/mL (50% of the limit of quantification, LOQ) for summarizing and graphical purposes. If more than one third of all values were BLOQ for a specific time point/treatment combination, the data point was not included in the summary/graph. For PK analysis, BLOQ data points were set to zero when not embedded between two measurable data points (i.e. >BLOQ) and occurring prior to the time at the observed maximum concentration (t_{max}). BLOQ data points were excluded from PK analysis when not embedded between two measurable data points and occurring after t_{max} , or when embedded between two measurable data points.

LPS/ALUMINIUM HYDROXIDE WHOLE BLOOD CHALLENGE Preceding the phase I clinical trial, the effect of *in vitro* TNF- α blockade on LPS/aluminium hydroxide-induced cytokine release in whole blood samples was explored. Blood specimens were obtained from four healthy male volunteers in sodium heparin tubes (Becton Dickinson). Fresh whole blood was (pre-) incubated in 96-well plates with Humira® EU at 37°C at 5% CO₂. The Humira® concentration ranged from 0.3125 to 10 μ g/mL, which was based on the expected maximum concentrations of 4.7 \pm 1.6 μ g/mL, observed after a single administration of 40 mg (11). After 90 min, 2 ng/mL LPS (Sigma-Aldrich, St Louis, Missouri, USA) and 100 μ g/mL Alhydrogel 85 (aluminium hydroxide, Brenntag, Frederikssund, Denmark) were added to the samples followed by an additional incubation period of 20 h. In the clinical study, LPS/aluminium hydroxide whole blood challenges were performed in a subset of study

participants, pre-dose (day 1) and on day 5, day 15, day 29 and day 64. Conditions for the whole blood challenges were similar as for the *in vitro* experiment above, except for the fact that the incubations were performed in a larger volume (2 mL), and no pre-incubation with Humira® EU was performed. Cytokine release was measured in the culture supernatants by an electrochemiluminescence assay (MSD, V-plex; TNF- α , IL-1 β , IL-6, IL-8 and IFN- γ , intra- and inter-assay variation: <10%) or enzyme-linked immunosorbent assay (ELISA, R&D Systems; IL-18).

IMMUNOGENICITY Blood samples for analysis of adalimumab-associated antibodies against ONS-3010 and Humira® were collected in 4 mL SST™ Gel and Clot Activator tubes (Becton Dickinson). A bridging ELISA assay was used to measure anti-adalimumab antibodies in serum samples by electrochemiluminescence. Positive immunogenicity samples were further investigated to confirm the specificity of binding. If a sample was confirmed positive for specific anti-adalimumab antibodies the neutralizing capacity of these antibodies was investigated. Binding specificity was determined by competitive inhibition with 5 mg/mL of unlabelled ONS-3010; samples with an inhibition >20.7% were confirmed positive for anti-drug antibody. Assay sensitivity was 2.463 ng/mL and inter-run assay precision 5.143%-11.354%.

ROUTINE SAFETY ASSESSMENTS Pre-dose (day 1) and on day 2 (haematology only), day 4, day 8, day 36 and day 72, blood and urine samples were collected for routine haematology, biochemistry and urinalysis safety parameter assessments. In addition, general safety measures such as vital signs, electrocardiography and symptoms were assessed throughout the study.

DATA ANALYSIS Demographic and PD data were summarized and presented by graphical and tabular presentations. For the inhibition of TNF- α and IFN- γ release after incubation with LPS/aluminium hydroxide and increasing adalimumab concentrations *in vitro*, a model was fitted to the data in R (v2.15.2, R Foundation for Statistical Computing, Vienna, Austria, 2012) and described by a maximal effect (E_{max}) and half maximal effect concentrations (EC_{50}).

A non-compartmental analysis was performed to describe the PK of the antibodies using software. The area under the curve (AUC) was computed from zero to the last measurement point (AUC_{0-last}). If the terminal phase was sufficiently well characterized (at least three data points after t_{max} and a linear regression $r^2 \geq 0.5$), the terminal half-life ($t_{1/2}$) and the AUC zero to infinity (AUC_{0-inf}) were estimated. PK profiles of the investigational product (ONS-3010) and the reference

products (Humira® EU and Humira® US) were compared using general linear model procedures in SAS®. An analysis of variance (ANOVA) was performed on the untransformed elimination rate constant (k_{el}), apparent terminal elimination half-life ($t_{1/2el}$) and ln-transformed AUC_{0-last} , AUC_{0-inf} , and C_{max} . The ANOVA model included treatment as a fixed effect. The ratio of means with the 90% geometric confidence interval (CI) was calculated for AUC_{0-last} , AUC_{0-inf} , and C_{max} . Bioequivalence was evaluated in accordance with EMA and FDA guidelines on the investigation of bioequivalence (30, 31). The hypothesis of bioequivalence for the PK parameters AUC_{0-last} , AUC_{0-inf} , and C_{max} was supported with 90% CI for the relative geometric means ratio fully enclosed in the equivalence bounds of 80-125%.

Results

DEMOGRAPHICS A total number of 90 male and 108 female subjects aged between 18 and 55 years, with a body mass index of 19-29 kg/m² and a body weight >50 kg were enrolled in the clinical trial with both sexes equally divided over the three treatment groups (ONS-3010 and Humira® EU/US, Figure 1 and Table 1).

PHARMACOKINETIC ANALYSIS Five subjects (four Humira® US; one Humira® EU) had an incomplete PK profile as a result of early study termination and therefore PK parameters could not be determined accurately. These participants were excluded from the statistical analysis on total exposure parameters (e.g. AUC_{0-last}). Two of these subjects had a PK profile up to 7 and 8 days, based on which C_{max} and t_{max} could be determined, and these data were included in the statistical analysis (Table 2).

Subcutaneous administration of adalimumab resulted in a steady increase in plasma concentrations starting at approximately 36 h post-dose to reach a maximum concentration after 6-7 days, followed by a log-linear decrease and a non-linear decrease once the plasma concentration reached lower levels, similar to other monoclonal antibodies (Figure 2). Large variability in antibody concentration was observed between subjects during the elimination phase, with some subjects having adalimumab plasma concentration levels BLOQ (<250 ng/mL) 5 weeks after dosing, while others continued to have measurable levels up to the last study visit (day 71). On the primary PK endpoints, AUC_{0-inf} and C_{max} , equivalence was demonstrated based on bounds of 80-125% for the ratio of the geometric means (ONS-3010/Humira®; Table 3). Equivalence was also demonstrated for secondary PK endpoint AUC_{0-last} .

LPS/ALUMINIUM HYDROXIDE WHOLE BLOOD CHALLENGE In a separate experiment preceding the clinical study, the effect of *in vitro* TNF- α blockade on LPS/aluminium hydroxide-induced cytokine release in whole blood samples was explored. Addition of adalimumab to the LPS/aluminium hydroxide-triggered whole blood samples resulted in dramatically reduced TNF- α levels measured in the culture supernatant. An average reduction in TNF- α level of $97 \pm 0.6\%$ was observed already at the lowest adalimumab concentration evaluated ($0.3125 \mu\text{g/mL}$), as compared to the LPS/aluminium hydroxide only samples. With increasing concentrations of adalimumab, further reductions in TNF- α levels were measured, up to $99 \pm 0.1\%$. In addition, TNF- α blockade affected the LPS/aluminium hydroxide-induced release of IFN- γ with a maximal reduction of $93 \pm 4\%$ observed at an adalimumab concentration of $10 \mu\text{g/mL}$. The adalimumab concentration-effect curves for TNF- α and IFN- γ are presented in Figure 3, with an E_{max} of 99% and 97% and an EC_{50} of $0.006 \mu\text{g/mL}$ and $0.6 \mu\text{g/mL}$ for TNF- α and IFN- γ , respectively. Increasing concentrations of adalimumab did not affect the release of IL-6, IL-1 β and IL-18 following LPS/aluminium hydroxide stimulation of whole blood (data not shown).

In the clinical study, adalimumab treatment resulted in a more than 99% reduction in measurable TNF- α levels in LPS/aluminium hydroxide-triggered whole blood samples (Figure 4A). This effect was maximal at the first time point investigated (day 5), and lasted until at least 3 weeks post-dose. Thereafter, TNF- α levels started to return to baseline with individual time courses depending on the adalimumab plasma concentration. On average, TNF- α levels were still approximately 85% reduced at the last time point investigated (day 64). The reduction in TNF- α levels did not differ between the three treatment groups.

LPS/aluminium hydroxide-induced release of IL-1 β and IL-6 was not inhibited by TNF- α blockade (Figure 4B, C). For all treatment groups, a slight increase over baseline cytokine levels was observed on day 29, both for IL-1 β (50%, 25% and 17% for treatment ONS-3010, Humira[®] EU and Humira[®] US, respectively) and IL-6 (25%, 29% and 19%). Administration of adalimumab resulted in a reduction of LPS/aluminium hydroxide-induced IL-8 release (Figure 4D). Minor differences were observed between treatment groups, with maximal reductions observed on day 5 (ONS-3010, -24% (CV 56%)) and day 15 (Humira[®] EU, -29% (CV 28%); Humira[®] US, -30% (CV 44%)), and a return to baseline levels between day 29 and day 64. Whereas adalimumab inhibited LPS/aluminium hydroxide-induced IFN- γ release in the preclinical *in vitro* experiment, this effect could not be confirmed in the clinical study. IFN- γ release was highly variable between subjects and BLOQ (<114 pg/mL) in the baseline samples of 21 out of the total number of 36 participants. IFN- γ release strongly differed between males and females with mean baseline

values of $1308 \pm 1803 \text{ pg/mL}$ and $144 \pm 278 \text{ pg/mL}$, respectively. Also for the other cytokines (TNF- α , IL-1 β , IL-6 and IL-8) sex differences were observed, but to a lesser extent (cytokine release on average 1.6-fold higher in the male subjects, data not shown).

IMMUNOGENICITY AND IMMUNE CELL COUNTS The immunogenicity profiles were well comparable between the ONS-3010, Humira[®] EU and Humira[®] US treatment groups for the confirmed and neutralizing antibodies (Table 4). Adalimumab administration resulted in a mild decrease in neutrophil count, amounting maximally 15-20% at day 8, and returning to baseline levels after 5 weeks (Figure 5A). Furthermore, adalimumab administration induced a mild increase in lymphocyte count, peaking 3 days after dose administration (Figure 5B). There were no indications for differences between treatment groups in neutrophil and lymphocyte cell counts over time.

Discussion

A phase I clinical study was performed to demonstrate biosimilarity between ONS-3010 and two reference adalimumab products (the EU and US approved forms of Humira[®]) in healthy volunteers. For the PK endpoints ($AUC_{0-\text{inf}}$, C_{max} , $AUC_{0-\text{last}}$) equivalence was demonstrated between ONS-3010 and the marketed products, based on bounds of 80-125% for the ratio of the geometric means (ONS-3010/Humira[®]). The immunogenicity profiles were comparable between treatment groups for the confirmed and neutralizing antibodies and there were no indications for differences between treatment groups in routine safety parameters, including neutrophil and lymphocyte cell counts. The adverse events (AEs) which were reported most frequently (probably, possibly or unlikely related to treatment) were a burning sensation upon injection at injection site, headache and nasopharyngitis. In general, the AEs were evenly divided over the treatments, mild in severity, and self-limiting. In addition to PK, safety and immunogenicity, the intended pharmacological activity of the compounds was assessed in this study using whole blood LPS/aluminium challenges. This PD endpoint was included to reduce the risk of late discovery of non-biosimilarity for the intended drug effect, even though this approach is rarely applied in biosimilarity trials in healthy volunteers. An LPS/aluminium challenge was used to induce TLR4-driven NF κ B signaling and NALP3/NLRP3 inflammasome activation. Both pathways are implicated in the pathogenesis of autoimmune diseases for which Humira[®] is being prescribed.

Preceding the clinical study, the effect of TNF- α blockade on LPS/aluminium hydroxide-induced cytokine release in whole blood samples was verified *in vitro*. TNF- α blockade resulted in dramatically reduced TNF- α levels (maximally 99%) measured in the culture supernatant. IFN- γ release was also strongly affected, with a maximal reduction of 93%. Previous studies also described a reduced production of IFN- γ following the use of TNF- α blockers. However, the underlying mechanism for the observed inhibition is not fully elucidated (32-34). IFN- γ can be produced by a variety of cells including T- and B-lymphocytes, antigen-presenting cells, and NK cells (35). NK cells are probably an important source of IFN- γ in our model. IFN- γ production is NF κ B-driven and supported by IL-12 and IL-18 (36-38). TNF- α may act synergistically with these cytokines, explaining the reduced IFN- γ release observed in our experiment.

In contrast to the effect on IFN- γ release, *in vitro* TNF- α blockade did not modulate the release of IL-1 β , IL-6 and IL-18. Although TNF- α -induced NF κ B signaling drives transcription of various cytokines, the unaffected IL-1 β , IL-6 and IL-18 release upon TNF- α blockade suggests that primary LPS-driven responses are sufficient to induce maximal cytokine release, and that secondary signaling via LPS-induced TNF- α does not augment the LPS-driven response.

The adalimumab induced reduction in TNF levels upon stimulation with LPS/aluminium hydroxide could be reproduced in the clinical samples of ONS-3010 and Humira[®] treated subjects. Treatment resulted in a more than 99% reduction in detectable TNF- α levels in the whole blood culture supernatant. The reduction in TNF- α levels did not differ between the three treatment groups in terms of magnitude or duration. Surprisingly, whereas adalimumab inhibited LPS/aluminium hydroxide-induced IFN- γ release in the preclinical *in vitro* experiment, this effect could not be confirmed in the clinical study. As described in the Section “Results”, the inter-individual variability in IFN- γ levels was substantial, and a large number of data points was BLOQ (<114 pg/mL). Strikingly, a major difference in IFN- γ release was observed between male and female subjects (baseline levels 1308 and 144 pg/mL, respectively). These data are in contrast to studies reporting no significant differences in IFN- γ cytokine levels between both sexes (39, 40) and we are not aware of studies reporting the existence of sex-dependent IFN- γ release. The different responsiveness in IFN- γ release observed in the current study upon TLR4/inflammasome stimulation may relate to sex differences in circulating cell populations producing IFN- γ , or hormonal influences that play a role in this specific immune response (41). IL-1 β , IL-6 and IL-8 responses were comparable for the three treatment groups. In line with the results from the preclinical *in vitro* experiment, LPS/aluminium hydroxide-induced release of IL-1 β and IL-6 was not

inhibited by anti-TNF- α treatment in the clinical study. In contrast, administration of adalimumab did result in a reduction of LPS/aluminium hydroxide-induced IL-8 release. A maximal decrease of approximately 30% was observed at day 15. Although this effect size is limited and the inter-individual variability relatively large, the timing of the IL-8 decrease suggests a causal relationship with the anti-TNF- α treatment. This observation may be explained by the role of TNF- α as an autocrine stimulator and a potent paracrine inducer of inflammatory cytokines (3), although the duration of the IL-8 reduction (i.e. shorter than the TNF- α reduction) and the absent effect on IL-6 release raises questions about the responsible mechanism.

The advised Humira[®] dose for the treatment of rheumatoid arthritis is 40 mg (11). Our data demonstrate that 40 mg adalimumab results in maximally reduced TNF- α levels in LPS-/aluminium-exposed whole blood cultures, persisting for at least a month (Figure 4A). During this period, the corresponding adalimumab concentrations ranged from 3800 (t_{max}) to 1050 ng/mL (day 36, Figure 2). A comparable adalimumab concentration range also resulted in a maximal reduction of TNF- α levels in our preclinical *in vitro* experiment (Figure 3), which demonstrates the excellent translatability between *in vitro* and *ex vivo* TNF- α blocking in an LPS/aluminium challenge model.

Importantly, our *in vitro* TNF- α blockade experiment shows that a dose of 40 mg Humira[®], which is applied in clinical practice, is a rational dose based on the observed PD effects in this study: circulating adalimumab concentrations below 1 μ g/mL (Figure 2, after day 36) translated into a sub-maximal reduction of LPS-/aluminium-induced TNF- α levels (Figure 4). Taken together, these data demonstrate the relevance of the LPS/aluminium challenge to monitor Humira[®] effects, and emphasize the value of whole blood challenges for monitoring of proximal drug effects in healthy volunteers, and potentially in the target population.

In conclusion, this healthy volunteer study demonstrated equivalence for PK endpoints and closely comparable PD biomarker profiles between ONS-3010 and the marketed Humira[®]. The immunogenicity profiles were well comparable between treatment groups, and there were no indications for differences in routine safety parameters. These data are promising for the further clinical development of ONS-3010, and underline the value of incorporation of PD measures in early clinical phase biosimilar trials.

FIGURE 1 Subject disposition.

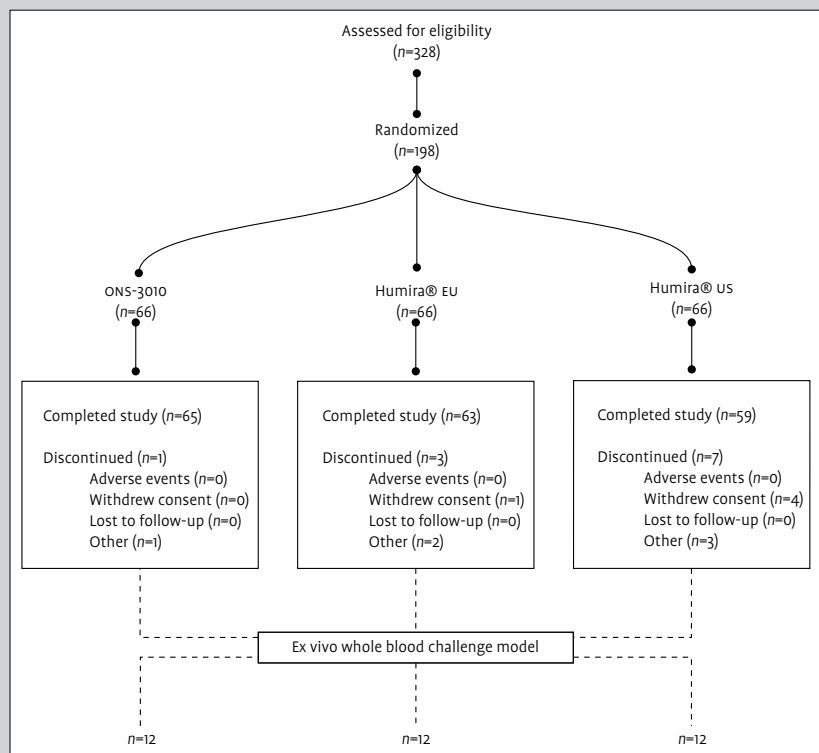


FIGURE 2 Adalimumab concentration-time profile for ONS-3010, Humira® EU and Humira® US with standard deviation as error bars; vertical line at day 1 denotes dosing.

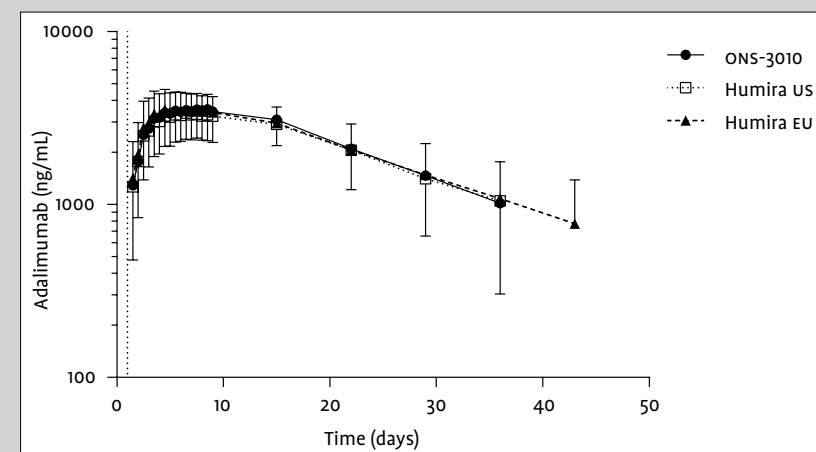


FIGURE 3 Mean reduction of *in vitro* tumour necrosis factor- α (TNF- α) and interferon- γ (IFN- γ) release (% with standard deviation as error bars; error bars smaller than the data point markers are not visible) after lipopolysaccharide (LPS)/aluminium hydroxide stimulation and incubation with increasing concentrations of adalimumab; curve fit presented as dotted line.

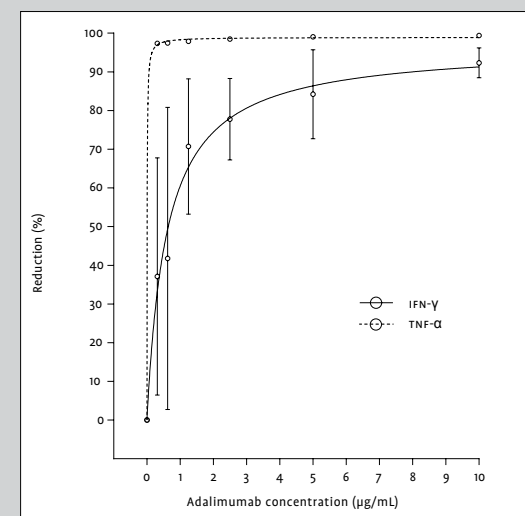


FIGURE 4 Tumour necrosis factor- α (TNF- α , A), interleukin (IL)-1 β (B), IL-6 (C) and IL-8 (D) release after *ex vivo* lipopolysaccharide (LPS)/aluminium hydroxide stimulation of blood samples collected from clinical study participants (change from baseline (CFB), %, with standard deviation as error bars).

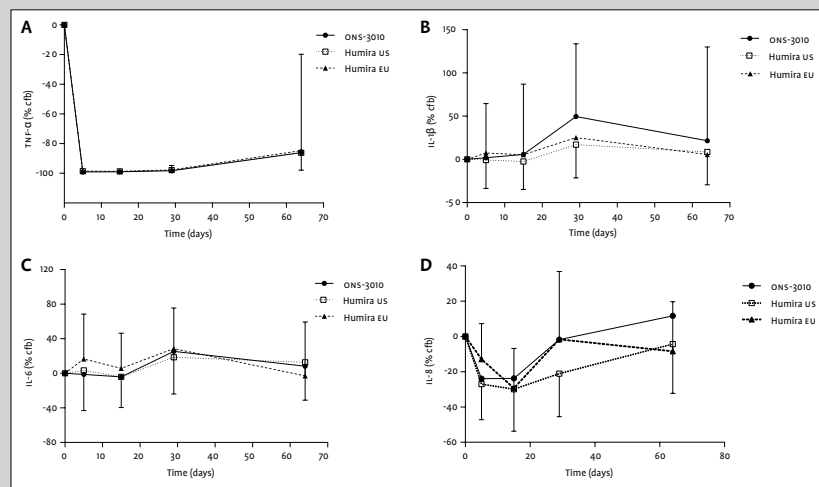


FIGURE 5 Neutrophil (A) and lymphocyte (B) count with standard deviation as error bars; vertical line at day 1 denotes dosing.

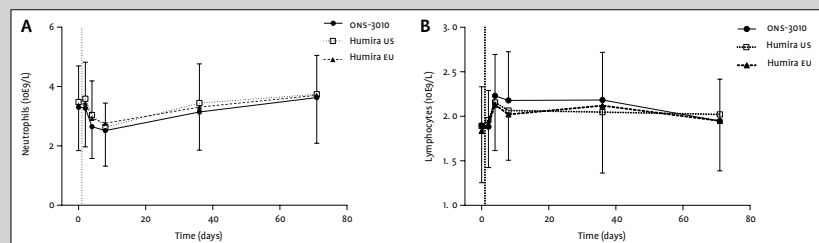


TABLE 1 Demographics and baseline characteristics.

	Humira® EU	Humira® US	ONS-3010
Age (years)			
n	66	66	66
Mean (sd)	25.4 (8.4)	25.6 (9.0)	25.9 (9.3)
Height (cm)			
n	66	65	66
Mean (sd)	175.8 (8.6)	176.8 (9.5)	177.3 (8.4)
Weight (kg)			
n	66	66	66
Mean (sd)	72.0 (11.1)	72.4 (11.5)	71.5 (9.4)
BMI (kg/m ²)			
n	66	66	66
Mean (sd)	23.2 (2.6)	23.1 (2.6)	22.7 (2.2)
Sex			
Female	36 (55%)	36 (55%)	36 (55%)
Male	30 (45%)	30 (45%)	30 (45%)
Race			
Asian	2 (3%)	0 (0%)	1 (2%)
Black or African American	7 (11%)	1 (2%)	5 (8%)
Hispanic or Latino	0 (0%)	2 (3%)	0 (0%)
White	50 (76%)	56 (85%)	58 (88%)
Mixed	6 (9%)	7 (11%)	2 (3%)

BMI: body mass index; SD: standard deviation.

TABLE 2 Non-compartmental pharmacokinetic analysis.

	ONS-3010 (n=66)	Humira® EU (n=66)	Humira® US (n=66)
AUC _{0-inf} (ng*h/mL)	2680234 (995883)	2631077 (1077199)	2577967 (1112632)
AUC _{0-last} (ng*h/mL)	2325364 (870647)	2376523 (891150)	2304145 (941728)
C _{max} (ng/mL)	3869 (842)	3898 (987)	3692 (1030)
t _{max} (h)	146 (59)	134 (70)	152 (82)
t _{1/2} (h)	317 (191)	307 (178)	318 (194)

Data are presented as mean (standard deviation). AUC: area under the curve; C_{max}: maximum concentration; t_{max}: time at observed maximum concentration; t_{1/2}: terminal half-life.

TABLE 3 Non-compartmental pharmacokinetic analysis – Contrasts of analysis of variance.

	Humira® EU vs. Humira® US			ONS-3010 vs. Humira® US			ONS-3010 vs. Humira® EU		
	Contrast	90% CI	p-value	Contrast	90% CI	p-value	Contrast	90% CI	p-value
AUC _{0-inf} (ng*h/mL)	1.04	0.92-1.17	0.6365	1.06	0.94-1.20	0.4061	1.03	0.91-1.16	0.7141
AUC _{0-last} (ng*h/mL)	1.05	0.92-1.20	0.5118	1.01	0.89-1.15	0.8705	0.96	0.85-1.09	0.6160
C _{max} (ng/mL)	1.07	0.99-1.15	0.1811	1.06	0.98-1.15	0.1899	1.00	0.92-1.08	0.9746

AUC: area under the curve; CI: confidence interval; C_{max}: maximum concentration; vs.: versus.

TABLE 4 Confirmed and neutralizing antibodies.

	Confirmed antibodies			Neutralizing antibodies		
	ONS-3010 (n=63)*	Humira® EU (n=62)*	Humira® US (n=65)*	ONS-3010 (n=66)	Humira® EU (n=65)**	Humira® US (n=66)
Day 15	20	17	13	8	8	3
Day 43	31	28	25	31	24	24
Day 57	39	38	37	41	37	37

Samples with normalized inhibition <0.886 were deemed positive for neutralizing antibodies. Subjects with a positive result for confirmed (*) and neutralizing (**) antibodies pre-dose, were excluded.

REFERENCE LIST

- Dillingham MR, Poelgeest van EP, Malone KE, Kemper EM, Stroes ESG, Moerland M, et al. Characterization of inflammation and immune cell modulation induced by low-dose LPS administration to healthy volunteers. *Journal of Inflammation*. 2014;11:28.
- Faustman D, Davis M. TNF receptor 2 pathway: drug target for autoimmune diseases. *Nat Rev Drug Discov*. 2010;9(6):482-93.
- Choy EH, Panayi GS. Cytokine pathways and joint inflammation in rheumatoid arthritis. *N Engl J Med*. 2001;344(12):907-16.
- Butler DM, Maini RN, Feldmann M, Brennan FM. Modulation of proinflammatory cytokine release in rheumatoid synovial membrane cell cultures. Comparison of monoclonal anti TNF-ALpha antibody with the interleukin-1 receptor antagonist. *Eur Cytokine Netw*. 1995;6(4):225-30.
- Gall JS, Kalb RE. Infliximab for the treatment of plaque psoriasis. *Biologics*. 2008;2(1):115-24.
- Gottlieb AB. Infliximab for psoriasis. *J Am Acad Dermatol*. 2003;49(2 Suppl):S112-57.
- Lipsky PE, van der Heijde DM, St Clair EW, Furst DE, Breedveld FC, Kalden JR, et al. Infliximab and methotrexate in the treatment of rheumatoid arthritis. Anti-Tumor Necrosis Factor Trial in Rheumatoid Arthritis with Concomitant Therapy Study Group. *N Engl J Med*. 2000;343(22):1594-602.
- Punzi L, Podswiadek M, Sfriso P, Oliviero F, Fiocco U, Todesco S. Pathogenetic and clinical rationale for TNF-blocking therapy in psoriatic arthritis. *Autoimmun Rev*. 2007;6(8):524-8.
- van Deventer SJ. Tumour necrosis factor and Crohn's disease. *Gut*. 1997;40(4):443-8.
- Weinblatt ME, Keystone EC, Furst DE, Moreland LW, Weisman MH, Birbara CA, et al. Adalimumab, a fully human anti-tumor necrosis factor ALpha monoclonal antibody, for the treatment of rheumatoid arthritis in patients taking concomitant methotrexate: the ARMADA trial. *Arthritis Rheum*. 2003;48(1):35-45.
- US Food and Drug Administration (FDA) – Highlights of Prescribing Information Humira. 2008.
- European Medicines Agency (EMA) – Guideline on similar biological medicinal products containing monoclonal antibodies; EMA/CHMP/BMWP/403543/2010. 2012.
- European Medicines Agency (EMA) – Guideline on similar biological medicinal products; CHMP/437/04 Rev 1. 2014.
- European Medicines Agency (EMA) – Guideline on similar biological medicinal products containing biotechnology-derived proteins as active substance; EMA/CHMP/BMWP/42832/2005 Rev1. 2014.
- US Food and Drug Administration (FDA) – Scientific Considerations in Demonstrating Biosimilarity to a Reference Product – Guidance for Industry. 2015.
- US Food and Drug Administration (FDA) – Quality Considerations in Demonstrating Biosimilarity of a Therapeutic Protein Product to a Reference Product – Guidance for Industry. 2015.
- European Medicines Agency (EMA) – Questions and answers on recommendation for refusal of marketing application on ALPheon. 2006.
- Eisenbarth SC, Colegio OR, O'Connor W, Sutterwala FS, Flavell RA. Crucial role for the NALP3 inflammasome in the immunostimulatory properties of aluminium adjuvants. *Nature*. 2008;453(7198):1122-6.
- Hoesel B, Schmid JA. The complexity of NF-kappaB signaling in inflammation and cancer. *Mol Cancer*. 2013;12:86.
- Kawai T, Akira S. Signaling to NF-kappaB by Toll-like receptors. *Trends Mol Med*. 2007;13(11):460-9.
- Kool M, Fierens K, Lambrecht BN. Alum adjuvant: some of the tricks of the oldest adjuvant. *J Med Microbiol*. 2012;61(Pt 7):927-34.
- Li H, Nookala S, Re F. Aluminum hydroxide adjuvants activate caspase-1 and induce IL-1beta and IL-18 release. *J Immunol*. 2007;178(8):5271-6.
- Li Q, Verma IM. NF-kappaB regulation in the immune system. *Nat Rev Immunol*. 2002;2(10):725-34.
- Li H, Willingham SB, Ting JP, Re F. Cutting edge: inflammasome activation by alum and alum's adjuvant effect are mediated by NLRP3. *J Immunol*. 2008;181(1):17-21.
- Sutterwala FS, Ogura Y, Szczepanik M, Lara-Tejero M, Lichtenberger GS, Grant EP, et al. Critical role for NALP3/CIA1/Cryopyrin in innate and adaptive immunity through its regulation of caspase-1. *Immunity*. 2006;24(3):317-27.
- Guo H, Callaway JB, Ting JP. Inflammasomes: mechanism of action, role in disease, and therapeutics. *Nat Med*. 2015;21(7):677-87.
- Liu Y, Yin H, Zhao M, Lu Q. TLR2 and TLR4 in autoimmune diseases: a comprehensive review. *Clin Rev Allergy Immunol*. 2014;47(2):136-47.
- Mathews RJ, Robinson JI, Battellino M, Wong C, Taylor JC, Eyre S, et al. Evidence of NLRP3-inflammasome activation in rheumatoid arthritis (RA); genetic variants within the NLRP3-inflammasome complex in relation to susceptibility to RA and response to anti-TNF treatment. *Ann Rheum Dis*. 2014;73(6):1202-10.

Summary and Discussion

- 29 Bauernfeind FG, Horvath G, Stutz A, Alnemri ES, MacDonald K, Speert D, et al. Cutting edge: NF-kappaB activating pattern recognition and cytokine receptors license NLRP3 inflammasome activation by regulating NLRP3 expression. *J Immunol.* 2009;183(2):787-91.
- 30 US Food and Drug Administration (FDA) – Statistical Approaches to Establishing Bioequivalence – Guidance for Industry. US Food and Drug Administration 2001.
- 31 European Medicines Agency (EMA) – Guideline on the investigation of bioequivalence; CPMP/EWP/QWP/1401/98 Rev.1. 2010.
- 32 Harris J, Keane J. How tumour necrosis factor blockers interfere with tuberculosis immunity. *Clin Exp Immunol.* 2010;161(1):1-9.
- 33 Popa C, Barrera P, Joosten LA, van Riel PL, Kullberg BJ, van der Meer JW, et al. Cytokine production from stimulated whole blood cultures in rheumatoid arthritis patients treated with various TNF blocking agents. *Eur Cytokine Netw.* 2009;20(2):88-93.
- 34 Wallis RS. Reactivation of latent tuberculosis by TNF blockade: the role of interferon gamma. *J Investig Dermatol Symp Proc.* 2007;12(1):16-21.
- 35 Schroder K, Hertzog PJ, Ravasi T, Hume DA. Interferon-gamma: an overview of signals, mechanisms and functions. *J Leukoc Biol.* 2004;75(2):163-89.
- 36 Kojima H, Aizawa Y, Yanai Y, Nagaoka K, Takeuchi M, Ohta T, et al. An essential role for NF-kappa B in IL-18-induced IFN-gamma expression in KG-1 cells. *J Immunol.* 1999;162(9):5063-9.
- 37 Matsumoto S, Tsuji-Takayama K, Aizawa Y, Koide K, Takeuchi M, Ohta T, et al. Interleukin-18 activates NF-kappaB in murine T helper type 1 cells. *Biochem Biophys Res Commun.* 1997;234(2):454-7.
- 38 Weinstock JV, Blum A, Metwali A, Elliott D, Arsenescu R. IL-18 and IL-12 signal through the NF-kappa B pathway to induce NK-1R expression on T cells. *J Immunol.* 2003;170(10):5003-7.
- 39 Biancotto A, Wank A, Perl S, Cook W, Olnes MJ, Dagur PK, et al. Baseline levels and temporal stability of 27 multiplexed serum cytokine concentrations in healthy subjects. *PLoS One.* 2013;8(12):e76091.
- 40 Eikelenboom MJ, Killestein J, Uitdehaag BM, Polman CH. Sex differences in proinflammatory cytokine profiles of progressive patients in multiple sclerosis. *Mult Scler.* 2005;11(5):520-3.
- 41 Vertehelyi D, Klinman DM. Sex hormone levels correlate with the activity of cytokine-secreting cells *in vivo.* *Immunology.* 2000;100(3):384-90.

The clinical pharmacology trials described in this thesis cover different aspects of question-based drug development which is a more agile approach to drug development compared to the traditional, linear phase I-IV approach (Figure 1).

It appears that within this linear approach to drug development, collected data is integrated predominantly at the transition to the subsequent phase. Several attempts have been made to improve this linear approach and accelerate the development process, for instance by the performance of so called 'concurrent engineering' (Figure 2).

This approach has definite value since information that becomes available during, and prior to completion of, a particular development phase is utilized to already initiate the next phase, and thereby increases the speed of drug development. However, it still lacks the urgency to prioritize important research questions to prevent failure in late stages of drug development. As mentioned in the introduction of this thesis, the advantage of the non-linear question-based drug development approach (Figure 3) is the possibility to resolve existing uncertainties already in an early stage of drug development when compared to the traditional, linear approach.

It turns out that the linear approach can be useful for the development of new compounds with only limited levels of uncertainty, while a non-linear approach would be more suitable for compounds for which clinical development is more uncertain, either because of their chemical novelty or because they are affecting a rather unexplored biological mechanism.

Question-based drug development also allows for concurrent engineering and thereby allowing an information-dense and accelerated drug development process, both approaches relying on the identification of informative biomarkers. Currently, a large number of pharmaceutical companies focus on the development of (immunomodulatory) biotherapeutics such as recombinant proteins and monoclonal antibodies, developed for therapeutic and diagnostic purposes. The development of these biotherapeutics is challenging, among others due to a lack of robust efficacy data when administered to patients (2-5). Hence, the identification of selective, early phase biomarkers is particularly needed in their process of development. By the identification of these biomarkers (for instance using *in vivo* or *ex vivo* challenge models), question-based drug development together with the performance of concurrent engineering provides the opportunity to collect and connect data already in the early stages of drug development resulting in an earlier assessment of the potential value of a new (biotherapeutic) compound and a potential increase in the drug development success rates.

Human recombinant placental alkaline phosphatase (hRESCAP, chapter 2), recombinant human pentraxin-2 (PRM-151, chapters 3 and 4) and an adalimumab biosimilar (ONS-3010, chapter 6) are immunomodulatory biotherapeutics of which the early pharmacological trials are described in this thesis. These studies were all performed according to the non-linear, question-based drug development approach.

Alkaline phosphatase (ALP) is an endogenous anti-inflammatory protein and the development of a human recombinant ALP (human recombinant placental alkaline phosphatase, hRESCAP) is thought to improve the treatment of an array of chronic inflammatory diseases.

Chapter 2 described the first study in which pharmacokinetic data of this new biotherapeutic compound ($[^{14}\text{C}]$ -hRESCAP) could be successfully obtained in a small number of healthy volunteers by using microdosing combined with ultrasensitive accelerator mass spectrometry, early in the drug development. The anticipated therapeutic dose was expected to result in an approximate 3-fold increase in endogenous healthy volunteer alkaline phosphatase levels (70-100 enzymatic units/L, after the initial elimination phase). Data analysis showed dose-proportional pharmacokinetics of hRESCAP in the investigated dose range, from 53 μg (microdose) up to 5300 μg (~ 5300 enzymatic units, the anticipated therapeutic dose).

In addition to an accurate prediction of the enzyme activity at the investigated doses by the use of the microdose radioactivity levels in healthy volunteers, this study demonstrates the value of a microdosing approach in a very small cohort to directly obtain human data and to accelerate the clinical development of biotherapeutic compounds by obtaining as much product information as possible, as early as possible in drug development. Based on these results microdosing may be considered a suitable strategy for the development of novel biotherapeutics, but it should be realized that it is not a panacea since it is known that the majority of biological compounds have non-linear pharmacokinetics.

As highlighted in one of the previous paragraphs, the identification of selective biomarkers in early drug development plays an important role in question-based drug development. Application of these biomarkers requires validation and also knowledge on their sensitivity to (biotherapeutic) compounds or interventions. These studies could be challenging though, when performed in a small group of subjects as described in chapters 3 and 4 of this thesis.

PRM-151 (recombinant human pentraxin-2 (PTX-2); also known as serum amyloid P, SAP) is under development for the treatment of pulmonary fibrosis and was first investigated in a single ascending dose study. This study was performed

for dose-finding and an initial comparison between the pharmacokinetic SAP profile in healthy volunteers and (idiopathic) pulmonary fibrosis patients. The observed pharmacokinetic comparability between the two subject populations together with linear pharmacokinetics in the healthy volunteers with increasing doses of PRM-151 showed an indication of the expected pharmacokinetic profiles to be observed in (idiopathic) pulmonary fibrosis patients after administration of increasing doses, to be confirmed in a multiple dose follow-up study.

The secondary study objectives were the identification of potential biomarkers (fibrocytes, CD45+/Procollagen-1+ cells) in the patient population and the investigation of the pharmacological effect ('proof of concept') of PRM-151 treatment on the proportion of fibrocytes using a fluorescence activated cell sorter (FACS) analysis, performed in a small cohort of (idiopathic) pulmonary fibrosis patients. Even though the patient number was small ($n=3$), a decrease in the number of circulating fibrocytes was observed. These results suggested a potential beneficial effect of PRM-151 in patients with elevated fibrocyte levels and therewith, circulating fibrocytes were regarded as a potential biomarker for future (idiopathic) pulmonary fibrosis studies.

Based on the results from the multiple dose follow-up study, pharmacokinetic linearity could be confirmed with increasing doses (1, 5 and 10 mg/kg) in a larger group of idiopathic pulmonary fibrosis patients ($n=21$, chapter 4). In addition, this study was performed to investigate the therapeutic and beneficial effects of PRM-151 in more detail. Although the single ascending dose study showed a potential effect of PRM-151 on fibrocyte levels with reduced levels observed at 24 h post-dose compared to baseline, this effect could not be confirmed in the follow-up study. Due to a high intra-subject variability in whole blood fibrocyte counts within the placebo group, it was not possible to interpret the data from the PRM-151 treated patients, and therefore, no conclusions could be drawn regarding potential pharmacodynamic effects of treatment on circulating fibrocyte levels. In an attempt to lower the risk of a high intra- or inter-assay variability, a mono-centre approach would be highly advisable for the performance of these type of sensitive, delicate (laboratory) assays.

Proceeding our search for selective, early phase (and non-invasive) biomarkers, retrospective analysis of high-resolution computed tomography (HRCT) data using a quantitative imaging modality demonstrated changes consistent with well-characterized pulmonary function outcomes by a strong negative correlation between the forced vital capacity (FVC) % predicted at screening and the percentage of lung volume unoccupied by interstitial lung abnormality ($n=16$, of

which five subjects received placebo treatment). This suggests the potential value of quantitative imaging as a biomarker in future clinical trials in (idiopathic) pulmonary fibrosis patients.

The examples above demonstrate the challenges that clinical pharmacologists face when they select biomarkers for early phase clinical trials, which are designed to explore pharmacological activity of an investigational immunomodulatory compound. In healthy volunteers the drug target may not be constitutively expressed, and in early phase trials in the target population the sample sizes are commonly small, and the treatment period too short to reach effective drug exposure level and duration. A low expression level of the drug target or low activity level of the pathophysiological pathway may be overcome by the application of challenge models to mimic disease or pathophysiological pathways. The *in vivo/ex vivo* lipopolysaccharide (LPS) whole blood challenge described in chapter 5 is a human model of systemic inflammation (the human endotoxaemia model) that can be applied in clinical pharmacology studies. It allows assessment of the effects of a specific compound or intervention, and exploration of the molecular mechanisms and physiological significance of the systemic inflammatory response encountered in acute as well as chronic inflammatory conditions, in a controlled and standardized experimental setting.

In the past such *in vivo* whole blood challenges have been performed using relatively high doses of LPS (2-4 ng/kg). In these endotoxaemia models, potential effects of immune-modulating compounds or interventions may not be observed because the elicited immune response is too strong which could also result in temporary impairment of other homeostatic mechanisms. In addition, it is impossible to repeat these challenges frequently over time, most importantly due to the burden on the subject but also because administration of high doses of LPS may have severe side effects or even sustained effects.

This is exactly why cell-based (*in vitro/ex vivo*) challenge models have been developed to assess drug effects outside the human body, on primary human cells. The results from the study described in chapter 5 showed inflammatory responses in C-reactive protein (CRP), interleukin (IL)-6, IL-8 and tumour necrosis factor- α (TNF- α) levels, which were clearly distinctive from baseline levels and elicited by a low-dose *in vivo* LPS challenge (≥ 0.5 ng/kg). Besides a lower risk for the subjects to experience side effects following the administration of low doses of LPS compared to higher LPS doses, we were able to demonstrate that this particular low-dose *in vivo* challenge in combination with repeated *ex vivo* LPS challenges

is a feasible methodological tool for future clinical studies exploring pharmacological (or nutritional) immune-modulating effects based on the observed *ex vivo* LPS-induced cytokine releases following an *in vivo* LPS dose administration.

In chapter 6, the *ex vivo* LPS/aluminium whole blood challenge was implemented in a clinical biosimilarity trial on ONS-3010. This biotherapeutic compound is developed as a biosimilar of adalimumab (Humira®), suppressing the immune system by blocking the activity of TNF- α . The patents of several originator's biotherapeutic compounds, such as adalimumab, are about to expire and therefore there has been an increasing interest in the development of products that are designed as a biosimilar of these original licensed products over the last years.

The study described in chapter 6 demonstrated equivalence between ONS-3010 and the EU and US approved forms of Humira® (reference products) based on the pharmacokinetic endpoints.

Compared to small molecules drugs of which the chemical structure can usually be completely defined and reproduced, the chemical structure of proteins is more complex which results in the possibility that the development of proteins could result in structural differences from their reference product. Even a minor structural difference could have an effect on the safety and efficacy and therefore, it is important to confirm biosimilarity on pharmacokinetic and pharmacodynamic endpoints. The US Food and Drug Administration (FDA) and European Medicines Agency (EMA) guidelines recommend the inclusion of pharmacodynamic endpoints in biosimilarity studies whenever feasible, but don't provide any guidance on the clinical development phase of the new compound in which these endpoints should be included (6-10).

In the current study, *ex vivo* LPS/aluminium challenges were implemented to assess the intended pharmacological activity of ONS-3010 in healthy volunteers in comparison with the reference products in this early stage of drug development, and to provide mechanistic insight into the secondary effects of TNF- α blockade (pharmacodynamic endpoints). Closely comparable effects of treatment were observed for the pharmacodynamic biomarkers in the three treatment groups (ONS-3010, Humira® EU and US) after *ex vivo* LPS/aluminium stimulation of blood samples. These study results demonstrate the relevance to incorporate pharmacodynamic endpoints in the early stages of clinical drug development to reduce the risk on discovery of drug non-similarity in later stages, and emphasize the value of the whole blood challenge to monitor primary and secondary pharmacodynamic drug effects, in healthy volunteers and potentially in the target population, in early biosimilarity and pharmacology trials.

In conclusion, this thesis provides an extended overview of different types of clinical pharmacology studies concerned with the complicated investigation of immunomodulatory biotherapeutics in the early stage of drug development. Key factors herein are the search for selective biomarkers in healthy volunteers and patients, the development of new methods, and optimization of existing methods to improve and potentially accelerate the development process of immunomodulatory biotherapeutics.

FIGURE 1 The linear clinical drug development process.

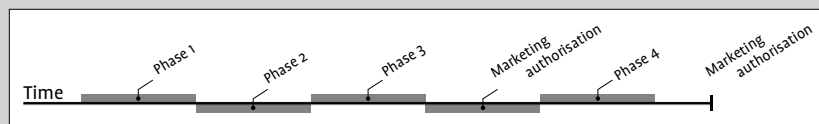


FIGURE 2 The clinical drug development process using concurrent engineering.

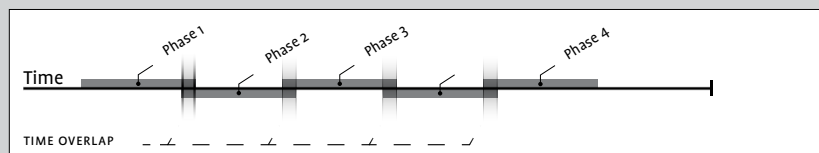
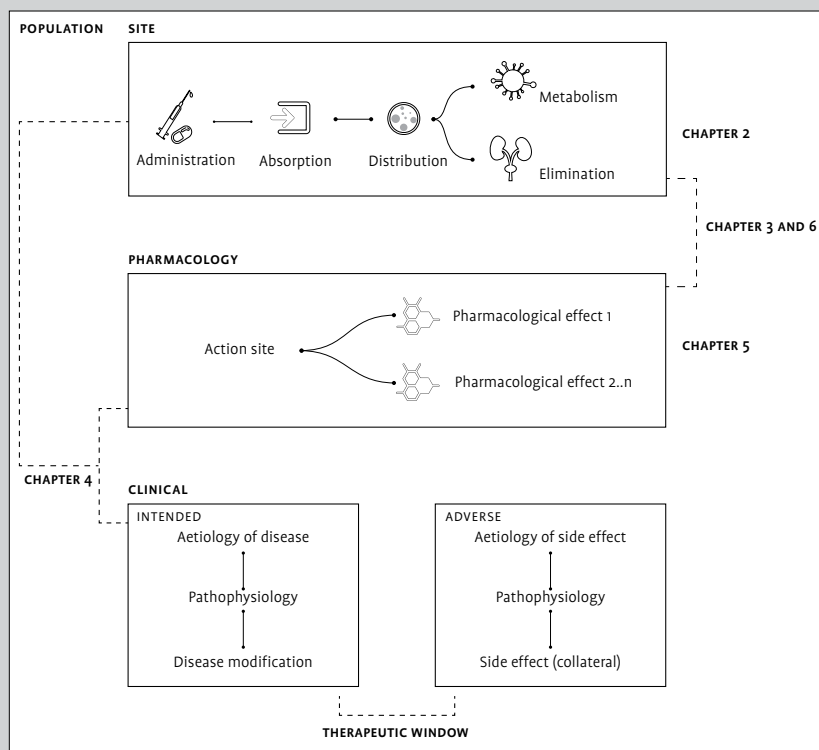


FIGURE 3 Areas of interest of question-based drug development (population, site, pharmacology, clinical and therapeutic window, source A.F. Cohen 2010 (1)).



REFERENCE LIST

- 1 Cohen AF. Developing drug prototypes: pharmacology replaces safety and tolerability? *Nat Rev Drug Discov.* 2010;9(11):856-65.
- 2 Arrowsmith J. Trial watch: Phase II failures: 2008-2010. *Nat Rev Drug Discov.* 2011;10(5):328-9.
- 3 Arrowsmith J. Trial watch: phase III and submission failures: 2007-2010. *Nat Rev Drug Discov.* 2011;10(2):87.
- 4 Denayer T, Stöhr T, Roy van M. Animal models in translational medicine: Validation and prediction. *New Horizons in Translational Medicine* 2014.
- 5 Hay M, Thomas DW, Craighead JL, Economides C, Rosenthal J. Clinical development success rates for investigational drugs. *Nat Biotechnol.* 2014;32(1):40-51.
- 6 European Medicines Agency (EMA) – Guideline on similar biological medicinal products containing monoclonal antibodies; EMA/CHMP/BMWP/403543/2010. 2012.
- 7 European Medicines Agency (EMA) – Guideline on similar biological medicinal products; CHMP/437/04 Rev 1. 2014.
- 8 European Medicines Agency (EMA) – Guideline on similar biological medicinal products containing biotechnology-derived proteins as active substance; EMEA/CHMP/BMWP/42832/2005 Rev1. 2014.
- 9 US Food and Drug Administration (FDA) – Scientific Considerations in Demonstrating Biosimilarity to a Reference Product – Guidance for Industry. 2015.
- 10 US Food and Drug Administration (FDA) – Quality Considerations in Demonstrating Biosimilarity of a Therapeutic Protein Product to a Reference Product – Guidance for Industry. 2015.

CHAPTER 8

Nederlandse samenvatting

De ontwikkeling van nieuwe geneesmiddelen is een ingewikkeld en tijdrovend proces. Het duurt gemiddeld ongeveer 12 jaar voordat een nieuw geneesmiddel uiteindelijk beschikbaar komt voor patiënten. Zodra een onderzoeksmiddel op basis van preklinische studies veilig wordt geacht voor toediening aan mensen, wordt het klinische onderzoek en de verdere ontwikkeling van het middel doorgaans opgedeeld in 4 opeenvolgende fasen: fase I-fase IV.

In de eerste fase wordt het middel voor het eerst toegediend aan een kleine groep gezonde vrijwilligers of patiënten. Uiteindelijk wordt in de laatste fase (fase IV) de effectiviteit van het geneesmiddel in een grote groep patiënten bepaald en wordt ook informatie verzameld over eventuele bijwerkingen na langdurig gebruik. Deze benadering is vooral toepasbaar voor het onderzoek naar en de ontwikkeling van onderzoeksmiddelen met een relatief geringe mate van onzekerheid en dus een hogere slagingskans hebben om op de markt te komen. De tijdslijnen van ontwikkeling zouden verkort kunnen worden door deze lineaire aanpak te combineren met het zogeheten 'concurrent engineering', waarbij een volgende fase van onderzoek wordt gestart op basis van de reeds beschikbare data alvorens die voorgaande fase volledig is afgerond.

De laatste jaren is de complexiteit van het traject voor geneesmiddelontwikkeling toegenomen. Daarvoor zijn twee belangrijke redenen aan te geven: de chemische structuur van de geneesmiddelen is complexer en/of het middel grijpt aan op een relatief onbekend biologisch mechanisme. Dit vergroot de kans dat een middel uiteindelijk niet het beoogde en gewenste therapeutische effect heeft in patiënten. Voor deze categorie geneesmiddelen, zoals bijvoorbeeld recombinante eiwitten en monoclonale antilichamen, biedt een niet-lineaire aanpak zoals de zogenoemde vraag-gestuurde geneesmiddelenontwikkeling ('question-based drug development') uitkomst. Deze aanpak is gebaseerd op het principe dat men door het stellen van de juiste (kritische) vragen in het juiste, meest relevante, stadium van onderzoek en ontwikkeling op een efficiëntere manier data verzamelt.

Binnen 'question-based drug development' speelt de identificatie van selectieve biomarkers een zeer belangrijke rol. Biomarkers kunnen worden gebruikt om bepaalde biologische- of ziekteprocessen te karakteriseren om vervolgens het farmacologisch effect van een onderzoeksmiddel te kunnen bepalen. De mogelijkheid om met behulp van biomarkers een farmacologisch effect in gezonde vrijwilligers vast te kunnen stellen is echter niet vanzelfsprekend. Dit is de reden waarom het Centre for Human Drug Research veel heeft geïnvesteerd in de ontwikkeling van diverse stimulatietesten en -modellen ('challenge models') om zo een specifieke ziekte of een specifiek pathofysiologisch proces na te kunnen bootsen en onderzoekers op die manier in de gelegenheid stelt om farmacologische effecten ook in gezonde vrijwilligers te onderzoeken. Deze stimulatietesten

en -modellen worden zowel in het menselijk lichaam (*in vivo*) als daarbuiten, in primaire humane cellen (*ex vivo/in vitro*) toegepast.

Ook binnen 'question-based drug development' kan 'concurrent engineering' worden toegepast. Het gebruik van selectieve biomarkers in combinatie met 'concurrent engineering' zal niet alleen resulteren in significant verkorte tijdslijnen met betrekking tot ontwikkeling van een potentieel geneesmiddel maar biedt ook de mogelijkheid om de waarde ervan in een eerder stadium vast te stellen. Dit leidt tot een efficiënter ontwikkelingsproces en bovendien tot eerdere identificatie van onderzoeksmiddelen die niet het gewenste therapeutische effect hebben, met een grote kostenbesparing tot gevolg. Dit proefschrift beschrijft klinisch-farmacologische onderzoeken met diverse immunomodulerende biotherapeutica en belicht daarbij verschillende aspecten van 'question-based drug development'.

Het toedienen van een microdosering (<1% van de verwachte therapeutische dosis gebaseerd op de beschikbare *in vitro* en *in vivo* farmacodynamische data, tot een maximale dosis van 100 µg of, in het geval van eiwitten, 30 nmol (1, 2)) aan een kleine groep gezonde vrijwilligers is een relatief nieuwe methode binnen klinisch geneesmiddelenonderzoek. Dit gebeurt op basis van beperkte preklinische veiligheidsdata in een zeer vroeg stadium van ontwikkeling, nog voordat er een uitgebreide fase I studie plaatsvindt. Het gebruik van een microdosering maakt het mogelijk om in een eerder stadium van ontwikkeling data in mensen te verzamelen en zo wellicht het ontwikkelingstraject van het desbetreffende middel te bespoedigen. Hoofdstuk 2 beschrijft het eerste klinische onderzoek waarbij we in staat waren de farmacokinetiek van een nieuw biotherapeutikum (humaan recombinant placentaal alkalisch fosfatase, hRESCAP) succesvol in kaart te brengen met behulp van een microdosering. Alkalisch fosfatase is een endogeen anti-inflammatoir eiwit en er zijn aanwijzingen dat hRESCAP een geschikte behandeling zou kunnen zijn voor een verscheidenheid aan chronische ontstekingsziekten. De resultaten van dit onderzoek suggereren dat microdosering ook waardevol en toepasbaar kan zijn voor onderzoek naar nieuwe recombinante eiwitten en mogelijk ook andere biotherapeutica.

In hoofdstuk 3 en 4 beschrijven we twee klinische onderzoeken met het nieuwe onderzoeksmiddel PRM-151, recombinant humaan pentraxin-2 (PTX-2), ook bekend als serum amyloid P (SAP). Dit recombinante eiwit wordt ontwikkeld voor de behandeling van longfibrose. Longfibrose is een chronische, zeer progressieve ziekte waarbij longweefsel ernstig wordt aangetast. De patiënten bij wie longfibrose wordt gediagnosticeerd hebben een levensverwachting van ongeveer drie jaar. De kwetsbaarheid van deze patiëntenpopulatie benadrukt zowel de noodzaak om een geschikte en effectieve behandeling voor deze patiënten te vinden als de noodzaak om voor klinische onderzoek uiterst selectieve en non-invasieve

biomarkers te identificeren. Naast onderzoek naar de veiligheid en verdraagbaarheid van het nieuwe onderzoeksmiddel bij toediening aan mensen was de identificatie van deze biomarkers dan ook een van de belangrijkste doelstellingen van de klinische onderzoeken die in deze hoofdstukken staan beschreven. In het eerste onderzoek werd PRM-151 voor het eerst en eenmalig aan gezonde vrijwilligers en een kleine groep longfibrose patiënten toegediend. Met deze efficiënte onderzoeksopzet kon er al in een vroeg stadium een vergelijkbare farmacokinetiek van PRM-151 worden vastgesteld in gezonde vrijwilligers en patiënten met longfibrose. In het vervolgonderzoek heeft een grotere groep longfibrose patiënten meerdere, opklimmende doses van het onderzoeksmiddel toegediend gekregen. Naast de identificatie van potentiële biomarkers tonen de onderzoeksresultaten de moeilijkheden die onderzoekers tijdens de zoektocht naar geschikte biomarkers kunnen ervaren door bijvoorbeeld een beperkte omvang van de onderzoekspopulatie, een te korte behandelperiode om effectiviteit te kunnen waarnemen of doordat het aangrijpingspunt van het potentiële geneesmiddel in beperkte mate tot expressie komt in gezonde vrijwilligers. Het gebruik van de eerder genoemde stimulatietesten en -modellen kan hierbij uitkomst bieden in het onderzoek naar de farmacologische effecten van o.a. immunomodulerende biotherapeutica.

De stimulatietesten met lipopolysaccharide (LPS) zijn een voorbeeld waarbij door middel van LPS een ontsteking in gezonde vrijwilligers kan worden nagebootst. Stimulatie met LPS kan zowel *in vivo* (intraveneuze toediening van LPS aan de gezonde vrijwilliger) als *ex vivo* (toevoeging van LPS aan een bloedmonster van de gezonde vrijwilliger) plaatsvinden. Dit biedt de mogelijkheid om de farmacologische effecten van immunomodulerende biotherapeutica ook in gezonde vrijwilligers te onderzoeken. Doorgaans wordt voor *in vivo* LPS-stimulatie gebruik gemaakt van een relatief hoge dosis LPS (2-4 ng/kg). Dit is echter niet zonder risico voor de vrijwilliger in verband met een verhoogde kans op bijwerkingen. Dit is een van de redenen waarom *in vivo* LPS stimulaties niet binnen korte tijd herhaald kunnen worden. Bovendien is er beschreven dat een vrijwilliger die blootgesteld is geweest aan LPS enige tijd verminderd gevoelig is voor LPS (3, 4). Dit maakt het aantrekkelijk om *ex vivo* LPS-stimulatietesten toe te passen in klinische onderzoeken als vervanging voor of ter ondersteuning van een, voor de vrijwillige belastende, *in vivo* LPS-stimulatie.

In hoofdstuk 5 wordt de mogelijkheid beschreven om *in vivo* LPS-stimulatietesten uit te voeren met een beduidend lagere dosis LPS dan de dosis die doorgaans gebruikt wordt. De onderzoeksresultaten tonen aan dat een LPS dosis van 0.5 ng/kg al een significant effect heeft op de ontstekingsreacties *in vivo* (C-reactief proteïne (CRP), interleukine (IL)-6, IL-8 en tumor necrosis factor- α (TNF- α)). De *in*

vivo LPS-stimulatietest vormt in combinatie met *ex vivo* LPS-stimulatietesten in volbloed een uitstekende methode om op een veilige manier farmacologische effecten van immunomodulerende middelen te onderzoeken op basis van de geïnduceerde ontstekingsreacties.

De *ex vivo* LPS-stimulatietest in volbloed is ook toegepast in het bioequivalentieonderzoek met ONS-3010 (hoofdstuk 6). Dit onderzoeksmiddel is ontwikkeld als biologisch vergelijkbaar geneesmiddel (biosimilar) van adalimumab (Humira®). Adalimumab onderdrukt het immuunsysteem door de werking van TNF- α te blokkeren. In het geval van biosimilars ligt de nadruk in de vroege stadia van ontwikkeling doorgaans op het onderzoek naar farmacokinetische bioequivalentie. Dat gaat echter voorbij aan het feit dat farmacokinetische bioequivalentie van eiwitten geen garantie biedt voor gelijke effecten ('farmacodynamische bioequivalentie'). Immers, een klein verschil in de chemische structuur van het eiwit kan een grote invloed hebben op de activiteit. Daarom is het belangrijk dat klinisch onderzoek zich richt op bevestiging van zowel farmacokinetische als farmacodynamische bioequivalentie. De US Food and Drug Administration (FDA) and European Medicines Agency (EMA) geven echter geen duidelijke richtlijn over de fase van onderzoek of het stadium van ontwikkeling waarin dit dient te gebeuren (5-9). Om te voorkomen dat farmacodynamische bioequivalentie tussen het onderzoeksmiddel en het referentieproduct in een later stadium van ontwikkeling niet kan worden bevestigd, of het risico daarop te verkleinen, is het raadzaam om ook de farmacologische effecten van het geneesmiddel al in een vroeg stadium te onderzoeken. We illustreren de waarde van deze aanpak met het onderzoek beschreven in hoofdstuk 6, waarin de resultaten een identieke farmacologische activiteit van het onderzoeksmiddel en de twee referentieproducten onderbouwen. De resultaten tonen tevens de waarde van de *ex vivo* LPS-stimulatietest in volbloed als een geschikte methode om zowel de primaire als de secundaire farmacodynamische effecten van een middel in kaart te brengen, in de vroege fase van klinisch geneesmiddelonderzoek.

Samenvattend geeft dit proefschrift een overzicht van klinisch-farmacologische onderzoeken waarbij het onderzoek naar immunomodulerende biotherapeutica in een vroeg stadium van ontwikkeling centraal staat. De zoektocht naar selectieve biomarkers, zowel in gezonde vrijwilligers als in patiënten, een efficiënte opzet van onderzoek, de ontwikkeling van nieuwe onderzoeksmethoden en de verbetering van reeds bestaande methoden speelt hierin een zeer belangrijke rol. De moeilijkheden, of beter gezegd uitdagingen, die men hierbij kan ervaren worden tevens belicht. De klinisch-farmacologische onderzoeken die in dit proefschrift staan beschreven zijn er allen op gericht het ontwikkelingsproces van immunomodulerende biotherapeutica te bespoedigen.

REFERENTIELIJST

1. European Medicines Agency (EMA) – Position Paper on nonclinical safety studies to support clinical trials with a single microdose – CPMP/SWP/2599/02/ Rev1. 2004.
2. US Food and Drug Administration (FDA) – Guidance for Industry, Investigators and Reviewers – Exploratory IND Studies. 2006.
3. Kox M, de Kleijn S, Pompe JC, Ramakers BP, Netea MG, van der Hoeven JG, et al. Differential ex vivo and in vivo endotoxin tolerance kinetics following human endotoxemia. *Crit Care Med.* 2011;39(8):1866-70.
4. Dillingh MR, Poelgeest van EP, Malone KE, Kemper EM, Stroes ESG, Moerland M, et al. Characterization of inflammation and immune cell modulation induced by low-dose LPS administration to healthy volunteers. *Journal of Inflammation.* 2014;11:28.
5. European Medicines Agency (EMA) – Guideline on similar biological medicinal products containing monoclonal antibodies; EMA/CHMP/BMWP/403543/2010. 2012.
6. European Medicines Agency (EMA) – Guideline on similar biological medicinal products; CHMP/437/04 Rev 1. 2014.
7. European Medicines Agency (EMA) – Guideline on similar biological medicinal products containing biotechnology-derived proteins as active substance; EMEA/CHMP/BMWP/42832/2005 Rev1. 2014.
8. US Food and Drug Administration (FDA) – Scientific Considerations in Demonstrating Biosimilarity to a Reference Product - Guidance for Industry. 2015.
9. US Food and Drug Administration (FDA) – Quality Considerations in Demonstrating Biosimilarity of a Therapeutic Protein Product to a Reference Product - Guidance for Industry. 2015.

Appendices

CURRICULUM VITAE

Marlous Dillingh was born on January 13th, 1984 in Dirksland. After graduation from secondary school *Regionale Scholengemeenschap Goeree Overflakkee (RGO)* in Middelharnis in 2002, she studied Biomedical Sciences at Leiden University. She completed two research internships during her study, at the Rheumatology department (from April till August 2005) and the Intensive Care department (from August 2006 till January 2007) of the Leiden University Medical Centre. In the final year of her master (specialization: management) she completed a third and final internship at Reed Elsevier, Amsterdam (Science Based Business, from September 2007 till March 2008).

In 2008 she obtained her master's degree and started working as a Clinical Research Associate at Quintiles, Hoofddorp. In 2010 she was appointed as a Clinical Scientist in the Vascular Medicine research group at the Centre for Human Drug Research (CHDR), Leiden. She focused on the clinical pharmacology of immunomodulatory biotherapeutics, and participated in several research projects, supervised by prof. dr. J. Burggraaf and prof. dr A.F. Cohen. Whilst working as a Clinical Scientist at CHDR, she also became a board certified clinical pharmacologist in 2016.

LIST OF PUBLICATIONS

- Recombinant human serum amyloid P in healthy volunteers and patients with pulmonary fibrosis. **M.R. Dillingh**, B. van den Blink, M. Moerland, M.G.J. van Dongen, M. Levi, A. Kleinjan, M.S. Wijsenbeek, M.L. Lupher Jr, D.M. Harper, J.A. Getsy, H.C. Hoogsteden, J. Burggraaf. *Pulmonary Pharmacology & Therapeutics*, 2013 Dec, 26(6):672-676.
- Characterization of inflammation and immune cell modulation induced by low-dose LPS administration to healthy volunteers. **M.R. Dillingh**, E.P. van Poelgeest, K.E. Malone, E.M. Kemper, E.S.G. Stroes, M. Moerland, J. Burggraaf. *Journal of Inflammation*, 2014, 11(28).
- Microdosing of a Carbon-14 Labeled Protein in Healthy Volunteers Accurately Predicts Its Pharmacokinetics at Therapeutic Dosages. M.L.H. Vlaming, E. van Duijn, M.R. **Dillingh**, R. Brands, A.D. Windhorst, N.H. Hendrikse, S. Bosgra, J. Burggraaf, M.C. de Koning, A. Fidder, J.A.J. Mocking, H. Sandman, R.A.F. de Ligt, B.O. Fabriek, W.J. Pasma, W. Seinen, T. Alves, M. Carrondo, C. Peixoto, P.A.M. Peeters, W.H.J. Vaes. *Clinical Pharmacology and Therapeutics*, 2015 Aug, 98(2):196-204.
- Recombinant human pentraxin-2 therapy in patients with idiopathic pulmonary fibrosis: safety, pharmacokinetics and exploratory efficacy. B. van den Blink, **M.R. Dillingh**, L.C. Ginns, L.D. Morrison, M. Moerland, M. Wijsenbeek, E.G. Trehu, B.J. Bartholmai, J. Burggraaf. *European Respiratory Journal*, 2016 Mar, 47(3):889-897.
- Clinical evaluation of Humira® Biosimilar ONS-3010 in Healthy Volunteers: Focus on Pharmacokinetics and Pharmacodynamics. **M.R. Dillingh**, J.A.A. Reijers, K.E. Malone, J. Burggraaf, K. Bahrt, L. Yamashita, C. Rehrig, M. Moerland. *Frontiers in Immunology*, 2016 Nov, 7(508).
- Topical Ionic Contra Viral Therapy comprised of digoxin and furosemide as a potential novel treatment approach for common warts. T. van der Kolk, **M.R. Dillingh**, R. Rijneveld, E.S. Klaassen, M.N.C. de Koning, S.T.P. Kouwenhoven, R.E. Genders, J.N. Bouwes Bavinck, G. Feiss, R. Rissmann, J. Burggraaf. *Journal of the European Academy of Dermatology & Venereology*, 2017 Aug DOI: 10.1111/jdv.14527.
- Characterization of immune cell, endothelial, and renal responses upon human low-dose experimental endotoxemia. E.P. van Poelgeest, **M.R. Dillingh**, M.L. de Kam, K.E. Malone, E.M. Kemper, E.S.G. Stroes, J. Burggraaf, M. Moerland. *Journal of Pharmacological and Toxicological Methods (Submitted)*.

AUTHOR AFFILIATIONS

Academic Medical Center, Amsterdam, The Netherlands

E.M. Kemper
E.S.G. Stroes

AMRIF B.V., Wageningen, The Netherlands

R. Brands
W. Seinen

Centre for Human Drug Research, Leiden, The Netherlands

J. Burggraaf
M.R. Dillingh
M.G.J. van Dongen
M. Levi
M. Moerland
P.A.M. Peeters
E.P. van Poelgeest
J.A.A. Reijers

Department of Medicine, Duke University, Durham, North Carolina, United States

L.D. Morrison

Department of Pharmacy and Clinical Pharmacology, VU University Medical Center, Amsterdam, The Netherlands

N.H. Hendrikse

Department of Pulmonary Medicine, Erasmus Medical Center, Rotterdam, The Netherlands

B. van den Blink
H.C. Hoogsteden
A. Kleinjan
M.S. Wijsenbeek

Department of Radiology and Nuclear Medicine, VU University Medical Center, Amsterdam, The Netherlands

N.H. Hendrikse
A.D. Windhorst

Division of Thoracic Radiology, Mayo Clinic, Rochester, Minnesota, United States

B.J. Bartholmai

Gen IBET/IBET, Oeiras, Portugal

T. Alves
M. Carrondo
C. Peixoto

Good Biomarker Sciences, Leiden, The Netherlands

K.E. Malone

Massachusetts General Hospital, Boston, Massachusetts, United States

L.C. Ginns

Oncobiologics Inc. Cranbury, New Jersey, United States

K. Bahr
L. Yamashita
C. Rehrig

Promedior, Inc., Lexington, Massachusetts, United States

J.A. Getsy
D.M. Harper
M.L. Luper Jr.
E.G. Trehu

TNO, Zeist, The Netherlands

S. Bosgra
E. van Duijn
B.O. Fabriek
A. Fidder
M.C. de Koning
R.A.F. de Ligt
J.A.J. Mocking
W.J. Pasman
H. Sandman
W.H.J. Vaes
M.L.H. Vlaming

Utrecht University, Utrecht, The Netherlands

W. Seinen

LIST OF ABBREVIATIONS

5HTP	5-hydroxytryptophan	K_{el}	Elimination rate constant (also represented by the abbreviation)
6MWT	6-min walk test	LC	Liquid chromatography
6MWD	6-min walking distance	LOQ	Limit of quantification
AE	Adverse event	LPS	Lipopolysaccharide
ALAT	Alanine aminotransferase	LSMS	Least square means
ALP	Alkaline phosphatase	MAPK	Mitogen-activated protein kinase
AMS	Accelerator mass spectrometry	MCP-1	Monocyte chemoattractant protein-1
ANOVA	Analysis of variance	MMP-7	Matrix metalloproteinase-7
ANU	Australian National University	MSD	Meso Scale Discovery
AP	Alkaline phosphatase	NALP3	NACHT, LRR and PYD domains-containing protein-3
APTT	Activated partial thromboplastin time	NBE	New biological entity
ASAT	Aspartate aminotransferase	ND	Not determined
ATS	American Thoracic Society	NFKB	Nuclear factor κ -B
AUC	Area under the curve	NK	Natural killer
BLOQ	Below the limit of quantification	NLRP3	NACHT, LRR and PYD domains-containing protein-3 encoding gene
BMI	Body mass index	NOAEL	No-observed-adverse-effect level
BPM	Beats per minute	PAMP	Pathogen-associated molecular patterns
CALIPER	Computer-aided lung informatics for pathology evaluation and rating	PBMC	Peripheral blood mononuclear cell
CD14	Cluster of differentiation 14	PD	Pharmacodynamics
CI	Confidence interval	PDGF	Platelet derived growth factor
C_{max}	Maximum concentration	PF	Pulmonary fibrosis
COPD	Chronic obstructive pulmonary disease	PK	Pharmacokinetics
CRP	C-reactive protein	PT	Prothrombin time
CV	Coefficient of variance	PTX	Pentraxin
DLCO	Diffusing capacity of the lung for carbon monoxide	QTC	Corrected QT interval
EC ₅₀	Half maximal effect concentration	rhSAP	Recombinant human serum amyloid-P
EC ₈₀	80% maximal effect concentration	SAP	Serum amyloid-P
EC ₁₀₀	Maximal effect concentration	SAR	Structure-activity relationships
ECG	Electrocardiogram	SD	Standard deviation
EDTA	Ethylenediaminetetraacetic acid	SEC-UV	Size-exclusion chromatography-ultraviolet
ELISA	Enzyme-linked immunosorbent assay	SEM	Standard error of the mean
EMA	European medicines agency	SGRQ	St George's Respiratory Questionnaire
E_{max}	Maximal effect	SHIP	SH2 domain-containing inositol 5'-phosphatase
Eq.	Equation	SOCs-1	Suppressor of cytokine signalling-1
EU	European Union	$t_{1/2}$	Terminal half-life
FACS	Fluorescence activated cell sorter	$t_{1/2 el}$	Terminal elimination half-life
FCS	Fetal calf serum	TGF- β	Transforming growth factor- β
FDA	Food and drug administration	THC	Tetrahydrocannabinol
FEV1	Forced expiratory volume in 1 second	TLR	Toll-like receptor
FIH	First-in-human	t_{max}	Time at observed maximum concentration
FVC	Forced vital capacity	TNF- θ	Tumour necrosis factor- θ
FVC % PRED	Forced vital capacity percentage predicted	TNFR1	TNF receptor type 1
GGT	Gamma glutamyl transferase	TNFR2	TNF receptor type 2
HPLC	High-performance liquid chromatography	TRIF	TIR domain-containing adapter inducing interferon-
HRCT	High-resolution computed tomography	UIP	Usual interstitial pneumonia
hRESCAP	Human recombinant placental alkaline phosphatase	US	United States
ICAM-1	Intercellular adhesion molecule-1	USA	United States of America
IFN- γ	Interferon- γ	UVDL	University Veterinary Diagnostic Laboratory
IIP	Idiopathic interstitial pneumonia	V_d	Volume of distribution
IL	Interleukin	VCAM-1	Vascular cell adhesion molecule-1
ILA	Interstitial lung abnormalities	VGEF	Vascular endothelial growth factor
IPF	Idiopathic pulmonary fibrosis		
IRAK-M	Interleukin-1 receptor-associated kinase-M		
JNK	c-Jun N-terminal kinase		

